APPLICATION OF THE ALGEBRAIC TECHNOLOGICAL FUNCTION TO THE OPTIMIZATION OF GROUNDWATER ABSTRACTION FROM AN UNCONFINED AQUIFER IN ZACATECAS, MEXICO.

by

Mariano Hernandez Narvaez

A Thesis Submitted to the Faculty of the

DEPARTMENT OF HYDROLOGY AND WATER RESOURCES

In Partial Fulfillment of the Requirements
For the Degree of

MASTER OF SCIENCE
WITH A MAJOR IN HYDROLOGY

In the Graduate College

THE UNIVERSITY OF ARIZONA

1 9 8 7

STATEMENT BY AUTHOR

This thesis has been submitted in partial fulfillment of requirements for an advanced degree at the University of Arizona and is deposited in the University Library to be made available to borrowers under rules of the Library.

Brief quotations from this thesis are allowable without special permission, provided that accurate acknowledgment of source is made. Request for permission for extended quotation from or reproduction of this manuscript in whole or in part may be granted by the head of the major department or the Dean of the Graduate Collage when in his or her judgment the proposed use of the material is in the interests of scholarship. In all other instances, however, permission must be obtained from the author.

SIGNED: M. Hernandez D.

APPOVAL BY THESIS DIRECTOR

This thesis has been approved on the date shown below:

Thomas Maddock III — 4/17/87

THOMAS MADDOCK III
Professor of Hydrology and
Water Resources

Date

This Thesis is dedicated to my parents

Ing. Mariano Hernandez Moedano and

Sra. Josefina Narvaez de Hernandez

and my sisters

Elisa, Carmen, Concepcion,

Gloria and Roxana "Gonini"

ACKNOWLEDGMENTS

I want to recognize the members of the Faculty of the Department of Hydrology and Water Resources for the knowledge I received from them, especially from Dr. Thomas Maddok III, my thesis director and academic advisor. I thank Dr. Nathan Buras and Dr. Martin Fogel for serving on my thesis committe, and Dr. Shlomo P. Neuman for his many suggestions and insights.

I want to express my gratefulness to Ing. Joaquin Mendez for providing the necessary information about the Calera aquifer in Zacatecas, Mexico. Special thanks are due to Javier Samper who patiently introduced me to the fascinating world of geostatistics and thoroughly reviewed chapter three. My most sincere gratitude and appreciation go to Ron Green, Gordon Wittmeyer, Javier Samper and Adolfo Chavez. I will be forever gratefull to them for their patient discussions, help, and support throughout my studies. Appreciation also goes to my friends in the Hydrology Department, too numerous to mention, who have given me moral support and encouragment over the years. Very special thanks are also extended to Augusta Davis who graciously devoted much of her time providing all manner of support.

Lastly, I wish to thank my family for their love and belief in me all these years.

TABLE OF CONTENTS

TABLE OF CONTENTS--Continued

LIST OF ILLUSTRATIONS

LIST OF ILLUSTRATIONS--Continued

LIST OF ILLUSTRATIONS--Continued

LIST OF TABLES

LIST OF TABLES--Continued

ABSTRACT

The use of systems analysis coupled with the simulation model provides the basis of a powerfull decision making tool. A groundwater simulation model is coupled with a mathematical optimization model through the Algebraic Technological Function (Response Function) to form the Groundwater Management Model for the Calera aquifer in Zacatecas, Mexico. The management model maximizes the amount of groundwater pumped from the Calera aquifer subject to the physical capability of the system.

A two dimensional finite difference code is used both to simulate the flow system in the aquifer and compute the response functions at specified locations. To overcome the lack of parameter information, the geostatistical technique of Kriging is used to estimate spatially-averaged log-transmissivities, point estimates of hydraulic head and kriging estimation errors at each cell or node. Semivariograms are validated using both "Jacknife" and Maximum Likelihood cross-validation methods. In addition, the hydraulic head kriging errors are used as a criterion to stop the calibration process of the simulation model.

Three alternatives are evaluated to obtain optimal pumping rates while meeting water demands for 1990 and 1995 by means of Linear Programming. These results may help to enhance future development of groundwater resources in the area.

CHAPTER 1

INTRODUCTION

The Calera Basin is one of the most important regions of the state of Zacatecas, and the socioeconomic development of the past thirty years has been due to its agricultural production. Water resources of the Calera Basin are primarily limited to groundwater which occurs in the alluvial sediments of the Calera aquifer. The early presence of springs and water levels close to the ground surface, in the northern region of the basin, gave the false impression of high water availability. As a result, an indiscriminately number of wells were installed in this area; therefore, by the end of 1975 most of the springs became dry and the hydraulic gradient steeper. Water levels have declined in the most heavily pumped area approximately 30 meters (98 ft) during the period of 1956-1985. Groundwater development in this area is presently characterized by narrowly-spaced and fairly high yield wells which supply water to irrigation and domestic use. However, the groundwater resources of the southern and central part of the region appear destined for medium scale development in the future. These areas have not been investigated for development of a water supply to support possible areas for irrigation use.

This report presents the development of ground water simulation and management models to quantify the water resources of the Calera Basin and predict the response of the hydrogeologic system to future

pumping stresses. Specifically, the study focuses on the estimation of the spatial distribution of the hydrogeologic parameters used in the models and the calculation of optimal pumping rates for two time periods.

Purpose and Scope

The purpose of the study is to obtain with the aid of the response fuction technique the maximum amount of water that can be pumped from the aquifer subject to physical constraints of the system. In addition, in order to meet the water demands at the end of 1990 and 1995, three optimal spatially distributed pumpage schemes are presented based on the 1985 useable saturated thickness. The study has been divided in three parts. The first part used the kriging technique for estimation of transmissivity and hydraulic heads at unsampled sites, and computation of the estimation kriging errors. The second part of the study used a two dimensional finite difference model to simulate the actual conditions of the system. The third part consisted of the formulation of the hydraulic management model and the application of the response function technique to couple the simulation model with the management model.

The following chapter of this report contains a physical description of the aquifer of the Calera Basin. The geography, climate, geology and hydrogeology are presented. The chapter concludes with a short history of groundwater development in the basin. Chapter 3 includes a general presentation and discussion of kriging theory. In

addition, application of kriging to log-transmissivity and hydraulic head data from the Calera Basin is reported. Chapter 4 deals with the application of the two dimensional finite difference model to simulate actual conditions in the Calera aquifer. Chapter 5 includes a general presentation of the response function technique to couple the simulation and management models, and the presentation of the objective function that maximizes the total amount of water that can be pumped from the aquifer subject to physical constraints of the system. Conclusions reached on the basis of results from kriging, simulation and management models are discussed individually within chapters 3, 4 and 5, and generally in chapter 6. The study should provide future investigators a guidance regarding the most critical data and most important areas to be studied in order to refine the predictive capabilities of the model for the basin.

Previous Investigations

The Calera Basin has been the subject of several geologic and hydrogeologic investigations. The first study was carried out by the federal agency Secretaria de Agricultura y Recursos Hidraulicos (SARH) in 1966. The objective of the study was primarily to collect and organize previous information concerning water level measurements performed since 1956. SARH performed the first hydrogeologic study, based on the previous study, in 1968. However, the results of the hydrogeologic study are highly questionable due to the very limited data concerning the spatial distribution of transmissivity and storativity.

In addition, the study was limited to the northern region of the basin. As a result, the regional behavior of the aquifer was unknown. SARH has been updating the data base every two years since 1970. One geologic and two hydrogeologic studies have been carried out since 1970. The first hydrogeologic study provided a better knowledge of the regional behavior of the aquifer. The second hydrogeologic study involved an electrical resistivity survey, which provided information about the relative thickness of the basin fill sediments and probable bedrock configuration. In addition, the study provided a quantitative assessment of the ground water resources of the entire basin. However, no attempts have been made to develop a computer model to assess the effect of the present pumpage policy on future water levels.

CHAPTER 2

SETTING OF THE STUDY AREA

Geographic Setting

The Calera Valley is an elongate basin located in the southeastern part of the state of Zacatecas, Mexico, figure 2.1. The drainage basin is approximately 48 Km (30 Miles) long, the width of the valley floor varies from 30 Km (19 Miles) to 18 Km (11 Miles) and covers an area of over 1200 Km^2 (463 $Miles^2$). The southern divide is the Villanueva Canyon, whereas the northern divide is the low lands basin. The western divide follows the crest of the Sierra Madre Occidental, whereas the eastern divide follows the crest of the Sierra of Zacatecas.

The topography of the area varies, the northern and central part of the valley are almost flat with an average slope of 0.6 %, whereas the eastern and western regions have an average slope of 0.9 %.

The basin is drained by small washes originated in the Sierra Madre Occidental and the southern part of the Sierra of Zacatecas. The flow is northward to a point just south of the town of Victor Rosales. The washes are perennial just during the rainy season in its upper reaches but ephemeral along most of the valley floor.

The Calera basin is one of the most important regions of the state of Zacatecas, major cities in the basin are Fresnillo and Victor

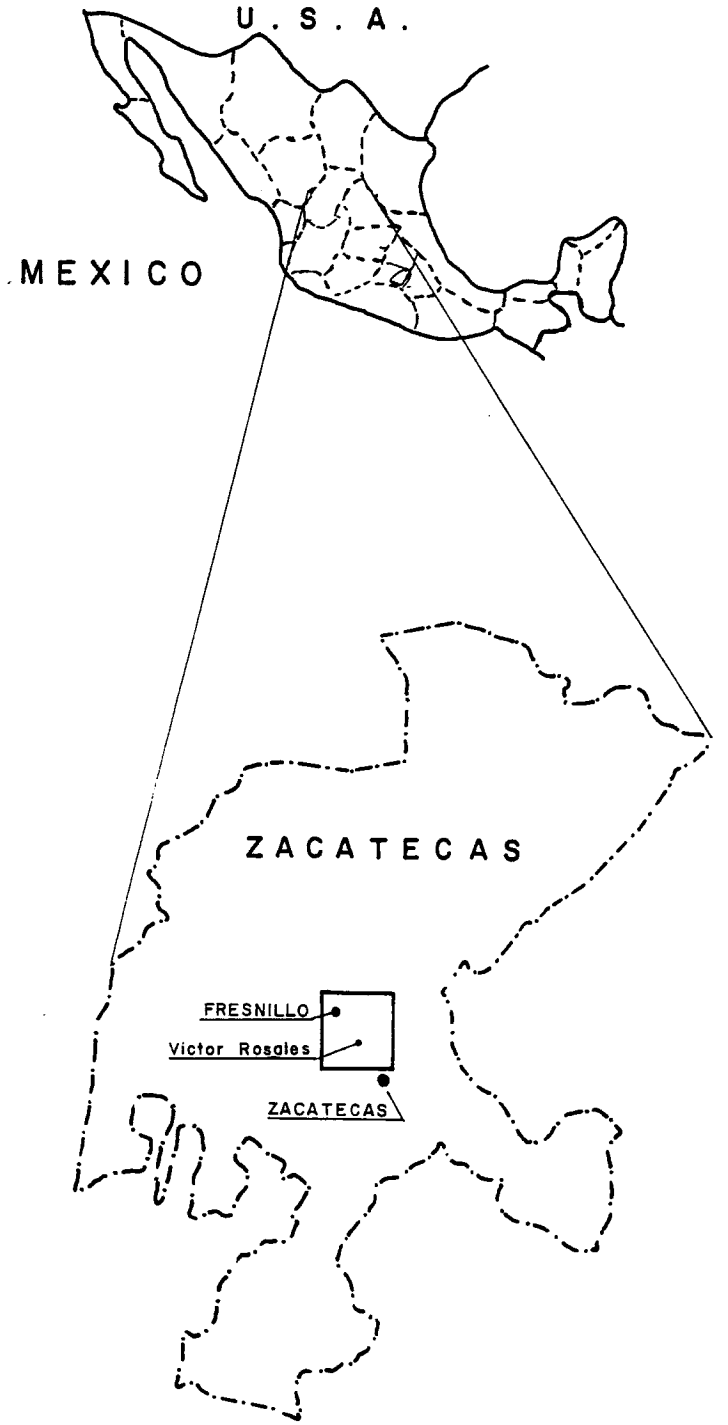

Figure 2.1 Location of study area in Zacatecas, Mexico.

Rosales with a present population of 70 and 20 thousand, respectively. Land use is predominately agriculture with the major portion of the income coming from soybeans and vegetables.

Climate

The climate of Calera Valley is semiarid with a mean annual temperature of 16 °C (62 °F). The monthly mean temperature reaches a maximum of 22 °C (72 °F) in June and a minimum of 10 °C (50 °F) in January. The average yearly precipitation is 450 mm (18 inches) to 600 mm (24 inches) with the northern region of the basin generally receiving less than the southern region. The hydroclimatology of the basin is characterized by distinct rainy and dry seasons. The rainy period, which extends from June through October, accounts for 82% of the total rainfall. During the dry season scattered thunderstorms produce the majority of the precipitation. The average yearly potential evaporation in the basin is 2200 mm (87 inches).

Geology

The structural basin was apparently formed by basin-range type normal faulting during the Miocene period. The Sierra of Zacatecas consists of Tertiary intrusive igneous rocks, Tertiary conglomerate, whereas the Sierra Madre Occidental consists of Tertiary conglomerate, Tertiary rhyolites and Tertiary volcanic tuff.

The bedrock in the study area is composed of metamorphic and granite rocks and tilts to the north. Depth to well consolidated

bedrock in the basin varies from less than 180 M (590 Ft) to more than 300 M (984 Ft) below land surface.

The lithology of the basin fill is typical of a continental basin in a semiarid climate. The rocks and sediments can be classified broadly into three hydrogeologic units. The first unit comprises all the permeable sediments such as alluvium composed of gravels, sands with loam and discontinous thin lenses of clay. Alluvial material outcrops mostly on the northeastern and central part of the basin. The second unit is characterized by less permeable material like medium to fine grained dolomite limestone, which is overlain by soil layers of 2 and 3 meters thick. This unit is exposed in the northern and western area of the basin. The third hydrogeologic unit consists of rhyolites, conglomerate, basalt flows and volcanic rocks. The latter unit is a characteristic of the Sierra of Zacatecas and Sierra Madre Occidental (figure 2.2).

Hydrogeology

The lower (northern) part of the basin is developed for irrigated agriculture. Available data indicate that withdrawals of significant amounts from the aquifer in the region started around 1966. Typically, groundwater extractions account for more than 90% of the total water usage during the dry season. As a result, it is during the dry season that the groundwater system is most highly stressed. According to the water level data groundwater flow follows a northerly pattern, with an average hydraulic gradient of 0.0027.

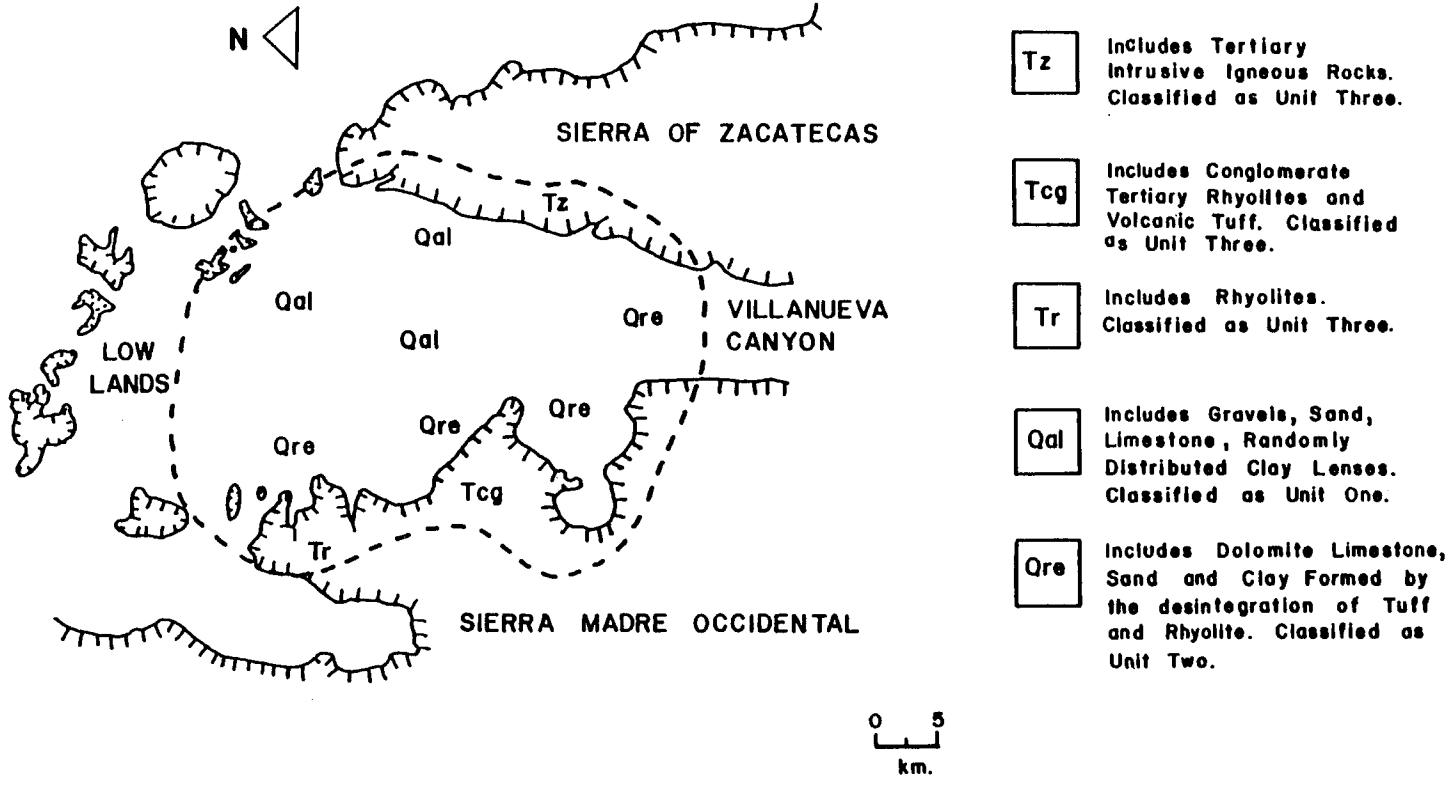

Figure 2.2 Hydrogeologic map of Calera basin.

The interpretation of field observations and well records indicates that the aquifer is anisotropic, heterogeneous and unconfined with lenses of more permeable sand that appear to be randomly distributed within a less permeable clay-rich matrix. As a result of the fairly large spatial variability of the sediments the hydraulic parameters of the aquifer are expected to vary spatially. Average values of aquifer parameters were obtained from previous work (SARH, 1980). Transmissivity was reported to have values ranging from 50 to 400 M^2/day (538 to 4300 Ft^2/day) and averaging 140 M^2/day (1500 Ft^2/day). The hydraulic conductivity of the aquifer ranges between 0.25 to 1.33 M/day (0.82 to 4.36 Ft/day). A value for the storage coefficient for the entire aquifer was reported to be 0.13.

Recharge to the goundwater system in the Calera Valley occurs from irrigation return flow, and precipitation. Irrigation return flow inferred from water level fluctuations is minimal. Precipitation on the valley floor of the upper valley and on mountain-front drainage add significant amount of water to the groundwater system. Recharge has been estimated from a hydrologic budget to equal 62 mm/yr (2.44 inches) (SARH, 1980). The aquifer discharges to springs in the lowlands.

History of Grounwater Development

For the past thirty years, the agricultural and urban development that has taken place in the Calera basin, Zacatecas, Mexico is due to the explotation of its groundwater resources.

A considerable number of wells have been installed in different

time periods. According to SARH the number of wells drilled up to 1984 are 1060. Water levels in the central area have declined about 30 M (98 Ft), the most pumped region. In fact, very few investigations dealing with the availability of water have been carried out.

Farmers in the region are concerned about the availability of water for the present demand, and future agricultural development of cultivable lands. This concern is coupled with the population growth of the comunities within the basin.

CHAPTER 3

KRIGING THEORY

Inasmuch as subsurface hydrology is an applied science a great deal of data of various types must be collected such as water levels, transmissivities determined by pumping test, aquifer thickness, etc. On the other hand, in practice, the groundwater flow equation is often solved numerically on computers by grid methods such as finite differences or finite elements. Whether the flow equation is solved by either method, values of the parameter at each node or cell should be provided. However, one does not have measured data at each node of the grid. In order to overcome the lack of parameter information at each node or cell one can either allow the value of the parameter to remain uniform over discrete subregions of the flow field or vary slowly in space. If the latter approach is considered, one has to account for the randomness of the spatial variations of the hydrologic parameters, therefore, the problem of insufficient information should be analyzed statistically instead of deterministically. One way to analyze the spatial variability of hydrological parameters is by means of geostatistical methods such as Kriging.

Kriging is based on the theory of regionalized variables developed mainly by Matheron (1963, 1971) for the estimation of ore reserves in mining engineering. The method which was originally limited to mining problems has been considerably extended during the last 10 years

to cover fields as varied as soils, geophysics, geology, hydrology, etc. In this method the data values $z(\underline{x}_i)$ at N locations $\underline{x}_1, \ldots, \underline{x}_N$ are interpreted as a realization of a random function $Z(\underline{x})$. This probabilistic interpretation allows obtaining not only estimated values at unsampled locations but also the variances of estimation. This characteristic of kriging is not considered by other interpolation methods such as inverse distance, trend surface analysis, etc.

We start discussing the basic concepts of Kriging theory. Then the application to log-transmissivity and hydraulic head. For details of kriging theory the reader is referred to Journel and Huijbregts (1978), Matheron (1963), Delhome (1978,1979), and Neuman (1984).

Basic Assumptions and Definitions

Kriging, as previously mentioned, is based on the theory of regionalized variables. In geostatistics, a regionalized variable (ReV) is interpreted as any realization of a random function (RF) $Z(\underline{x})$. Then a RF $Z(\underline{x})$ can be seen as a set of random varibles (RV) $Z(\underline{x}_i)$ defined at each point $\underline{x}_i$ of the domain D.

In linear geostatistics, only the first two moments of the RF $Z(\underline{x})$ are required. The first moment of $Z(\underline{x})$, $m(\underline{x}) = E[Z(\underline{x})]$, generally a function of the location $\underline{x}$ is called drift or trend. The second moments of $Z(\underline{x})$ include the variance, the autocovariance and the semivariogram which are defined respectively as

$$VAR[Z(\underline{x})] = E\{[Z(\underline{x}) - m(\underline{x})]^2\} \quad \text{----} \quad (1)$$

$$COV[Z(\underline{x}),Z(\underline{x}+\underline{h})] = E\{[Z(\underline{x})-m(\underline{x})][Z(\underline{x}+\underline{h})-m(\underline{x}+\underline{h})]\} \text{ --- (2)}$$

$$\delta(\underline{x},\underline{x}+\underline{h}) = 1/2\ E\{[Z(\underline{x}) - Z(\underline{x}+\underline{h})]^2\} \text{ ---- (3)}$$

Inasmuch as is not possible to infer the probability distribution of the RF $Z(\underline{x})$ from a single realization, it is necessary to make some assumptions about $Z(\underline{x})$, like the stationarity assumption. A RF $Z(\underline{x})$ is said to be strictly stationary if for any set of n points $\underline{x}_1$, $\underline{x}_2$,...., $\underline{x}_n$, and for any vector $\underline{h}$, the distribution function of the n random functions $Z(\underline{x}_i)$, i= 1, 2,..., n is the same as that of $Z(\underline{x}_i+\underline{h})$.

Since one is dealing with the first two moments of the RF $Z(\underline{x})$, the previous assumption can be relaxed to stationarity of the first two moments. Therefore, a RF $Z(\underline{x})$ is said to be second order stationary if

$$E[Z(\underline{x})] = m \quad \text{--- (4)}$$

$$COV[Z(\underline{x}),Z(\underline{x}+\underline{h})] = E[Z(\underline{x})Z(\underline{x}+\underline{h})] - m^2 = C(\underline{h}) \text{ --- (5)}$$

for a second order stationary random function the drift $m(\underline{x})$ exists and is not dependent on $\underline{x}$. In addition, the covariance between any two points $\underline{x}$ and $\underline{x}+\underline{h}$ depends only on the separation vector $\underline{h}$ and not on the points. A consequence of the stationarity of the covariance is that the variance of $Z(\underline{x})$, $Var[Z(\underline{x})] = \sigma^2$ exists, is finite and does not depend on $\underline{x}$.

Random functions not satisfying the previous conditions are not stationary. The type of non stationary RF that has stationary

increments are called intrinsic random functions. Then a RF $Z(\underline{x})$ is intrinsic if all the increments $Z(\underline{x}) - Z(\underline{x}+\underline{h})$ are second order stationary. That is

$$E[Z(\underline{x}) - Z(\underline{x}+\underline{h})] = 0 \quad \text{----} \qquad (6)$$

$$\text{Var}[Z(\underline{x}) - Z(\underline{x}+\underline{h})] = 2\delta(\underline{h}) \quad \text{-----} \qquad (7)$$

where $\delta(\underline{h})$ is the semivariogram function introduced first by Matheron (1963). Notice that the semivariogram of an intrinsic random function is only a function of the separation vector $\underline{h}$. The semivariogram $\delta(\underline{h})$ is a statistic that measures the variability of the RF $Z(\underline{x})$ and the spatial correlation between two points separated by a vector $\underline{h}$. Notice that a second order stationary random function is always intrinsic. The reciprocal, however, is not always true. The relation between the semivariogram and the covariance for a second order random function is

$$\delta(\underline{h}) = \text{Var}[Z(\underline{x})] - C(\underline{h}) \quad \text{-----} \qquad (8)$$

which is depicted in figure 3.1.

For a stationary random function, the semivariogram usually increases with distance until at a certain distance reaches its sill, which is equal to the variance of the data in the field and stays there. This distance is generally denoted by "a" and defines the distance within which samples are correlated. Points farther apart than distance "a" are uncorrelated, thus "a" is referred to as the range of influence of a point within the aquifer (figure 3.2). In theory, a semivariogram of a continuous random function should be equal to zero

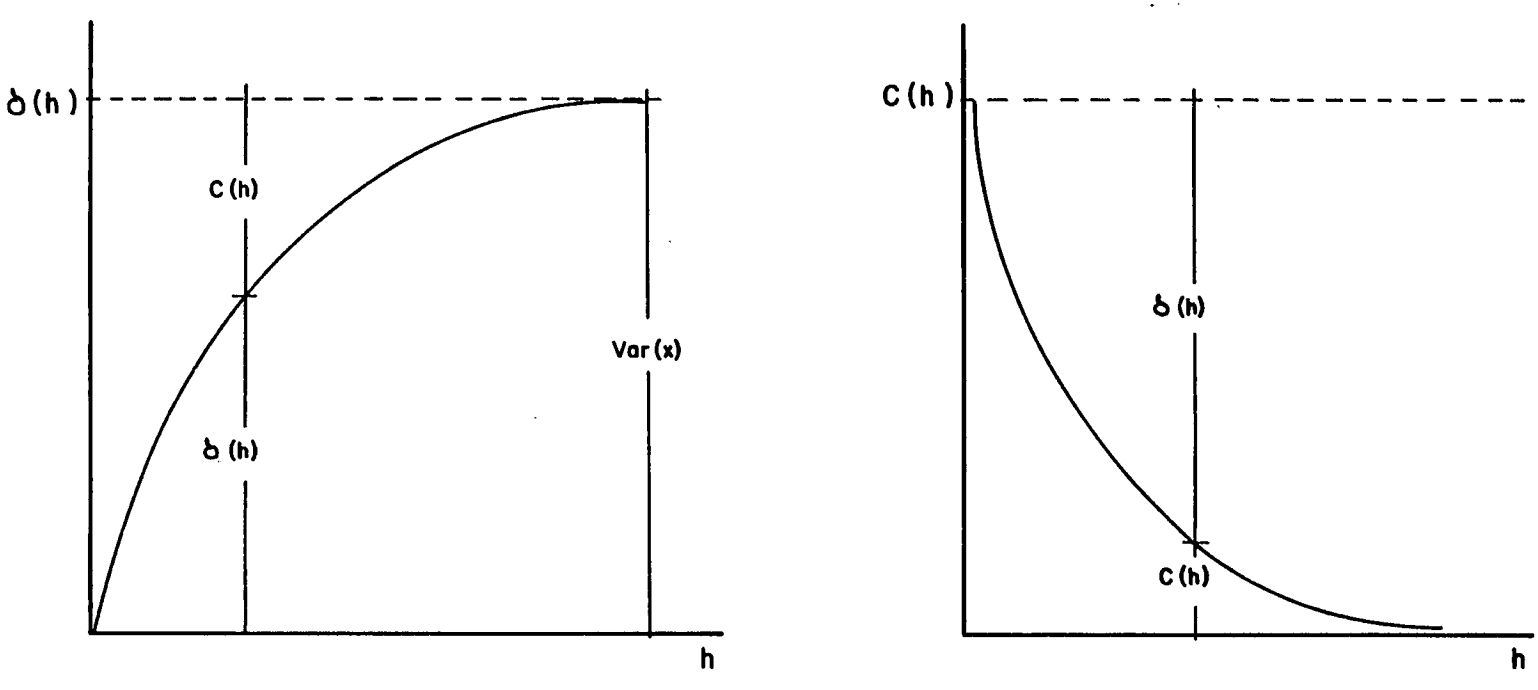

Figure 3.1 Relation between the semivariogram and the covariance.

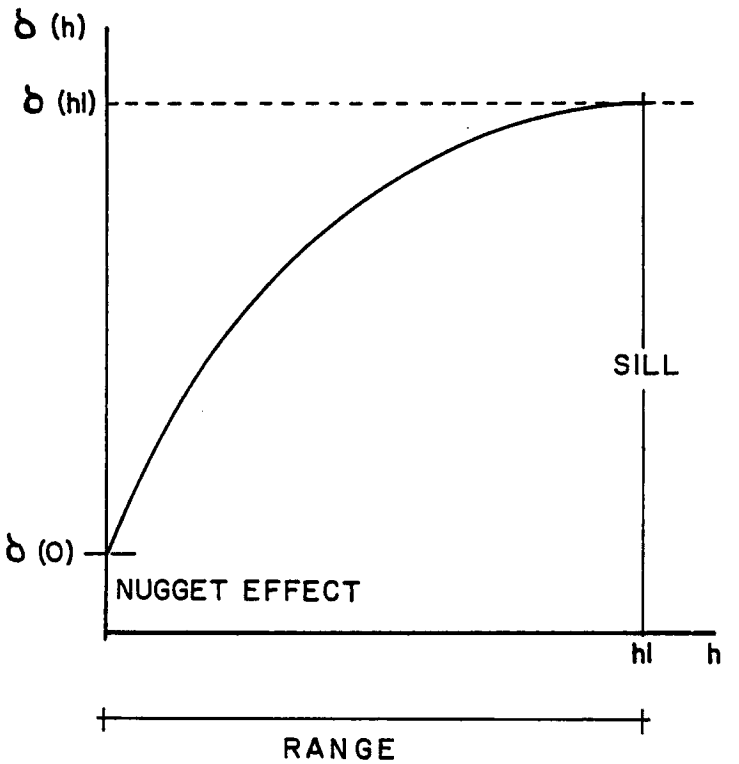

Figure 3.2 Components of the semivariogram.

at the origin. However, often a discontinuity is present in the semivariogram at the origin. This discontinuity is called "nugget effect" and could be explained, among other things, by measurement errors (Clifton and Neuman,1982).

Introduction to Kriging

The procedure for making a geostatistical hydrological parameter estimation can be divided in two parts. The first is the investigation and modeling of the physical and statistical structure of the basin for which the estimation is being made. The concept of spatial variability of the random variable is considered during the first step. The second step of the procedure is the estimation process itself, kriging, which depends entirely on the semivariogram obtained during the first step. The next section will be devoted to construct and model the semivariogram.

Semivariogram Estimation

The process of estimating the semivariogram is usually referred as structural analysis. One of the earliest semivariogram estimators is the proposed by Matheron (1963)

$$\delta^*(\underline{h}) = \frac{1}{2N(h)} \sum_{i=1}^{N(h)} [Z(\underline{x}_i + \underline{h}) - Z(\underline{x}_i)]^2 \quad ----- \quad (9)$$

where $Z(\underline{x}_i)$ is the experimental value at point $\underline{x}_i$ and N(h) is the

number of pairs of data points separated by a distance equal to $\underline{h}$. Because the observed points are rarely evenly spaced in the plane, they are regrouped by classes of distance and angle so that mean square differences can be calculated. In general, a semivariogram is assumed isotropic, that is, the semivariogram depends only on the modulus h of the vector $\underline{h}$. However, it is often useful to compute a semivariogram assuming that $\gamma^*(\underline{h})$ is a function of the direction as well as of the modulus of $\underline{h}$. A comparison of the semivariograms obtained for different directions will reveal the anisotropies of the random variable under study.

The sample semivariogram generally exhibits very poor statistical behavior because of sampling problems (Journel and Huijbregts, 1978). If an experimental semivariogram has been constructed it must be related to some theoretical model. The usual way to fit a semivariogram model $\gamma(\underline{h})$ to the observed sample semivariogram involves several steps some of them are tedious and time consuming.

Firstly, one chooses a theoretical model among the list of currently available (quadratic, spherical, exponential, etc). The second step involves selecting values of the semivariogram parameters (nugget, sill, range) that produce a good fit to $\gamma^*(\underline{h})$. This fit is usually done by eye and is not intended to be optimal. This preliminary fitting provides a set of parameters to start the third step, the validation process. Validation of the semivariogram is a technique to check whether or not the semivariogram is adequate. This process commonly called "cross-validation" consists of dropping one of the data

points $\underline{x}_i$ from the estimation process, obtaining the kriging estimate at that point, and computing the difference between the kriging estimate value and the actual measurement. The output obtained by performing cross-validation consists of a set of values of:

$$a)\ e_i = Z(\underline{x}_i) - Z^*(\underline{x}_i)$$

$$b)\ \sigma^2_{ki}$$

where e_i is the difference between observed $Z(\underline{x}_i)$ and kriged values $Z^*(\underline{x}_i)$, σ^2_{ki}, is the kriging variance of the error e_i for all the points i where cross-validation is performed. The optimum parameters of the semivariogram are those that induce some desired properties on the cross-validation errors e_i and the variances σ^2_{ki} such as

a) The errors $e_i = Z(\underline{x}_i) - Z^*(\underline{x}_i)$ have zero mean

$$1/N \sum_{i=1}^{N} [Z(\underline{x}_i) - Z^*(\underline{x}_i)] \approx 0$$

b) and are consistent with the computed kriging errors.

$$[1/N \sum_{i=1}^{N} (e_i^2/\sigma^2_{ki})] \approx 1$$

Moreover, BLUEPACK a geostatistical package developed at the Ecole des Mines in Fontainebleau, France, uses additional criteria such as

c) The correlation coefficient of $Z(\underline{x}_i)$ versus $Z^*(\underline{x}_i)$ is close to 1.

d) The correlation coefficient of e_i versus $Z^*(\underline{x}_i)$ should be close to zero.

If the desired properties are not met, the parameters of the semivariogram are changed, then the whole cross-validation process is repeated again until the above criteria are more or less satisfied.

Kriging Equations

As indicated at the begining of this chapter, geostatistical estimation techniques provide a measure of the error associated with the estimates, namely the variance of the error of distribution. Furthermore, it is also possible to find the set of weighting coefficients that minimizes this estimation variance.

The kriging problem is usually posed as follow: given the measurements of $Z(\underline{x})$ at a set of n points $\underline{x}_1$, $\underline{x}_2$, $\underline{x}_3$,., $\underline{x}_n$, estimate the value of $Z(\underline{x}_0)$ at a point $\underline{x}_0$ or its average value $Z(v_0)$.

$$Z^*(\underline{x}_0) = \sum_{i=1}^{N} \lambda_i \, Z(\underline{x}_i) \text{ ----- } (10)$$

where the λ_i are the kriging coefficients that are determined by requiring $Z^*(\underline{x}_0)$ to be unbiased and of minimum variance. The unbiasedness of $Z^*(\underline{x}_0)$ leads to

$$\sum_{i=1}^{N} \lambda_i = 1$$

Minimization of the estimation variance leads to a system of N + 1 linear equations

$$\delta(\underline{x}_i,\underline{x}) = \sum_{j=1}^{N} \lambda_j \delta(\underline{x}_i,\underline{x}_j) + v \qquad i=1,..,n \qquad \text{--- (11)}$$

$$\sum_{i=1}^{N} \lambda_i = 1 \qquad \text{---- (12)}$$

Once the λ_j's and v are computed the estimated value $Z^*(\underline{x}_0)$ is obtained from equation 10 and the estimation variance by

$$\text{Var}[Z(\underline{x}_0)-Z^*(\underline{x}_0)] = 2\sum_{i=1}^{N} \lambda_i \delta(\underline{x},\underline{x}_i) - \sum_{i=1}^{N}\sum_{j=1}^{N} \lambda_i \lambda_j \delta(\underline{x}_i,\underline{x}_j) \qquad \text{---- (13)}$$

The previous equations can be extended for the estimation of the average value of $Z(\underline{x})$ over a zone R_n. For that, one has to replace $\delta(\underline{x}_i,\underline{x})$ by $\delta(\underline{x}_i,R_n)$ which is equal to the average value of $\delta(\underline{x}_i,\underline{s})$ for all $\underline{s} \in R_n$. Kriging variance is now given by

$$\sigma^2_k = -\delta(R_n,R_n) + \sum_{i=1}^{N} \lambda_i \delta(\underline{x}_i,R_n) + v \qquad \text{--- (14)}$$

Where $\delta(R_n,R_n)$ is the average value of $\delta(\underline{s},\underline{t})$ for all $\underline{s},\underline{t} \in R_n$

Residual Kriging

Up to now, the random function was assumed to be intrinsic. Generally this assumption does not hold for hydraulic head data. Therefore, in order to use kriging equations, the drift must first be removed from the data. This section discusses a method based on a stepwise iterative regression process that yields simultaneous

estimates of the drift and the residual semivariogram. Much of the following discussion is taken from Fennessy (1982), and Neuman, Jacobson and Fennessy (1983).

Let $H(\underline{x})$ be the hydraulic head at a point $\underline{x}$. By definition, the drift or trend is the expectation of the random function.

$$E[H(\underline{x})] = m(\underline{x})$$

$H(\underline{x})$ can be expressed as the sum of the deterministic drift, $m(\underline{x})$, and a residual term $R(\underline{x})$. Thus,

$$H(\underline{x}) = m(\underline{x}) + R(\underline{x}) \text{ ----- } (15)$$

where the residual term $R(\underline{x})$ has zero expectation.

$$E[R(\underline{x})] = 0$$

According to Fennessy (1982) the drift term $m(\underline{x})$ expresses the regular and continous variations of $H(\underline{x})$ at the scale of observation and the residual $R(\underline{x})$ accounts for erratic fluctuations of the data about the mean. Let the drift may be expressed as

$$m(\underline{x}) = \sum_{j=1}^{J_o} a_j \; f(x_i)_j \text{ ----- } (16)$$

where:

a_j, coefficients to be determined, and $f(x_i)_j$, prescribed basis functions. Suppose that $H(\underline{x})$ was observed at I locations, $\underline{x}_1, \underline{x}_2, ., \underline{x}_I$. Let H_i be the measured value of $H(\underline{x})$ at each point $\underline{x}_i$. Then (15) can be rewritten by virtue of (16) as:

$$\underline{H} = \underline{\underline{F}}\ \underline{a} + \underline{R} \text{ ----- (17)}$$

where

$$\underline{H} = \begin{Bmatrix} H_1 \\ \cdot \\ \cdot \\ H_I \end{Bmatrix} \quad ; \quad \underline{\underline{F}} = \begin{Bmatrix} f(x_1)_1 & \cdots & f(x_1)_{jp} \\ \cdot & & \cdot \\ \cdot & & \cdot \\ f(x_I)_1 & \cdots & f(x_I)_{jp} \end{Bmatrix}$$

$$\underline{a} = \begin{Bmatrix} a_1 \\ \cdot \\ \cdot \\ a_{jp} \end{Bmatrix} \quad ; \quad \underline{R} = \begin{Bmatrix} R_1 \\ \cdot \\ \cdot \\ R_I \end{Bmatrix}$$

If the covariance matrix of the residuals $\underline{\underline{V}}_k$ is known, then an unbiased estimate $\underline{a}^*$ of "a" is obtained by minimizing the following generalized least square criterion (Beck and Arnold, 1977; and Fennessy, 1982)

$$J(\underline{a}) = [\underline{H} - \underline{\underline{F}}\ \underline{a}]^T\ \underline{\underline{V}}_k^{-1}\ [\underline{H} - \underline{\underline{F}}\ \underline{a}]$$

The minimization leads to the following equation

$$\underline{a}^* = [\underline{\underline{F}}^T\ \underline{\underline{V}}_k^{-1}\ \underline{\underline{F}}]^{-1}\ \underline{\underline{F}}^T\ \underline{\underline{V}}_k^{-1}\ \underline{H} \text{ ------ (18)}$$

Having computed $\underline{a}^*$, the estimate of m, m^*, is

$$m^* = \underline{\underline{F}}\ \underline{a} \text{ ------- (19)}$$

and the residuals are given by,

$$\underline{R}^* = \underline{H} - \underline{m}^* \text{ ------- (20)}$$

Kriging is used to estimate the residuals. Because the drift and the

semivariogram must be determined simultaneously, the generalized least square process consists of two parts.

First part.- Stepwise least squares is used to identify the degree of the polynomial representing the drift. Since correlation between the residuals is unknown, one assumes as a first approximation that $\underline{\underline{V}}_k = \underline{\underline{I}}$ where $\underline{\underline{I}}$ is the identity matrix. Then equation 18 can be rewritten as

$$\underline{a}^* = [\underline{\underline{F}}^T \underline{\underline{F}}]^{-1} \underline{\underline{F}}^T \underline{H} \text{ ------- (21)}$$

Using (21), coefficients of increasingly higher order polynomial are calculated until the residuals behavior is stationary, that is, until the sample semivariogram shows a distinct sill.

Second part.- The sample semivariogram of the residuals implies a correlation structure that is used to fit a new polynomial by generalized least squares. Equation (18) is used to compute new coefficients of the polynomial whose degree was chosen in the first part. A new semivariogram of the residuals is obtained, and the process is repeated until the residual semivariogram does not change significantly from one iteration to the next.

Kriging of Calera Basin Data

In this section, geostatistical methods are applied to transmissivities and water level data from Calera basin, Zacatecas, Mexico.

Transmissivity

Transmissivity measured from aquifer tests is available at 49 sites (figure 3.3). These points are not evenly distributed and scarce

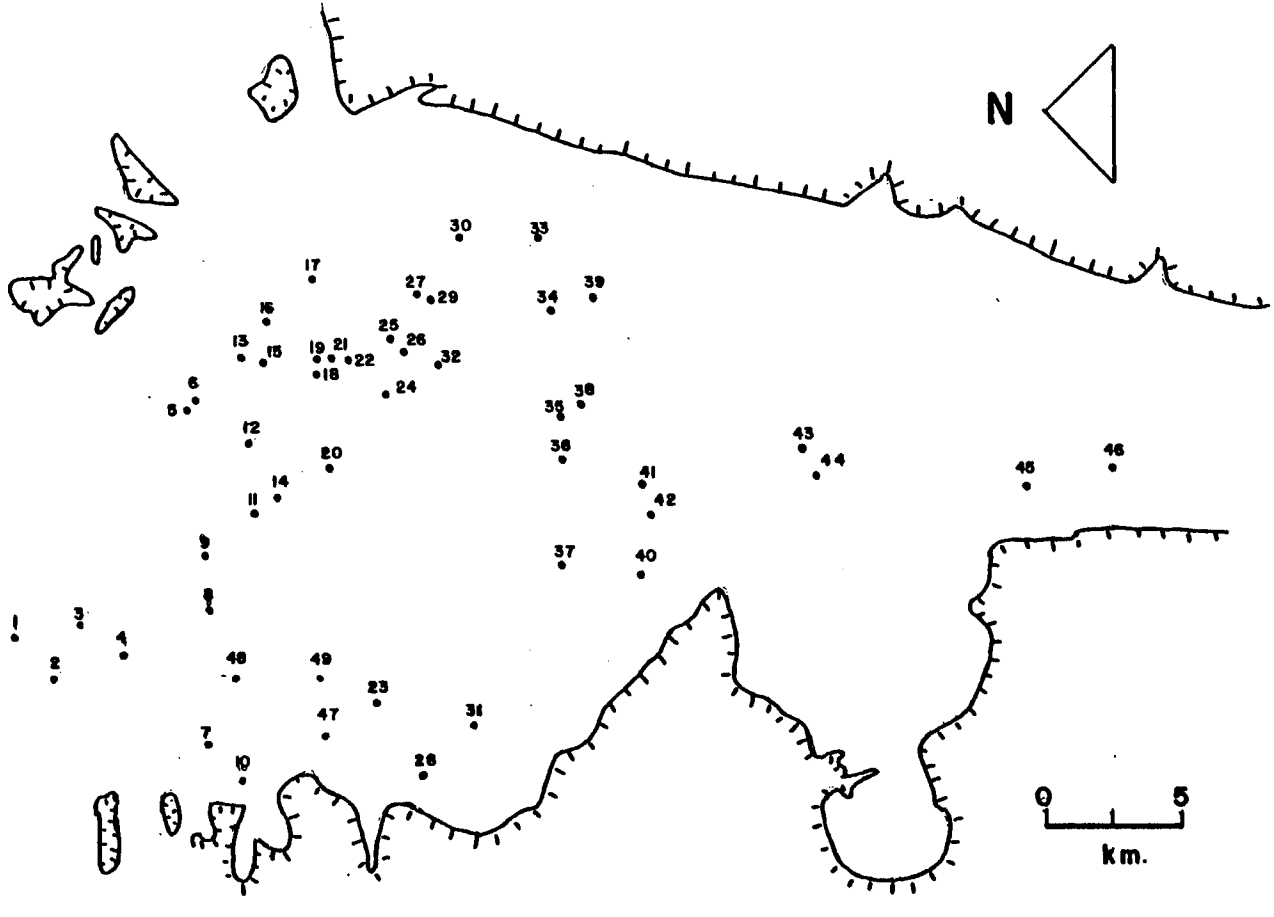

Figure 3.3 Location of transmissivity measurement sites in Calera basin.

in some areas. The data were reported by SARH (Secretaria de Agricultura y Recursos Hidraulicos).

Instead of working with Z = transmissivity, one generally uses their logarithm Z = log (transmissivity). Numerous studies have shown that transmissivities are lognormal distributed in an aquifer (Fennessy, 1982). Matheron has also shown that if Z is lognormal the semivariogram of log Z behaves better than the semivariogram of Z. As a check of log normality, frequency distribution plot was produced (figure 3.4). The Weibull plotting position was used,

$$p = \frac{d}{n + 1}$$

where:

d, the rank in ascending values, and

n, the number of data points plotted

The graph shows a fairly good fit of a lognormal distribution for the transmissivity data.

The sample semivariogram was obtained using eq. (9). Semivariograms calculated for different directions had insufficient number of pairs to reliably determine anisotropy (figure 3.5). Therefore, the assumption of isotropic semivariogram was the only choice. This average semivariogram for all 49 sites was calculated using the computer code Geos developed by Samper (1986). The trial and error cross-validation method presented in a previous section was used to fit a spherical model to the sample semivariogram (figure 3.6). The optimum estimates of the sill and the range of this spherical semivariogram

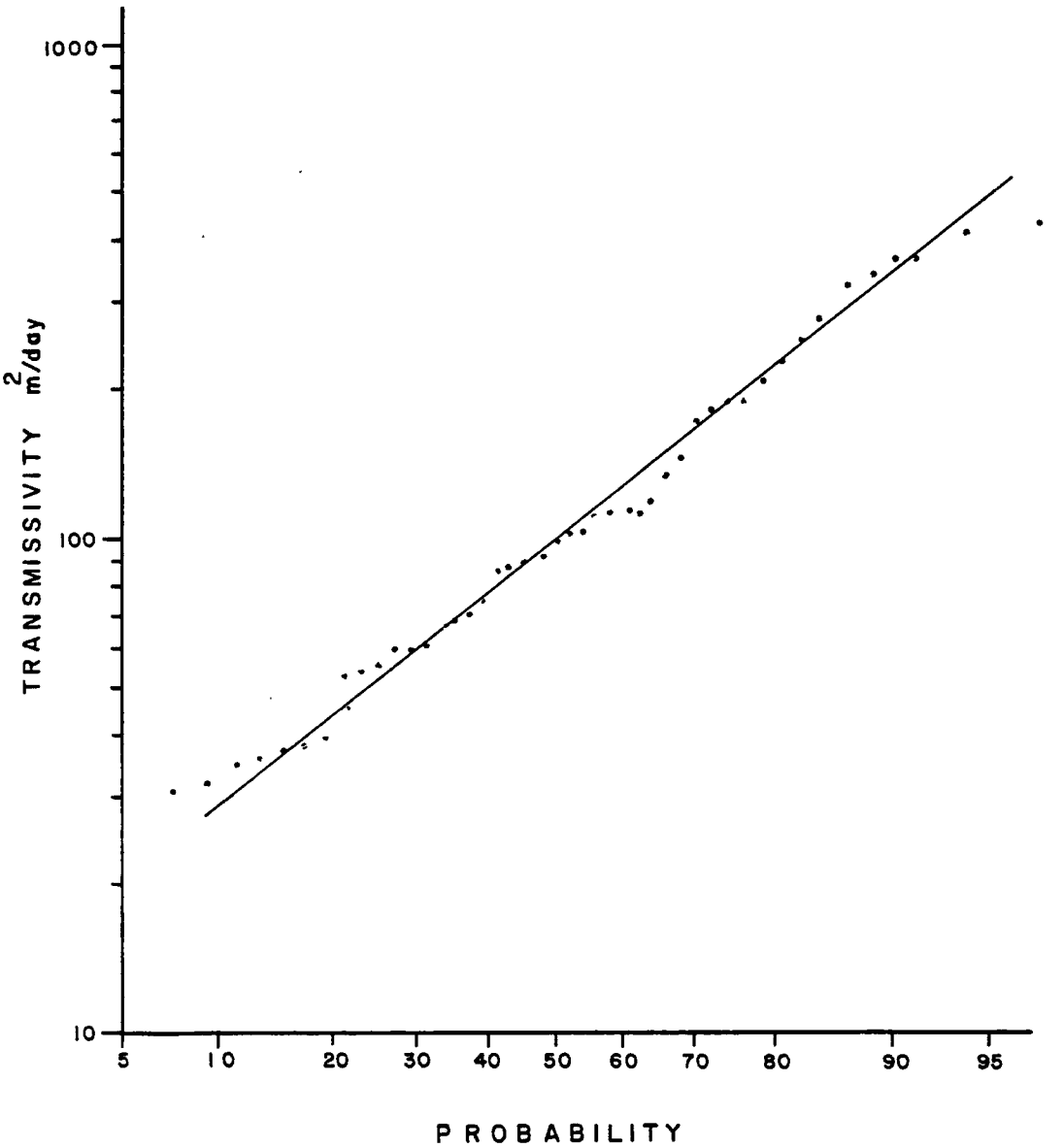

Figure 3.4 Frequency distribution plot to transmissivity data.

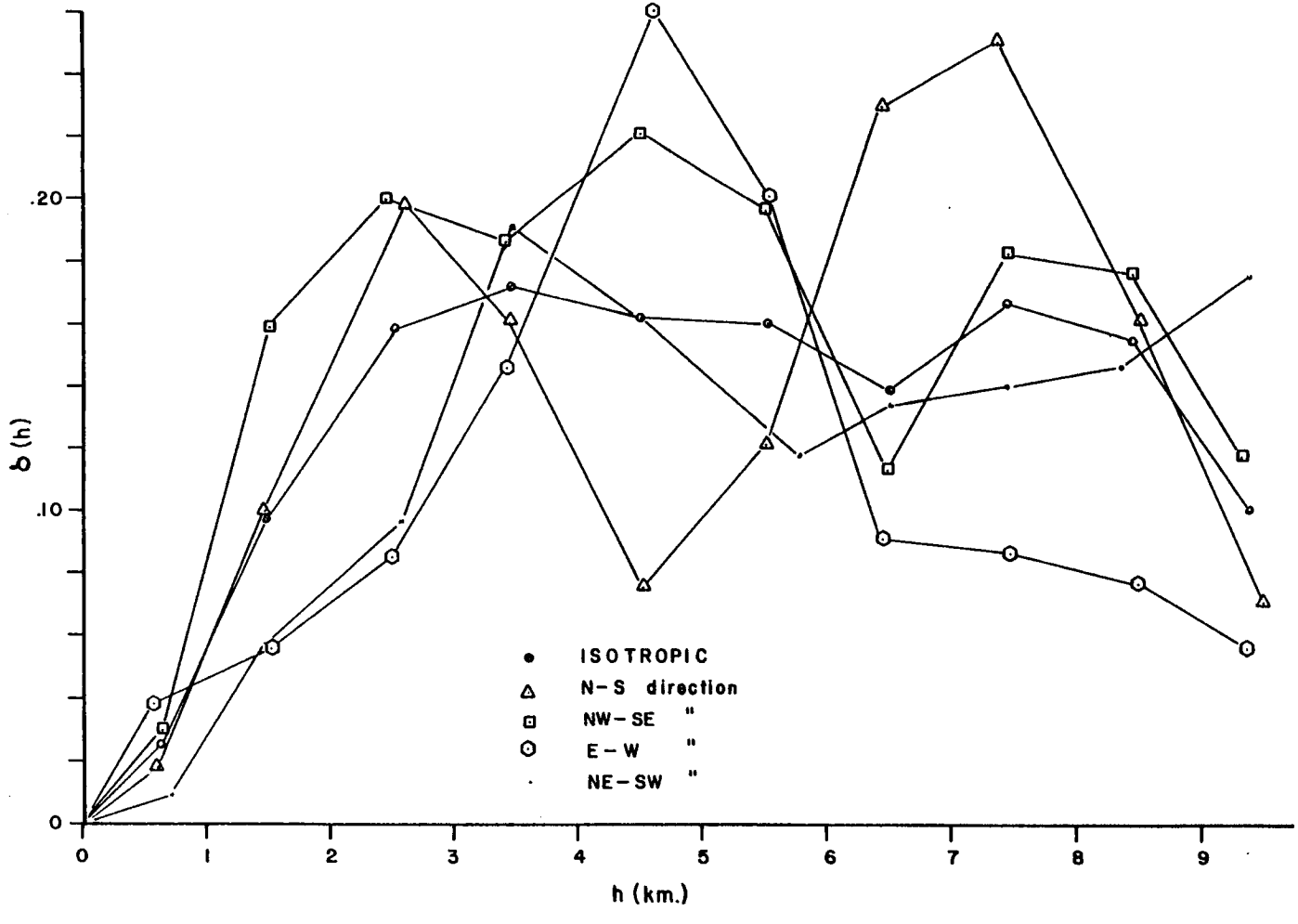

Figure 3.5 Directional sample semivariograms of log-transmissivity.

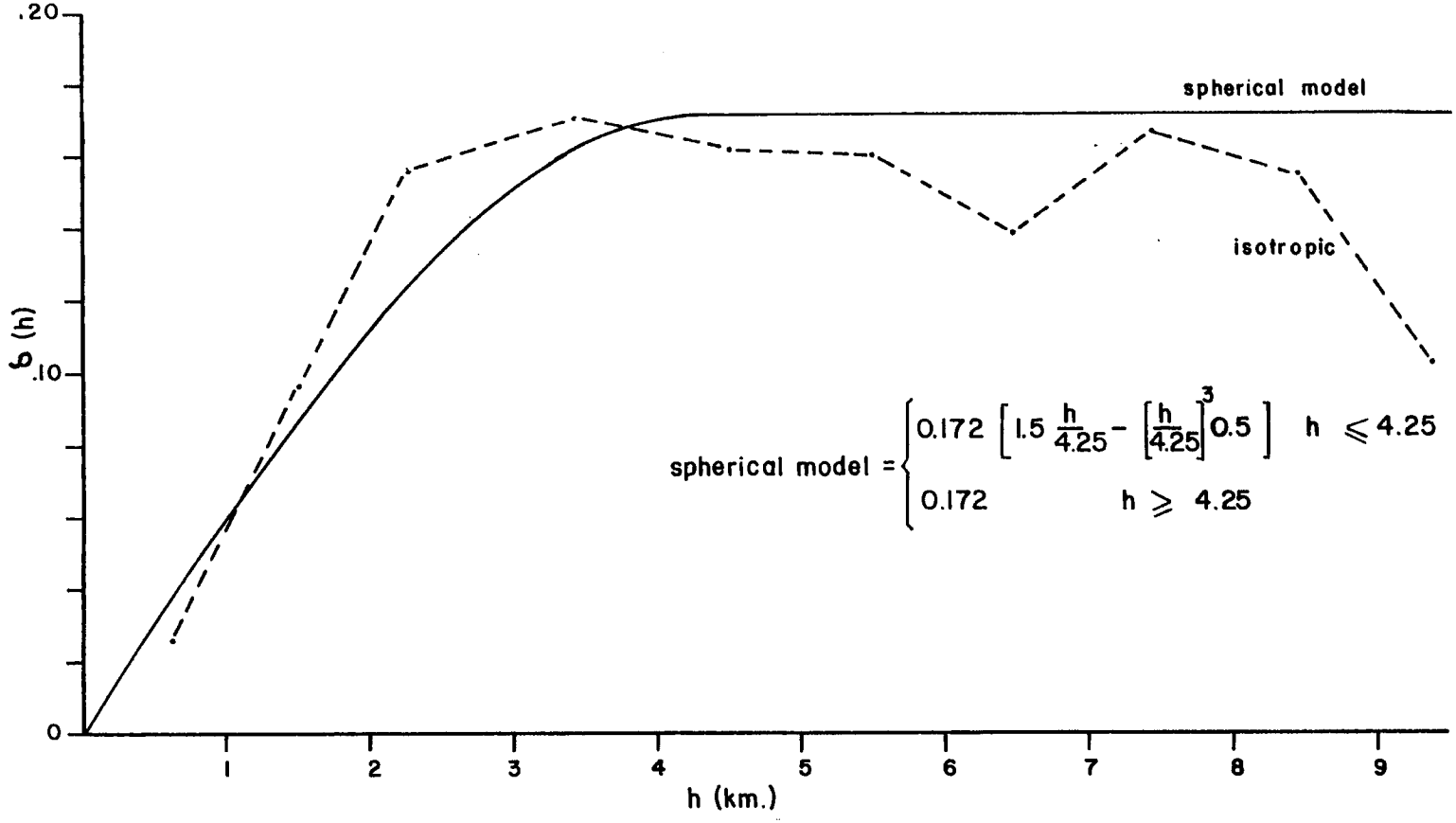

Figure 3.6 Sample semivariogram of log-transmissivity and fitted spherical model.

were found to be S= 0.1729 m^2 and a= 4250 m (13940 ft), respectively. The final results of the cross-validation for these values of the parameters are shown in table 3.1.

Table 3.1. Log-transmissivity validation test results.

a) mean difference between measured and kriged values

$$1/N \sum_{i=1}^{N} [(Z(\underline{x}_i) - Z^*(\underline{x}_i)] = -0.030$$

b) dimensionless mean square error

$$[1/N \sum_{i=1}^{N} (e_i^2/\sigma^2_{ki})]^{1/2} = 1.014$$

Clearly the mean square error is close to zero and the dimensionless error is close to 1. Notice that since no nugget effect is present, a relatively high correlation between transmissivity values at two close location is expected. On the other hand, the relatively small range value suggests that, although high, the correlation extends over a fairly small region.

If the fitted semivariogram is the true semivariogram of log-transmissivity for our field, then future measurements should be taken at distances not further than 4250 m (13940 ft).

Kriging average log-transmissivities were estimated at 84 zones. Figure 3.7 illustrates the zonation pattern of log-transmissivity in the Calera basin. Size and shape of zones depended

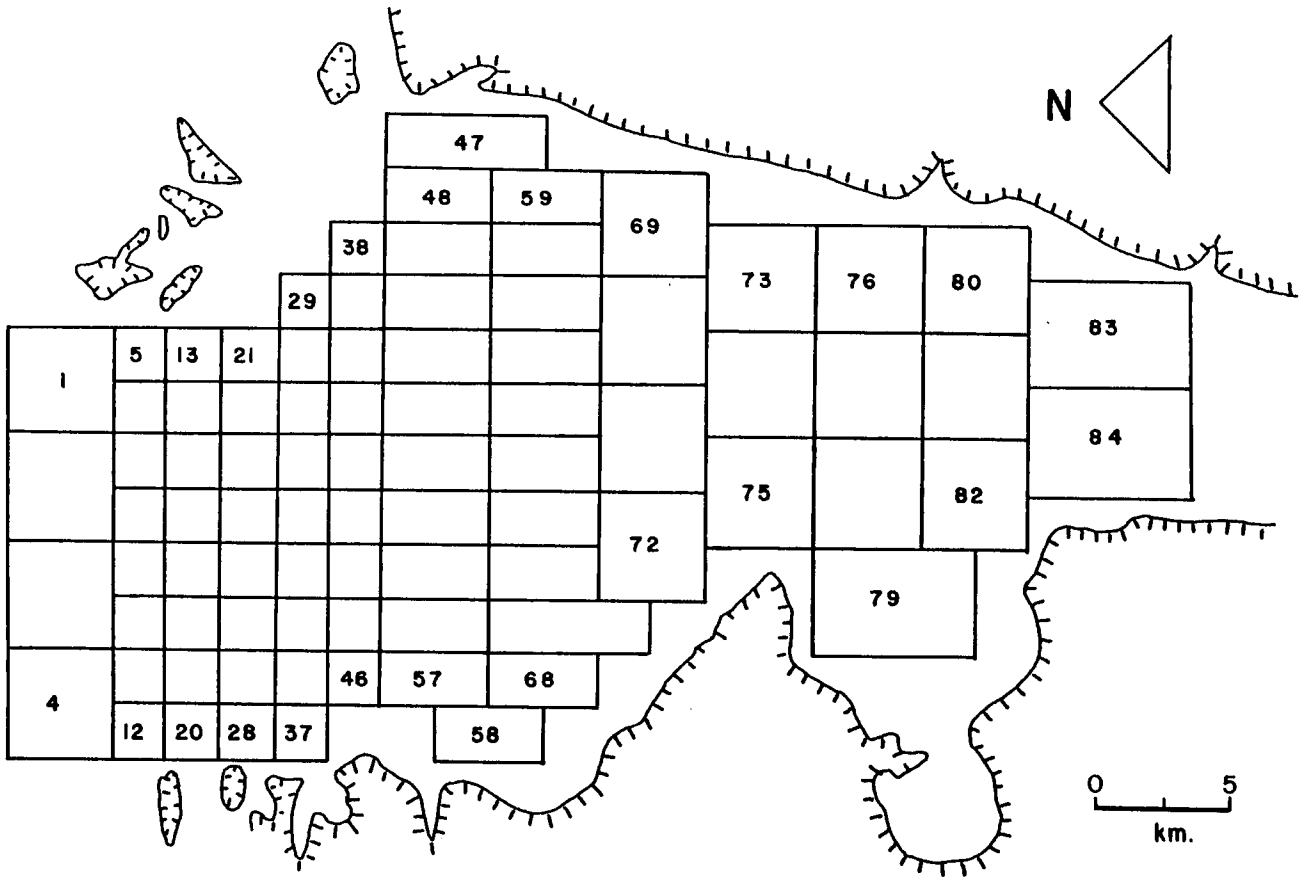

Figure 3.7 Zonation pattern for log-transmissivity in Calera basin.

on the distribution and variability of data. Larger zones were chozen in area where data were scarce and/or uniform in value. Kriged log-transmissivities and associated kriging errors are contoured in figures 3.8 and 3.9, respectively. It is important to point out that kriged log-transmissivities estimates are spatial averages over zones and may differ from point log-transmissivities as determined by aquifer tests. Regarding the spatial distribution of errors, it is apparent from the contour map that the largest values are found along the margins of the basin where data are scarce indicating that in these areas the reliability of the kriging estimates is fairly low.

Corresponding transmissivity estimates, T^*_n, were computed from kriged estimates Y^*_k, and kriging errors e_k, by the following equation (Hines and Montgomery, 1980; Clifton and Neuman, 1982; Fennessy, 1982).

$$T^*_n = EXP[2.303\ Y^*_k + 0.5(2.303\ e_k)^2] \text{ ----- } 22$$

Transmissivity estimates and estimation errors are listed in table 3.2. Transmissivity estimates are shown in figure 3.10. Kriged estimates in the northern and central areas of the basin agree with values that one may expect on the basis of geological considerations.
However, kriged estimates in the southeastern area are relatively low, the area consists of gravels and alluvium which are expected to have higher transmissivity than the estimated. Low kriging estimates in this area are due in part to the lack of sufficient data which translates in high errors of estimation and by the influence of the low transmissivities in the central region.

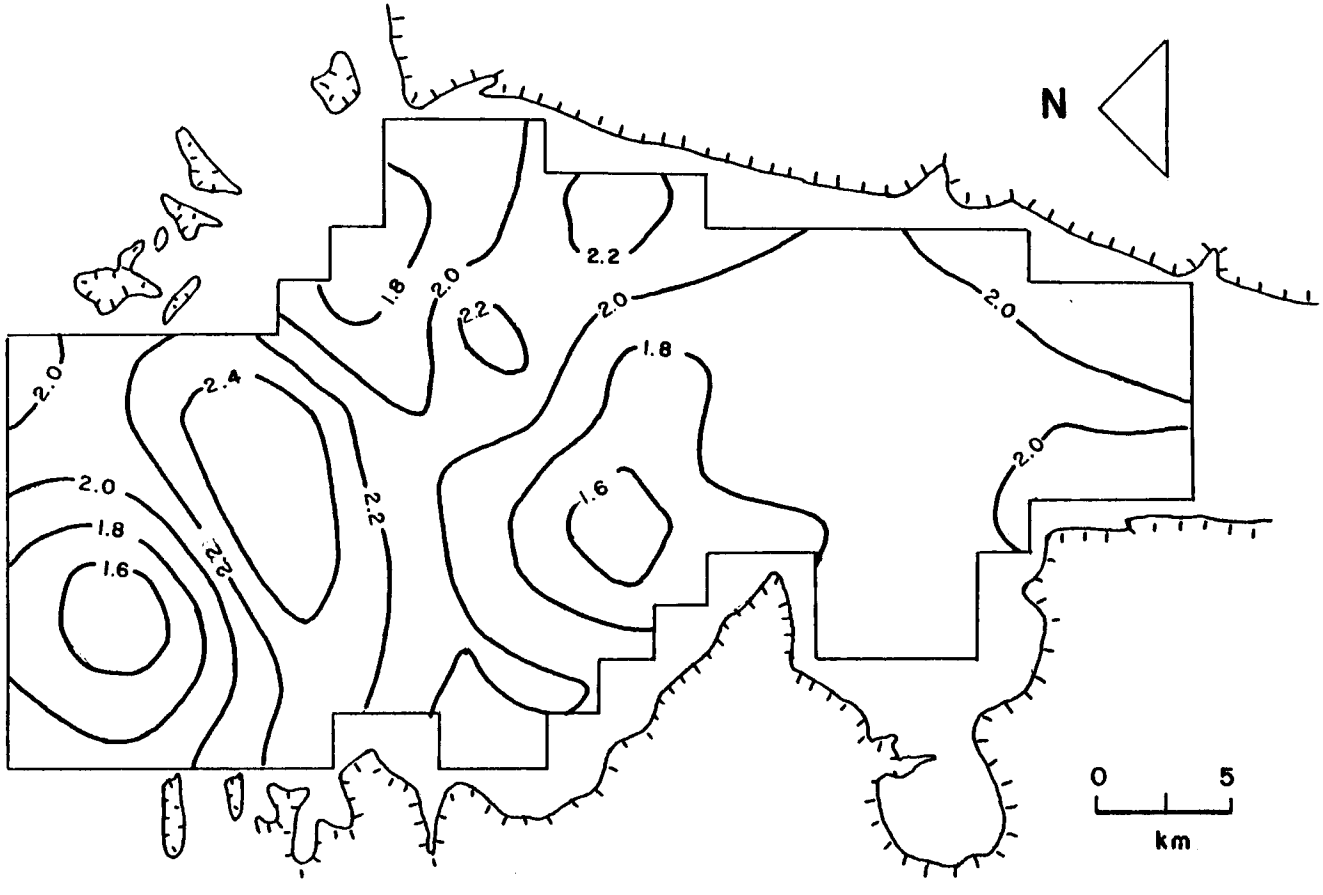

Figure 3.8 Contour map of kriged log-transmissivity.

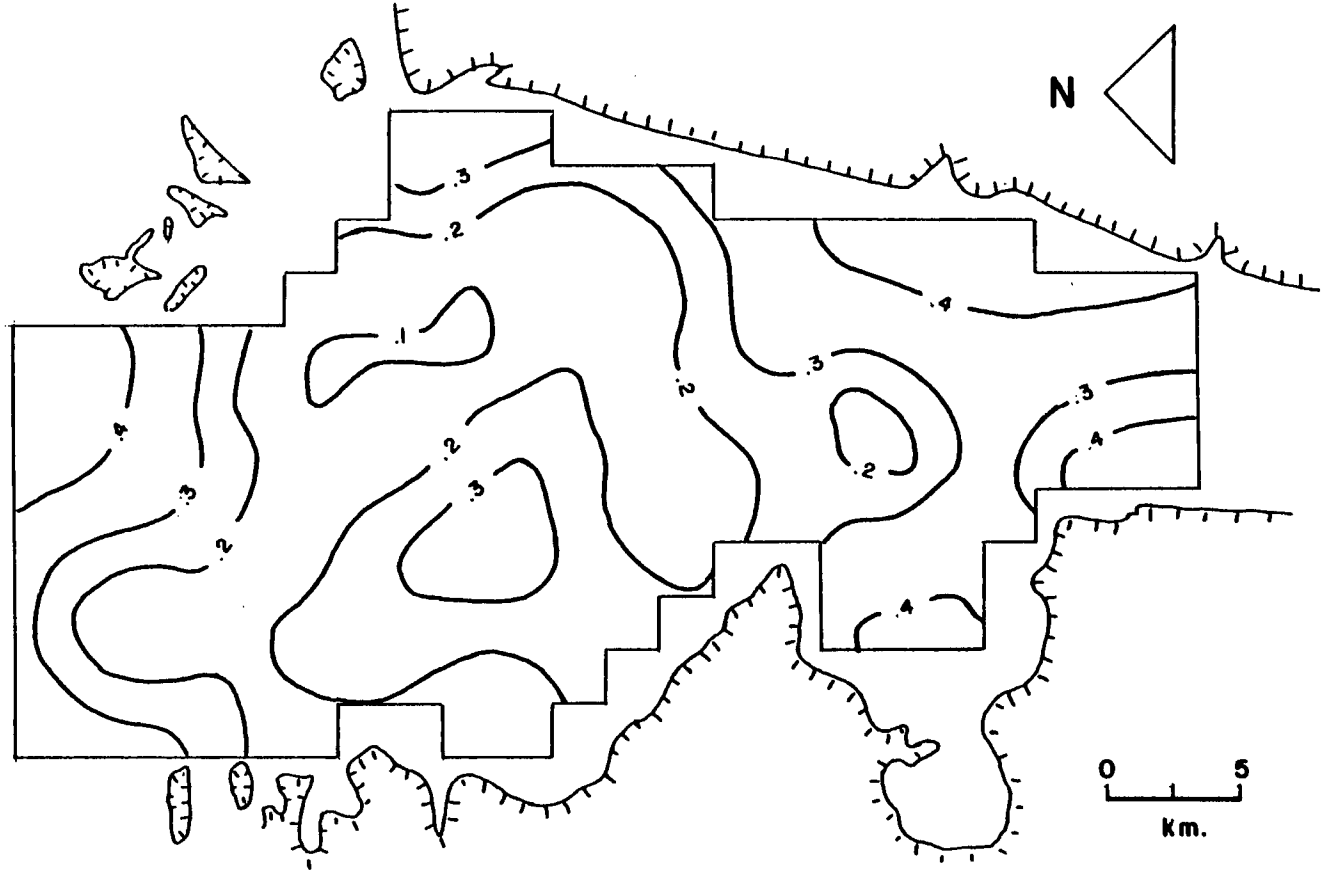

Figure 3.9 Contour map of log-transmissivity kriging errors.

TABLE 3.2

Kriged Transmissivities and Kriging Errors for Zones of Calera Basin.

Zone	Transmissivity m^2/day	Transmissivity ft^2/day	Kriging Errors
1	174.74	1880.89	0.43
2	129.93	1398.55	0.40
3	45.39	488.57	0.26
4	79.87	859.71	0.31
5	248.21	2671.71	0.39
6	284.97	3067.39	0.38
7	197.83	2129.42	0.37
8	100.98	1086.94	0.32
9	38.64	415.92	0.19
10	26.51	285.35	0.09
11	48.04	517.09	0.18
12	81.15	873.49	0.31
13	279.06	3003.77	0.30
14	368.04	3961.55	0.28
15	320.27	3447.36	0.30
16	202.63	2181.09	0.28
17	89.65	964.98	0.21
18	50.70	545.73	0.10
19	71.75	772.31	0.21
20	117.44	1264.11	0.28
21	255.20	2746.95	0.15
22	420.39	4525.04	0.13
23	476.27	5126.53	0.22
24	403.07	4338.60	0.15
25	263.52	2836.51	0.14
26	159.41	1715.88	0.19
27	137.38	1478.75	0.19
28	159.05	1712.00	0.17
29	75.45	812.14	0.15
30	138.08	1486.28	0.09
31	330.81	3560.81	0.09
32	359.78	3872.64	0.13
33	375.62	4043.14	0.11

Table 3.2 -- Continued

Zone	Transmissivity m^2/day	Transmissivity ft^2/day	Kriging Errors
34	355.53	3826.89	0.17
35	295.16	3177.08	0.24
36	220.62	2374.73	0.23
37	203.20	2187.23	0.12
38	50.10	539.27	0.16
39	49.92	537.33	0.10
40	90.44	973.49	0.09
41	153.52	1652.48	0.16
42	154.69	1665.07	0.09
43	219.43	2361.92	0.22
44	255.19	2746.84	0.29
45	245.66	2644.26	0.29
46	210.93	2270.43	0.27
47	117.96	1269.71	0.33
48	81.38	875.97	0.26
49	78.49	844.86	0.19
50	130.50	1404.69	0.12
51	110.42	1188.55	0.09
52	114.56	1233.11	0.15
53	112.76	1213.74	0.20
54	130.75	1407.38	0.30
55	146.85	1580.68	0.33
56	137.74	1482.62	0.24
57	109.29	1176.39	0.20
58	81.82	880.70	0.14
59	152.70	1643.65	0.19
60	141.10	1518.79	0.17
61	141.84	1526.75	0.15
62	135.13	1454.52	0.18
63	109.78	1181.66	0.23
64	71.27	767.14	0.27
65	57.19	615.58	0.30
66	67.39	725.38	0.31
67	96.51	1038.83	0.25
68	125.81	1354.20	0.20
69	184.17	1982.39	0.20
70	73.29	788.88	0.19

Table 3.2 -- Continued

Zone	Transmissivity m^2/day	Transmissivity ft^2/day	Kriging Errors
71	54.04	581.68	0.17
72	40.61	437.12	0.18
73	126.42	1360.77	0.35
74	85.58	921.17	0.29
75	72.69	782.43	0.22
76	126.88	1365.73	0.39
77	76.82	826.88	0.25
78	79.49	855.62	0.24
79	112.53	1211.26	0.39
80	157.58	1696.18	0.44
81	119.63	1287.89	0.31
82	125.90	1355.17	0.33
83	151.89	1634.93	0.37
84	115.31	1241.19	0.42

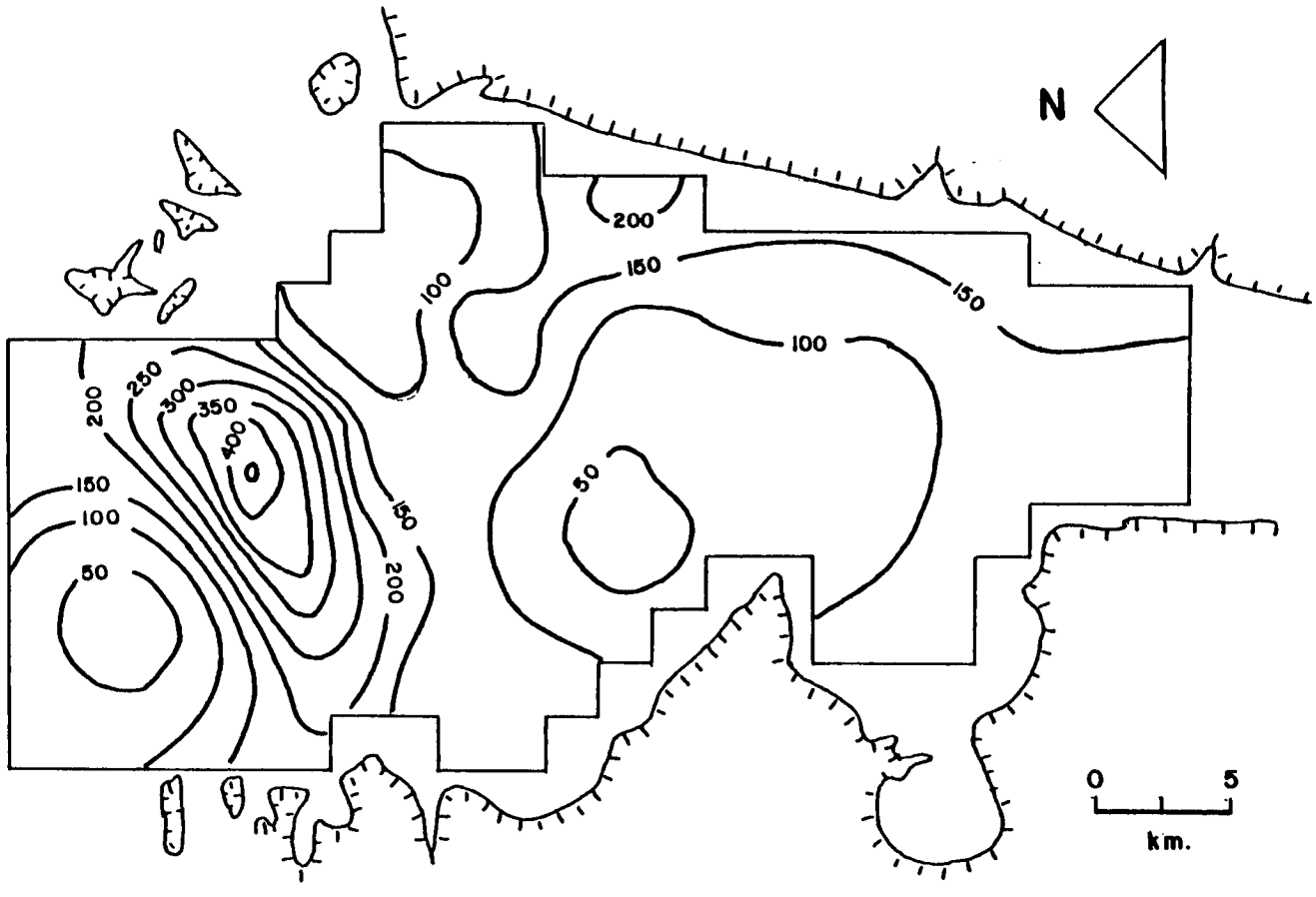

Figure 3.10 Contour map of transmissivity derived from kriged log-transmissivity.

Hydraulic Head

Water level measurements from 1956 and 1985 are available for 50 and 115 wells, respectively in the Calera basin. The data were provided by the federel agency SARH and are listed in appendix A. In order to have an idea about the distribution of the hydraulic head over the aquifer in 1956, figure 3.11 shows the location of measurement sites, and a hand contour map was drawn with the available data, (figure 3.12).

As previously stated, hydraulic head can not be treated as a stationary process because they are associated with a non constant drift. Therefore, in order to use the kriging equations, the drift must be removed first from the data. For that we use an iterative generalized least square method presented by Neuman, Jacobson and Fennesy (1983).

We started computing the 1956 average and directional sample semivariograms (figure 3.13). The directional semivariograms were obtained along the N-S, NW-SE, E-W and NE-SW directions; in this aquifer the hydraulic gradient goes from south to north. The sample semivariogram along this direction shows a rapid increase with distance indicating clearly that a drift in this direction is present in the data. The semivariogram along the perpendicular direction (E-W), however, remains constant for all distances.

As suggested by Fennessy (1982) residual kriging was carried out in two steps. In the first one, one estimates the order of the polynomial drift $m(\underline{x})$. In the second step, the estimation of the drift

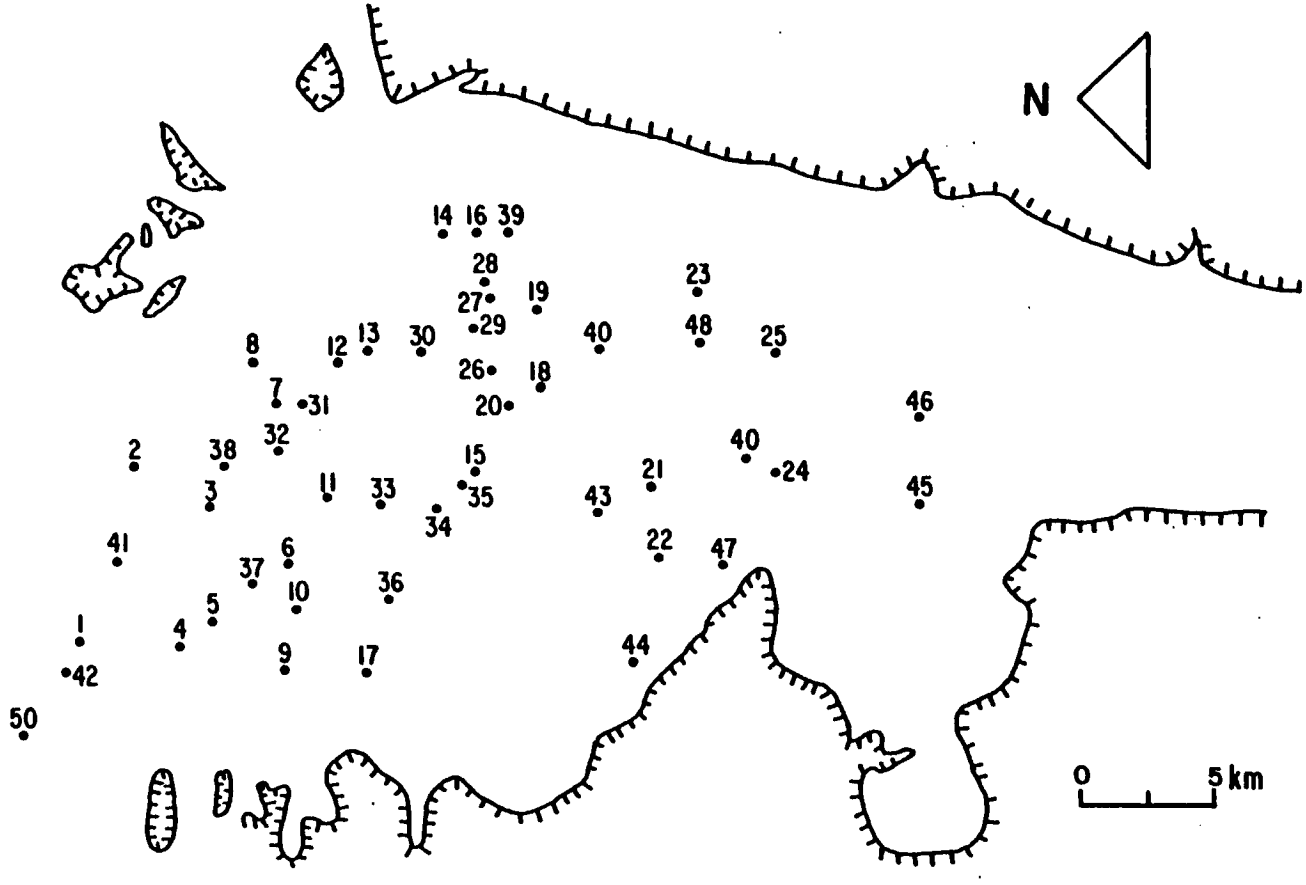

Figure 3.11 Location of 1956 water level measurement sites in Calera basin.

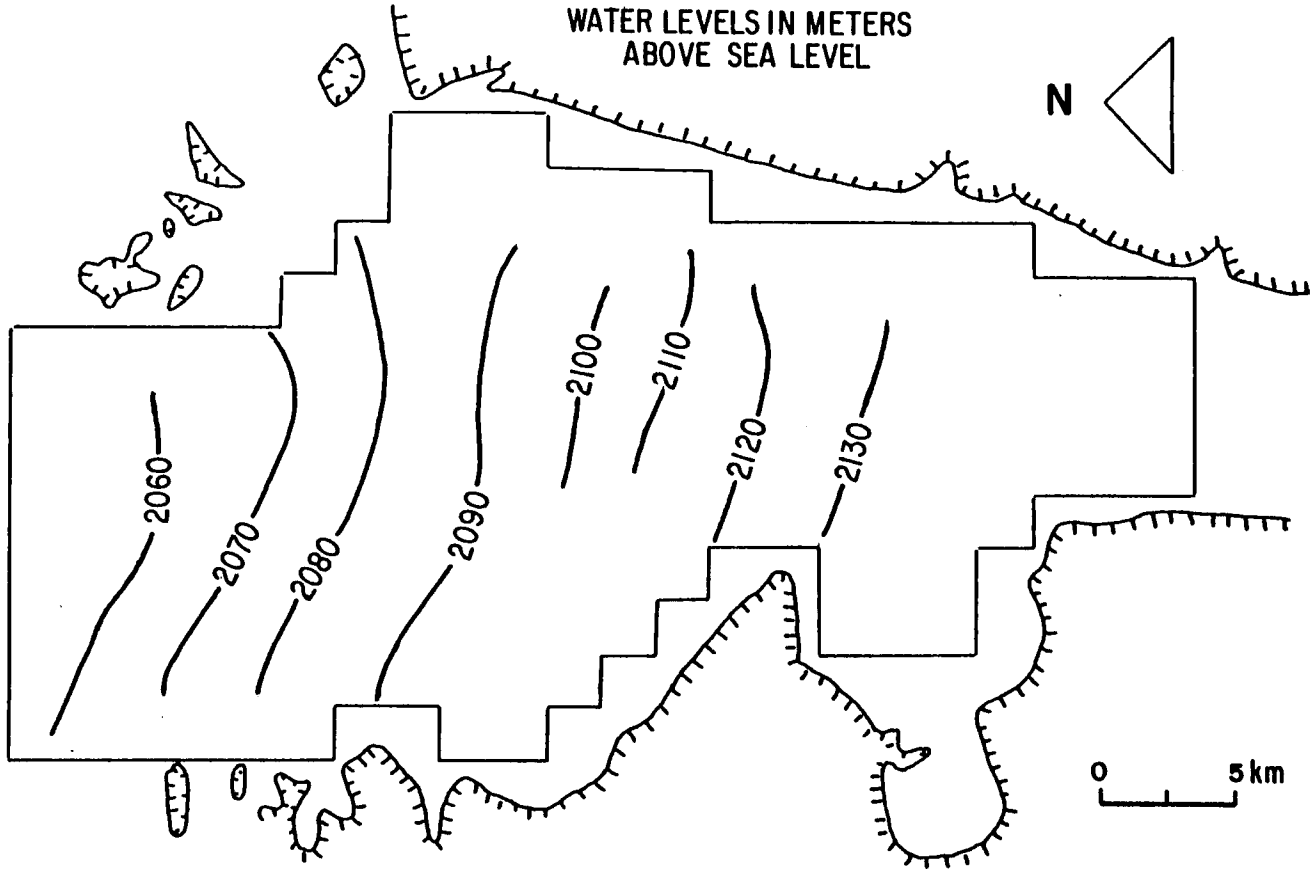

Figure 3.12 Hand drawn contour map of 1956 water levels in Calera basin.

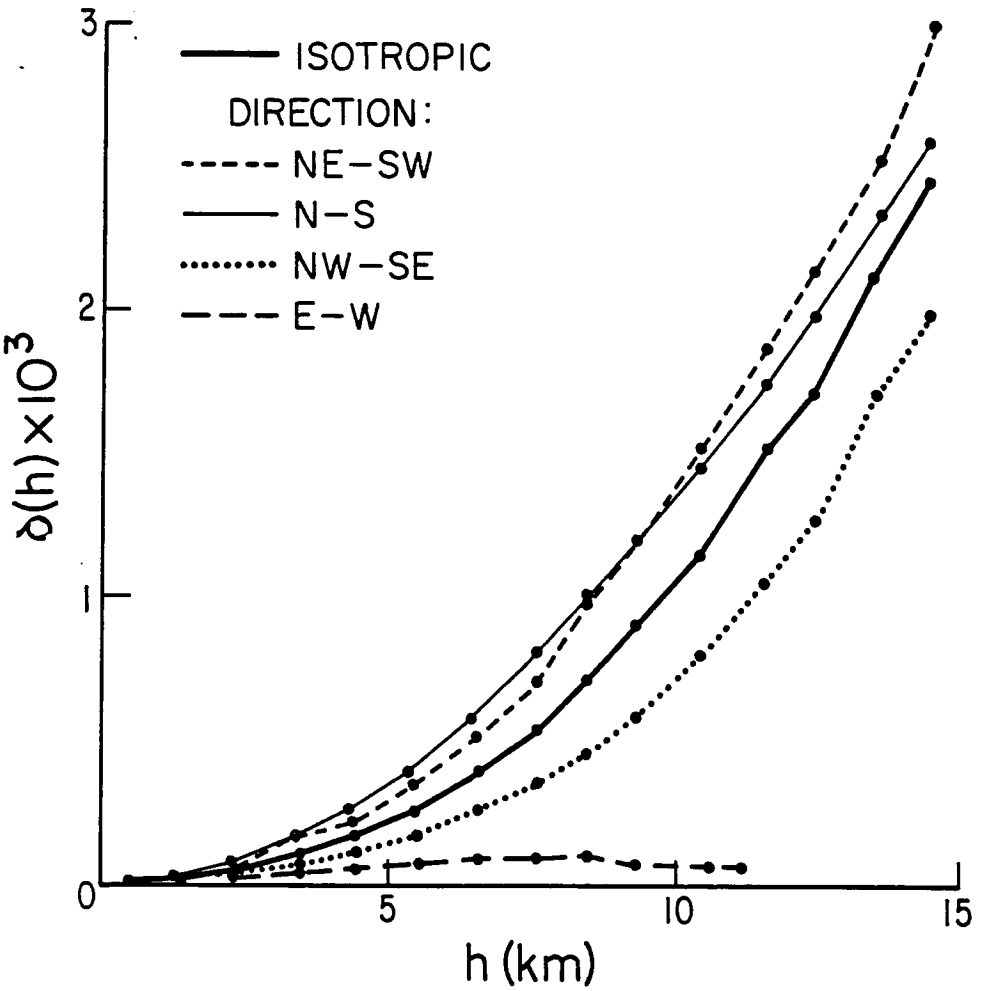

Figure 3.13 Directional and isotropic semivariograms of 1956 water levels in Calera basin.

and the semivariogram of the residuals is refined by accounting for the correlation among the residuals.

Step one.- Ordinary least squares was used to fit successively higher order polynomial trends to the water level data until the sample semivariogram of the residuals showed a distinct sill. As the degree of the polynomial was increased, the sill of the average sample semivariogram decreased and approached a constant value. In our case, a first order polynomial produced a residual semivariogram with distinct sill (figure 3.14). Attempts to fit higher order polynomials resulted in poorer estimates and did not lead to satisfactory results. Hence, the first order polynomial was chosen to represent the drift.

Step two.- The semivariogram obtained from the ordinary least squares procedure was used to start the first iteration of the generalized least squares method. New residuals were calculated and a new residual semivariogram was obtained. This residual semivariogram produced information for the next iteration. The process was repeated until the semivariograms computed at two consecutive iterations were essentially identical. In our case, three iterations were required to achieve the convergence of the sample semivariogram of the residuals. Figure 3.15 shows the sample semivariogram of the residuals at each of the three iterations.

The fitted drift was a first order polynomial of the form

$$m(\underline{x}) = a_0 + a_1 x + a_2 y$$

where x and y are components of $\underline{x}$ in two dimensions. The coefficients

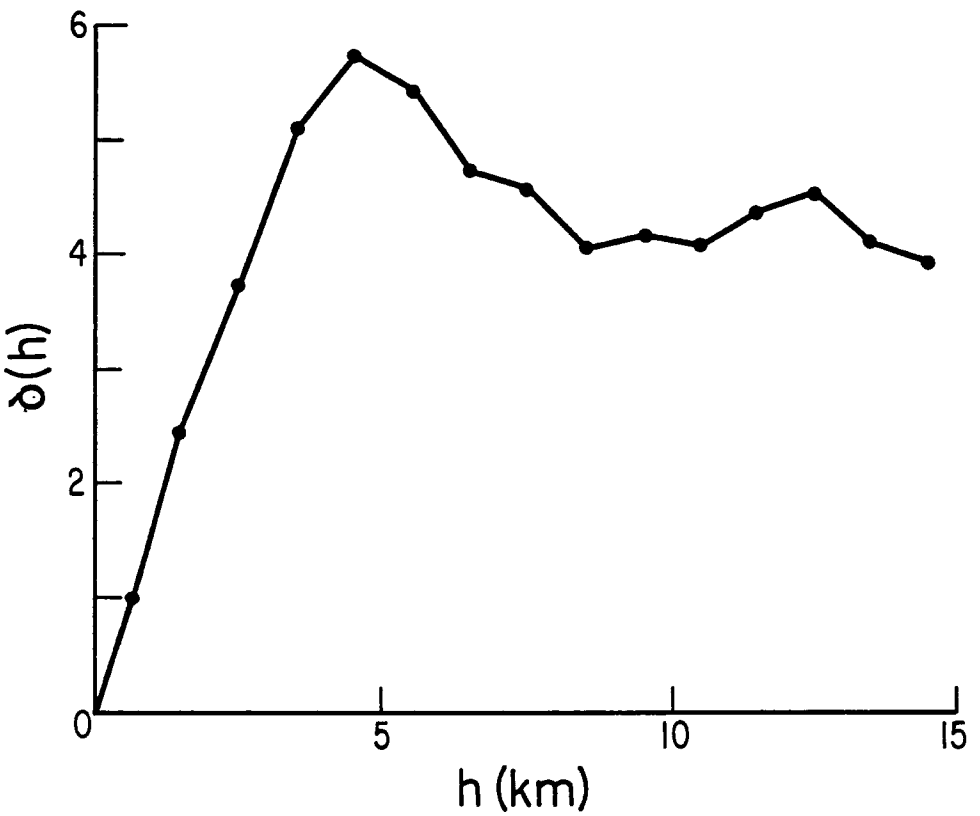

Figure 3.14 Sample semivariogram of residual hydraulic heads in Calera basin based on linear drift determined by ordinary least squares.

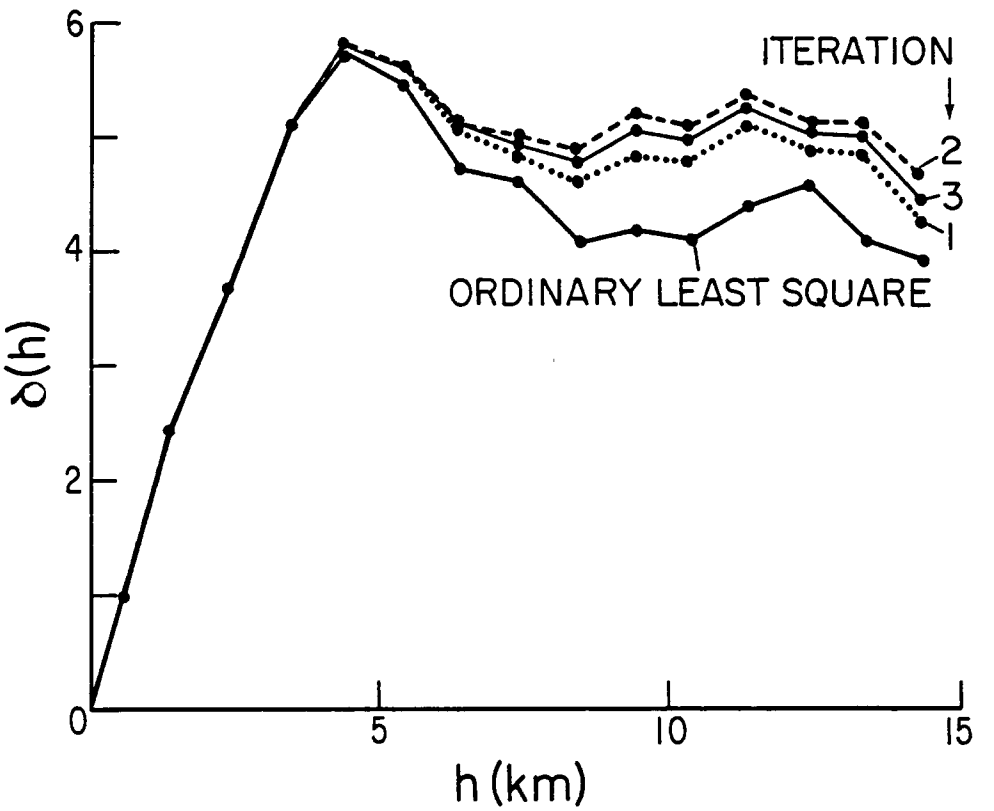

Figure 3.15 Sample semivariograms of residual hydraulic heads in Calera basin based on linear drift determined by generalized least squares.

a_0, a_1, a_2 were determined to take on values a_0 = 2052.10; a_1 = 5.30; a_2 = -1.18. The corresponding final residual semivariogram and fitted spherical model are shown in figure 3.16. The model was validated as in the case of log-transmissivity by deleting each data point and kriging that value using the remaining data points. The results of the validation test are presented in table 3.3. Once the drift and the semivariogram of the residuals were estimated, residual kriging was used to obtain hydraulic head estimates at the center of each cell of the grid shown in figure 3.17. Residual kriging was performed using the computer code Geos (Samper,1986).

The kriged hydraulic heads and kriging estimation errors are listed in table 3.4, and contoured in figures 3.18 and 3.19, respectively. Kriging estimates tend to give smoother contour maps than those obtained using hydrogeological information. This is true because hydrogeological factors such as mountain front recharge are not considered in the kriging method. In general, hydraulic head estimates agree with the hand contoured map, although, estimates at the central and western region were expected to be parallel to the no flow boundary. It should be noted that as in the case of log-transmissivity the areas where the performance is poorest correspond to areas of highest kriging errors.

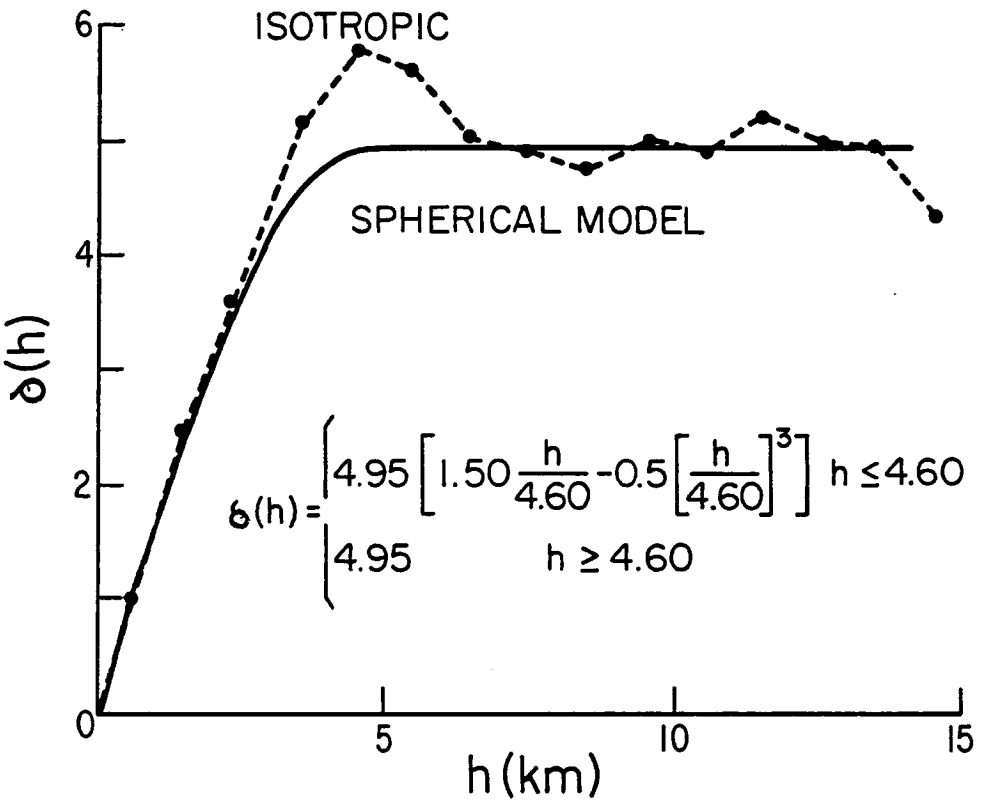

Figure 3.16 Final sample semivariogram of residual hydraulic heads and fitted spherical model.

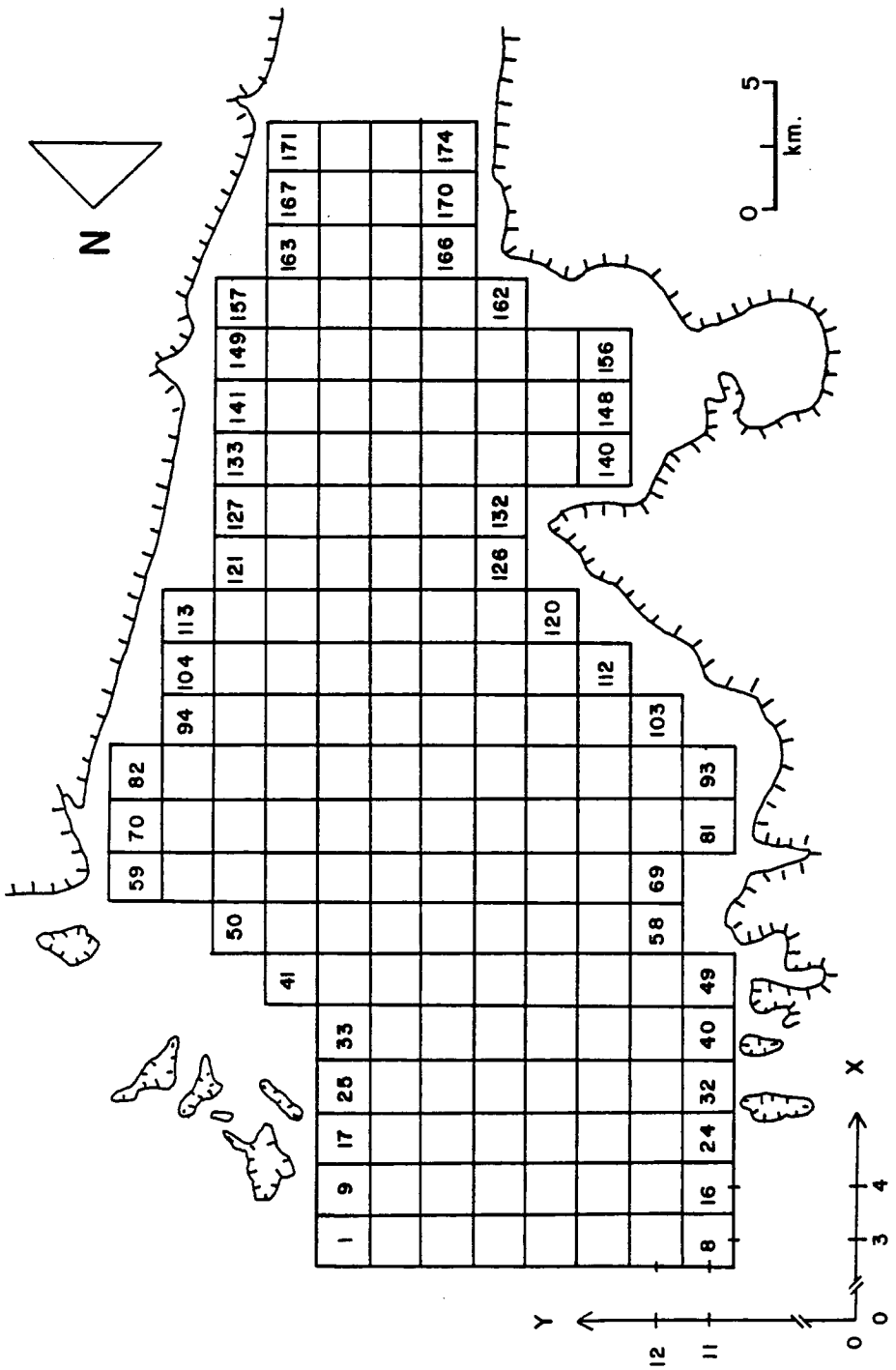

Figure 3.17 Zonation pattern for hydraulic head in Calera basin.

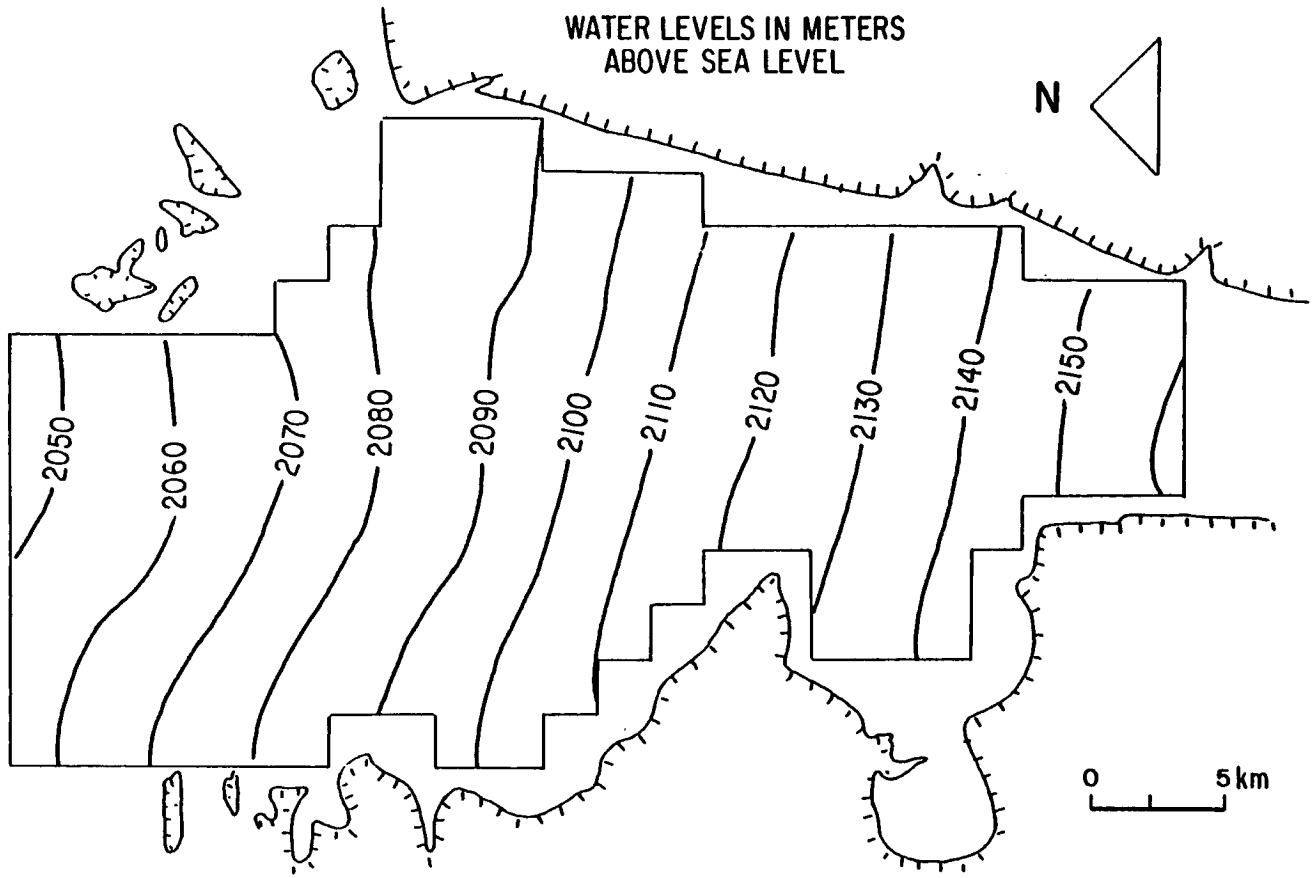

Figure 3.18 Contour map of 1956 kriged hydraulic head estimates based on results of generalized least squares.

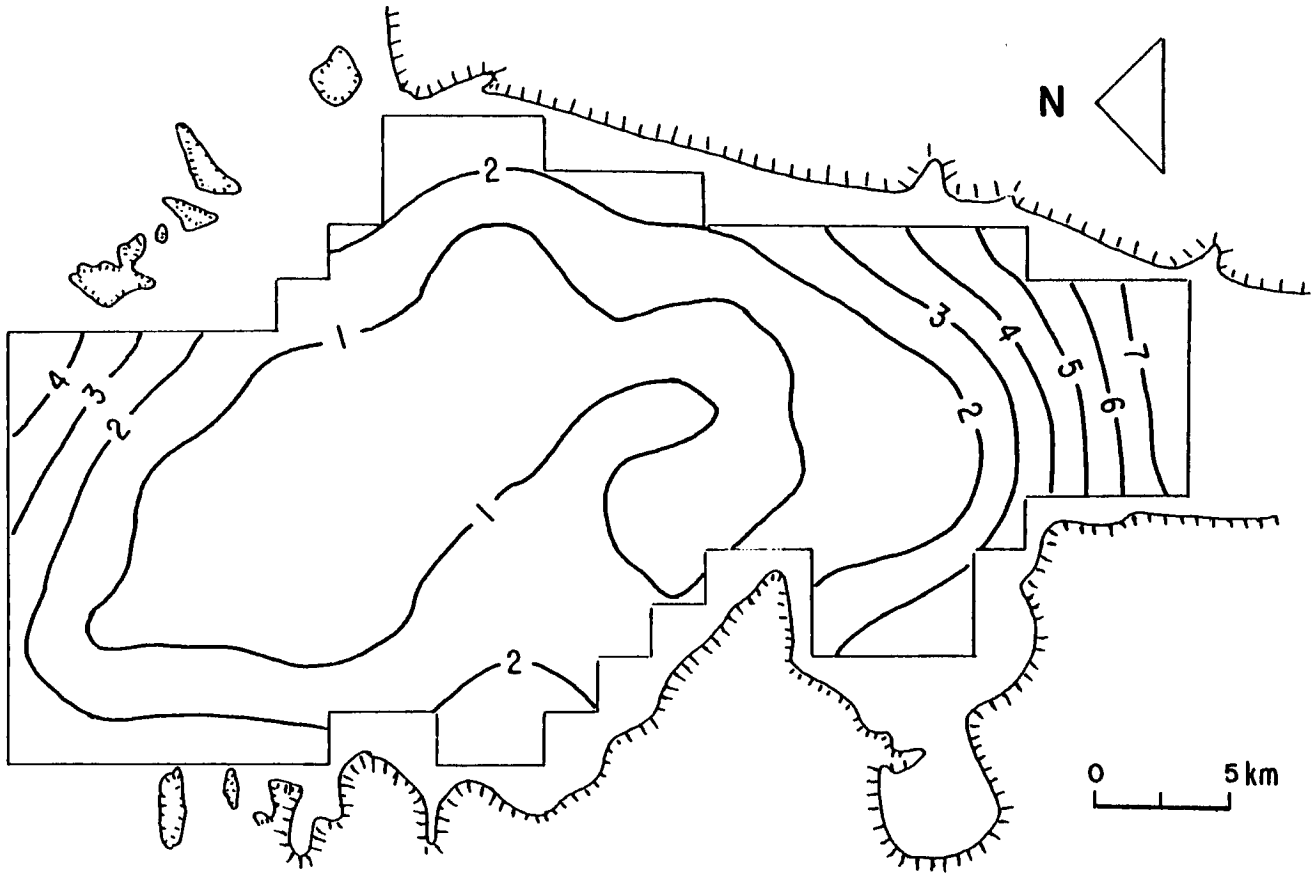

Figure 3.19 Contour map of 1956 hydraulic head kriging errors based on results of generalized least squares.

Table 3.3.- Hydraulic Head validation test results (1956).

a) mean difference between measured and kriged values

$$1/N \sum_{i=1}^{N} [Z(\underline{x}_i) - Z^*(\underline{x}i)] = 0.083$$

b) dimensionless mean square error

$$[1/N \sum_{i=1}^{N} (e_i^2/\sigma^2_{ki})]^{1/2} = 0.939$$

Maximum Likelihood Cross Validation Method

As indicated before the iterative generalized least squares method ends its iterative process when the sample residual semivariogram appears to have converged to a stable shape. However, when data are limited, the sample semivariogram may lead to suboptimal estimates because of its poor statistical behavior. In other words, convergence of the sample semivariogram does not necessarily means convergence to the true semivariogram. Samper (1986) has proposed a maximum likelihood cross-validation method to estimate the optimum parameters P_j^* of the semivariogram of the residuals. The philosophy of the method consists of minimizing the function:

$$S = N \ln 2\pi + \sum_{i=1}^{N} \ln\sigma^2_{ki} + \sum_{i=1}^{N} \left(\frac{e_i^2}{\sigma^2_{ki}}\right) \quad \text{-----(23)}$$

where:

N, is the number of pairs at which cross-validation is performed.

e_i, difference between observed $Z(\underline{x}_i)$ and kriged values $Z^*(\underline{x}_i)$

σ_{ki}, kriging variance of the error e_i

S, negative log likelihood function

Actually, the method proposed by Samper is a modification of the iterative generalized least squares method (Neuman, Jacobson and Fennessy, 1983). Samper proposed that instead of using the sample semivariogram as the criterion for convergence one should validate the semivariogram of the residuals by minimizing S in equation 23 at each iteration. The optimum parameters obtained at the end of an iteration are used as an input for the next iteration. The method converges when the optimum parameters at two consecutive iterations are essentially identical. The method can better be seen in the following chart.

Identification of drift.
Computation of the sample
semivariograms of the residuals
obtained with ordinary least square.

Switch to generalized least squares.

Select a type of semivariogram model
and assign preliminary values to its
parameters P_{j0} (sill,range,nugget).

Starting with P_{j0} values, find the
optimum parameters P^*_{j1} by
minimizing S.

Use P^*_{j1} values for the next iteration
and find the optimum parameter P^*_{j2} by
minimizing S.

Compare P^*_{j1} and P^*_{j2}.
If $P^*_{j1} - P^*_{j2} < \varepsilon$ for all j

Stop the iterative process
otherwise perform another iteration.
Where ε is a given prescribed positive tolerance.

In our case, the process required four iterations to obtain the optimum parameters. Figure 3.20 shows the sample semivariograms of the residuals at each of the four iterations. The final semivariogram of the residuals obtained with the maximum likelihood cross-validation method is depicted in figure 3.21. It is clear that the resulting optimum semivariogram $\delta(P^*_{jn},h)$ is far apart from the sample semivariogram $\delta^*(h)$ obtained by performing ordinary least squares. The coefficients of the drift in this case were found to be

$$a_0 = 2057.49 \; ; \; a_1 = 5.24 \; ; \; a_2 = -1.42$$

The cross-validation results for the final parameters of the semivariogram of the residuals are presented in table 3.5.

Having estimated both the optimal residual semivariogram and the drift, the next step was to obtain the kriging estimates. The resulting water level estimates and its associated kriging errors are listed in table 3.4 and shown in figures 3.22 and 3.23, respectively.

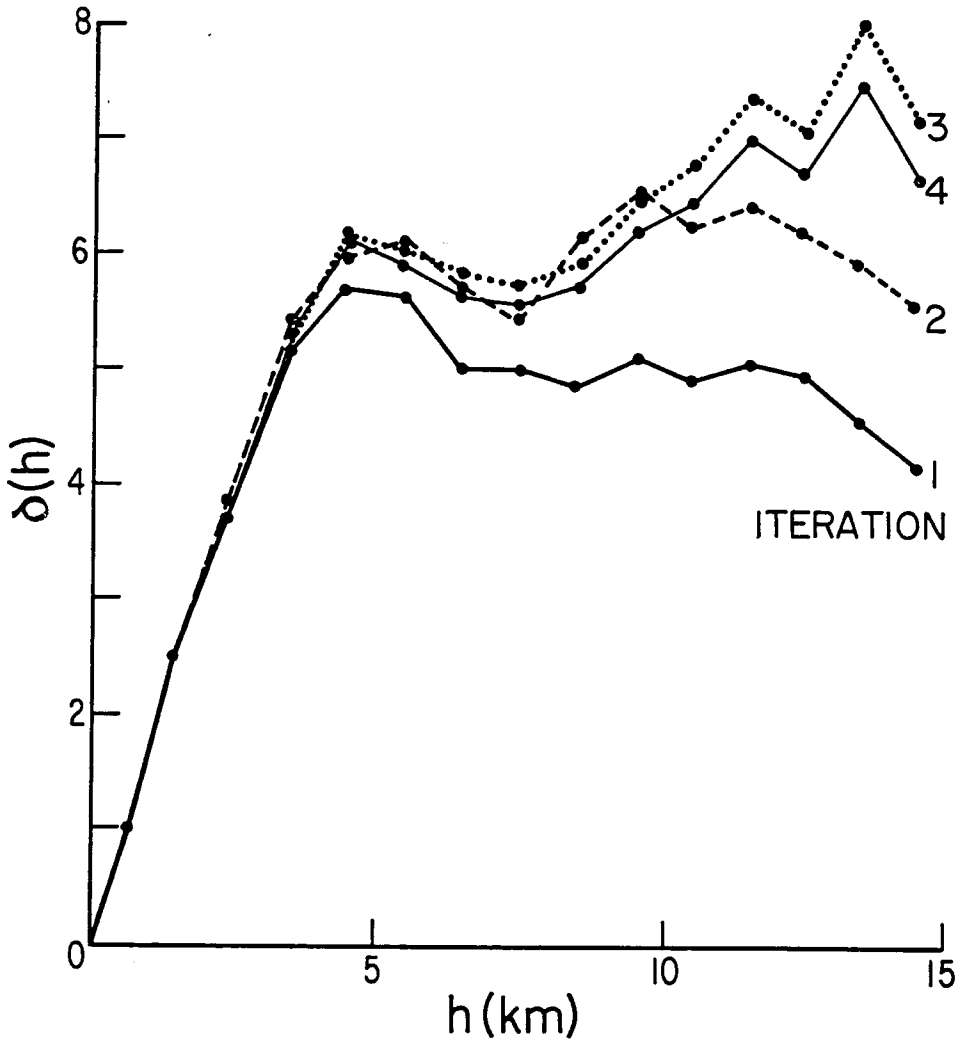

Figure 3.20 Sample semivariograms of residual hydraulic heads in Calera basin based on linear drift determined by maximum likelihood cross-validation.

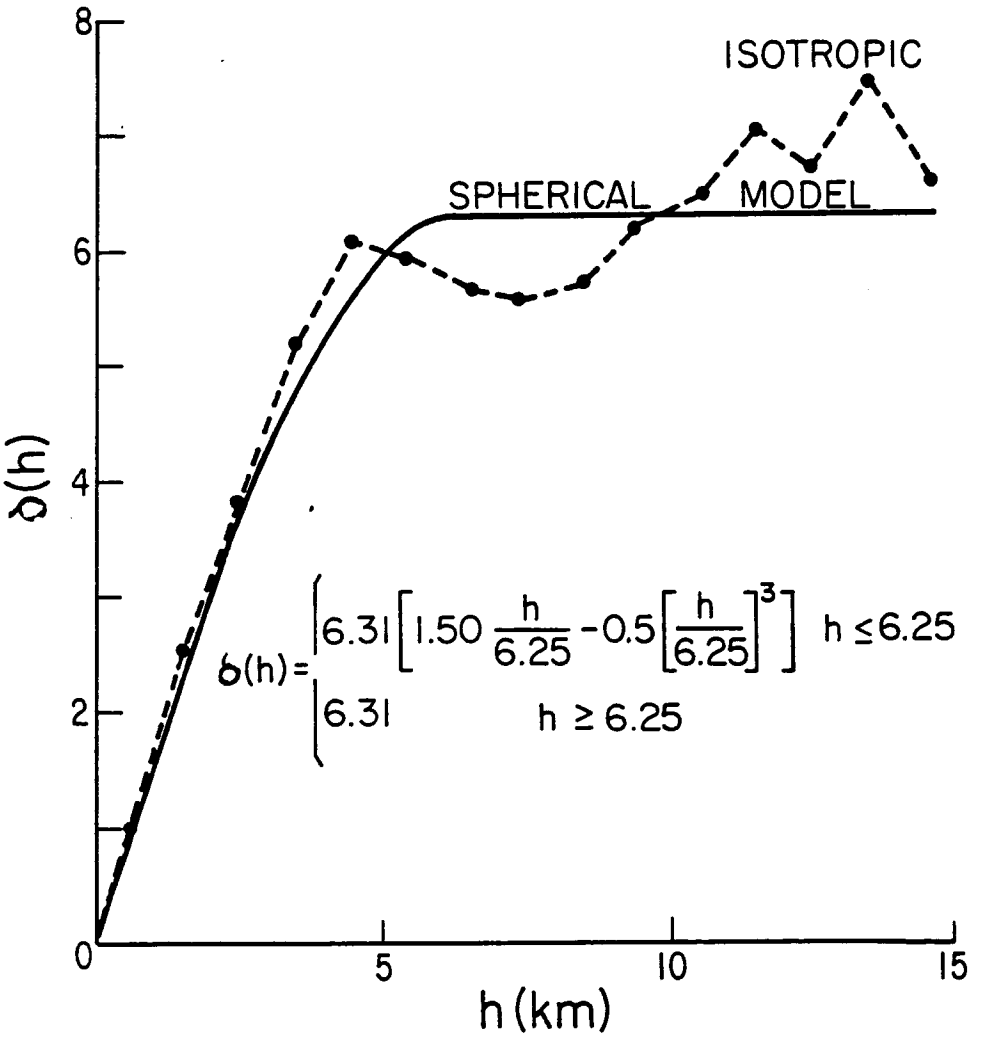

Figure 3.21 Final sample semivariogram of residual hydraulic heads and fitted spherical model.

TABLE 3.4

Kriged Hydraulic Head Estimates and Kriging Errors obtained by the GLS and ML Methods for Nodes of the Calera Basin in 1956 and 1985. Data are given in meters.

Cell	Kriged Hydraulic Head			Kriging Errors		
	1956		1985	1956		1985
	GLS	ML	ML	GLS	ML	ML
1	2047.12	2047.41	2053.35	4.85	4.65	3.32
2	2048.11	2048.06	2053.15	3.94	3.70	3.09
3	2048.47	2048.70	2052.65	3.23	2.96	2.52
4	2049.90	2049.95	2053.41	2.72	2.50	2.37
5	2051.83	2052.03	2054.34	2.26	1.98	2.07
6	2054.54	2054.62	2056.87	1.87	1.62	1.73
7	2056.30	2057.03	2059.45	2.01	1.90	1.86
8	2057.77	2058.84	2063.73	3.02	3.12	2.21
9	2052.99	2052.99	2051.92	3.67	3.67	2.64
10	2052.90	2052.96	2047.35	2.65	2.36	2.09
11	2053.11	2053.18	2042.32	1.94	1.68	1.92
12	2053.99	2053.99	2045.61	1.58	1.58	1.58
13	2056.29	2056.34	2034.50	1.23	0.99	1.34
14	2059.91	2059.89	2039.94	0.82	0.59	1.31
15	2062.99	2062.99	2062.84	1.07	1.07	1.49
16	2063.85	2064.55	2061.51	2.35	2.21	1.97
17	2058.08	2058.04	2055.70	2.77	2.55	2.04
18	2057.67	2057.66	2042.88	1.67	1.40	1.54
19	2057.28	2057.28	2038.45	0.96	0.72	1.17
20	2057.99	2057.99	2035.92	0.92	0.92	1.08
21	2059.34	2059.35	2029.76	0.84	0.75	0.91
22	2065.03	2065.02	2032.75	0.91	0.79	1.03
23	2067.99	2067.99	2055.53	1.32	1.32	1.19
24	2069.36	2069.87	2065.72	2.33	2.09	1.83
25	2062.90	2062.84	2055.21	1.81	1.59	1.45
26	2062.33	2062.34	2046.52	1.19	1.10	1.08
27	2060.99	2060.99	2035.04	0.78	0.78	0.94
28	2061.95	2061.95	2034.27	0.86	0.71	0.89
29	2064.99	2064.99	2038.40	0.88	0.88	0.82
30	2068.99	2069.00	2036.41	0.75	0.75	0.96

Table 3.4 -- Continued

Cell	Kriged Hydraulic Head 1956		1985	Kriging Errors 1956		1985
	GLS	ML	ML	GLS	ML	ML
31	2072.46	2072.53	2061.69	1.40	1.19	1.08
32	2074.52	2074.94	2070.57	2.36	2.08	1.98
33	2067.07	2067.10	2051.91	1.03	0.81	1.28
34	2065.99	2066.00	2045.17	0.82	0.82	0.99
35	2066.56	2066.61	2041.79	0.71	0.55	0.73
36	2067.99	2067.99	2042.53	0.83	0.83	0.78
37	2070.63	2070.63	2047.08	0.68	0.59	0.80
38	2074.60	2074.58	2058.71	0.78	0.57	0.95
39	2077.99	2078.00	2068.92	1.30	1.30	1.00
40	2079.71	2080.07	2073.46	2.32	2.11	2.06
41	2072.99	2072.99	2057.88	1.58	1.58	1.39
42	2071.10	2071.14	2049.19	0.81	0.63	1.14
43	2069.57	2069.58	2051.90	0.63	0.48	0.82
44	2071.99	2071.99	2051.65	0.76	0.76	0.64
45	2074.51	2074.50	2049.32	0.78	0.70	0.60
46	2076.99	2076.99	2054.01	0.67	0.67	0.82
47	2080.33	2080.29	2064.14	0.76	0.55	0.99
48	2083.99	2084.00	2072.62	1.06	1.06	1.70
49	2084.68	2085.09	2073.12	2.24	2.03	2.38
50	2078.99	2078.99	2069.75	1.96	1.96	1.63
51	2078.81	2078.78	2055.39	1.28	1.12	1.04
52	2077.68	2077.68	2061.91	0.70	0.58	0.95
53	2076.99	2077.00	2065.78	0.95	0.95	0.89
54	2077.96	2077.96	2062.99	0.83	0.67	0.61
55	2078.99	2078.99	2061.14	0.81	0.81	0.78
56	2082.36	2082.34	2060.95	0.89	0.73	0.92
57	2084.99	2084.99	2067.49	0.84	0.84	1.16
58	2087.68	2087.84	2075.00	1.09	0.85	1.99
59	2079.94	2079.90	2074.75	3.24	3.00	2.41
60	2080.99	2081.99	2074.63	1.97	1.97	1.87
61	2083.12	2083.11	2061.58	1.37	1.18	1.45
62	2083.79	2083.79	2059.06	1.03	0.96	1.01
63	2083.36	2083.36	2057.53	0.75	0.53	0.84
64	2082.99	2082.99	2072.08	1.09	1.09	0.79
65	2083.03	2083.03	2071.22	0.85	0.67	0.79

Table 3.4 -- Continued

Cell	Kriged Hydraulic Head 1956		1985	Kriging Errors 1956		1985
	GLS	ML	ML	GLS	ML	ML
66	2083.99	2083.99	2070.44	0.82	0.82	0.98
67	2086.72	2086.74	2069.89	0.89	0.70	1.09
68	2089.99	2089.99	2072.19	1.02	1.02	1.46
69	2092.00	2092.25	2080.01	1.41	1.14	1.81
70	2084.70	2084.62	2075.21	2.75	2.54	2.30
71	2085.99	2086.00	2076.32	1.26	1.26	1.98
72	2086.62	2086.63	2065.22	0.71	0.51	1.25
73	2088.40	2088.40	2067.37	0.70	0.55	0.90
74	2088.00	2088.00	2067.20	0.74	0.51	0.72
75	2087.99	2087.99	2077.39	0.90	0.90	0.69
76	2087.62	2087.63	2076.94	0.65	0.47	0.86
77	2087.99	2087.99	2074.75	0.93	0.93	1.08
78	2090.89	2090.91	2079.03	1.36	1.17	1.37
79	2094.99	2094.99	2080.11	1.61	1.61	1.66
80	2097.20	2097.55	2090.91	1.98	1.71	1.89
81	2098.63	2099.14	2103.17	2.74	2.55	2.26
82	2087.99	2088.00	2080.79	2.65	2.65	2.38
83	2088.89	2088.91	2081.07	1.22	1.08	1.81
84	2088.24	2088.25	2075.91	0.68	0.54	1.05
85	2091.15	2091.17	2071.17	0.60	0.45	0.89
86	2091.99	2091.99	2071.51	0.64	0.64	0.65
87	2092.52	2092.53	2075.16	0.72	0.62	0.67
88	2093.33	2093.34	2077.53	0.94	0.77	0.96
89	2093.99	2093.99	2084.05	1.29	1.29	1.08
90	2097.39	2097.33	2092.84	1.64	1.43	1.48
91	2100.99	2100.99	2096.58	1.87	1.87	1.66
92	2102.97	2103.35	2103.38	2.26	1.98	1.83
93	2103.56	2104.04	2118.79	2.92	2.79	2.26
94	2092.99	2093.00	2089.28	1.80	1.80	1.92
95	2093.90	2093.90	2084.55	1.22	1.10	0.90
96	2095.37	2095.38	2083.26	0.89	0.77	0.84
97	2097.87	2097.87	2075.94	0.76	0.67	0.61
98	2098.99	2098.99	2083.00	0.99	0.99	0.79
99	2100.22	2100.30	2086.95	1.11	0.88	0.85
100	2101.62	2101.65	2098.73	1.24	1.02	0.93

Table 3.4 -- Continued

Kriged Hydraulic Head Estimates and Kriging Errors obtained by the GLS and ML Methods for Nodes of the Calera Basin in 1956 and 1985. Data are given in meters.

Cell	Kriged Hydraulic Head			Kriging Errors		
	1956		1985	1956		1985
	GLS	ML	ML	GLS	ML	ML
101	2104.30	2104.25	2102.23	1.51	1.28	1.28
102	2106.99	2106.99	2105.27	1.65	1.65	1.56
103	2108.33	2108.72	2118.43	2.01	1.80	1.89
104	2099.71	2099.74	2094.87	2.30	2.10	2.05
105	2101.78	2101.76	2093.98	1.56	1.38	1.00
106	2101.99	2101.99	2093.94	1.08	1.08	0.81
107	2104.17	2104.18	2083.94	0.86	0.66	0.64
108	2105.99	2105.99	2093.30	1.12	1.12	0.59
109	2107.82	2107.86	2096.34	0.95	0.76	0.77
110	2108.99	2108.99	2105.33	0.80	0.80	0.88
111	2111.06	2111.02	2112.22	1.12	0.90	1.01
112	2112.99	2112.99	2122.97	1.10	1.10	1.44
113	2105.99	2106.00	2100.88	2.54	2.54	2.02
114	2107.47	2107.44	2101.58	1.50	1.28	1.41
115	2108.99	2108.99	2102.24	0.91	0.91	0.91
116	2110.39	2110.39	2098.03	0.95	0.72	0.79
117	2111.99	2111.99	2106.39	1.13	1.13	0.61
118	2114.90	2114.89	2100.12	0.90	0.77	0.72
119	2115.99	2115.99	2114.03	0.74	0.74	0.82
120	2117.16	2117.14	2128.01	0.90	0.73	0.98
121	2114.07	2114.07	2111.70	1.66	1.48	1.52
122	2114.99	2114.99	2110.44	0.87	0.87	0.99
123	2115.74	2115.76	2110.00	0.87	0.64	0.81
124	2117.07	2117.07	2112.16	1.00	0.84	0.88
125	2118.99	2118.99	2110.90	0.83	0.83	0.87
126	2120.70	2120.70	2120.42	0.87	0.69	0.93
127	2119.90	2119.90	2119.22	2.26	2.10	1.69
128	2120.91	2120.92	2118.06	1.30	1.13	1.01
129	2120.99	2120.99	2116.03	0.90	0.90	0.95
130	2122.03	2122.02	2118.18	1.00	0.84	0.96
131	2123.99	2123.56	2118.60	0.80	0.80	0.97
132	2124.83	2124.86	2124.25	1.16	0.99	1.09
133	2125.04	2125.05	2123.06	2.92	2.72	1.85
134	2125.99	2126.00	2123.83	1.93	1.93	1.40
135	2126.47	2126.46	2124.13	1.37	1.18	1.37

Table 3.4 -- Continued

Cell	Kriged Hydraulic Head			Kriging Errors		
	1956		1985	1956		1985
	GLS	ML	ML	GLS	ML	ML
136	2127.73	2127.74	2120.21	1.25	1.18	1.04
137	2127.99	2127.99	2120.70	1.21	1.21	1.03
138	2129.66	2129.70	2127.21	1.49	1.27	1.56
139	2131.41	2131.59	2131.35	2.08	1.76	2.05
140	2132.89	2133.25	2141.64	2.90	2.61	2.50
141	2130.12	2130.12	2128.84	3.63	3.36	2.01
142	2131.07	2131.07	2127.60	2.53	2.28	1.86
143	2131.99	2131.99	2127.35	1.63	1.63	1.75
144	2132.58	2132.61	2125.24	1.09	0.85	1.62
145	2133.45	2133.47	2124.54	1.05	0.82	1.75
146	2134.99	2134.99	2130.18	1.44	1.44	2.07
147	2136.41	2136.57	2135.05	2.37	2.08	2.44
148	2137.83	2138.14	2143.29	3.42	3.31	3.00
149	2135.13	2135.14	2130.54	4.41	4.10	2.30
150	2136.18	2136.15	2131.41	3.18	2.88	2.03
151	2136.99	2136.99	2130.04	2.10	2.10	2.05
152	2137.57	2137.59	2129.55	1.21	1.00	2.04
153	2138.52	2138.53	2130.78	1.12	0.90	2.11
154	2139.99	2139.99	2135.49	1.72	1.72	2.47
155	2141.59	2141.62	2138.07	2.86	2.66	2.84
156	2142.93	2143.02	2146.08	4.05	4.00	3.24
157	2140.29	2140.27	2135.39	5.30	4.99	2.74
158	2141.55	2141.52	2136.48	4.20	3.89	2.66
159	2142.99	2142.99	2137.74	3.23	3.23	2.55
160	2143.00	2143.02	2136.43	2.58	2.40	2.56
161	2143.67	2143.69	2138.93	2.47	2.27	2.85
162	2144.99	2144.99	2140.79	2.92	2.92	3.07
163	2146.96	2146.91	2142.58	5.46	5.17	3.03
164	2147.99	2147.99	2143.43	4.66	4.66	3.05
165	2148.56	2148.61	2143.17	4.14	3.92	3.05
166	2149.33	2149.39	2142.58	4.05	3.77	3.09
167	2152.03	2151.92	2149.34	6.89	6.55	3.80
168	2153.08	2153.00	2150.22	6.20	5.98	3.53
169	2153.99	2153.99	2150.04	5.77	5.77	3.71
170	2154.91	2154.95	2149.30	5.68	5.43	3.75
171	2157.15	2156.91	2163.16	7.50	7.46	4.40
172	2158.30	2158.16	2164.13	7.80	7.69	4.24
173	2159.29	2159.29	2164.05	7.40	7.34	4.27
174	2160.44	2160.56	2165.07	7.30	7.30	4.10

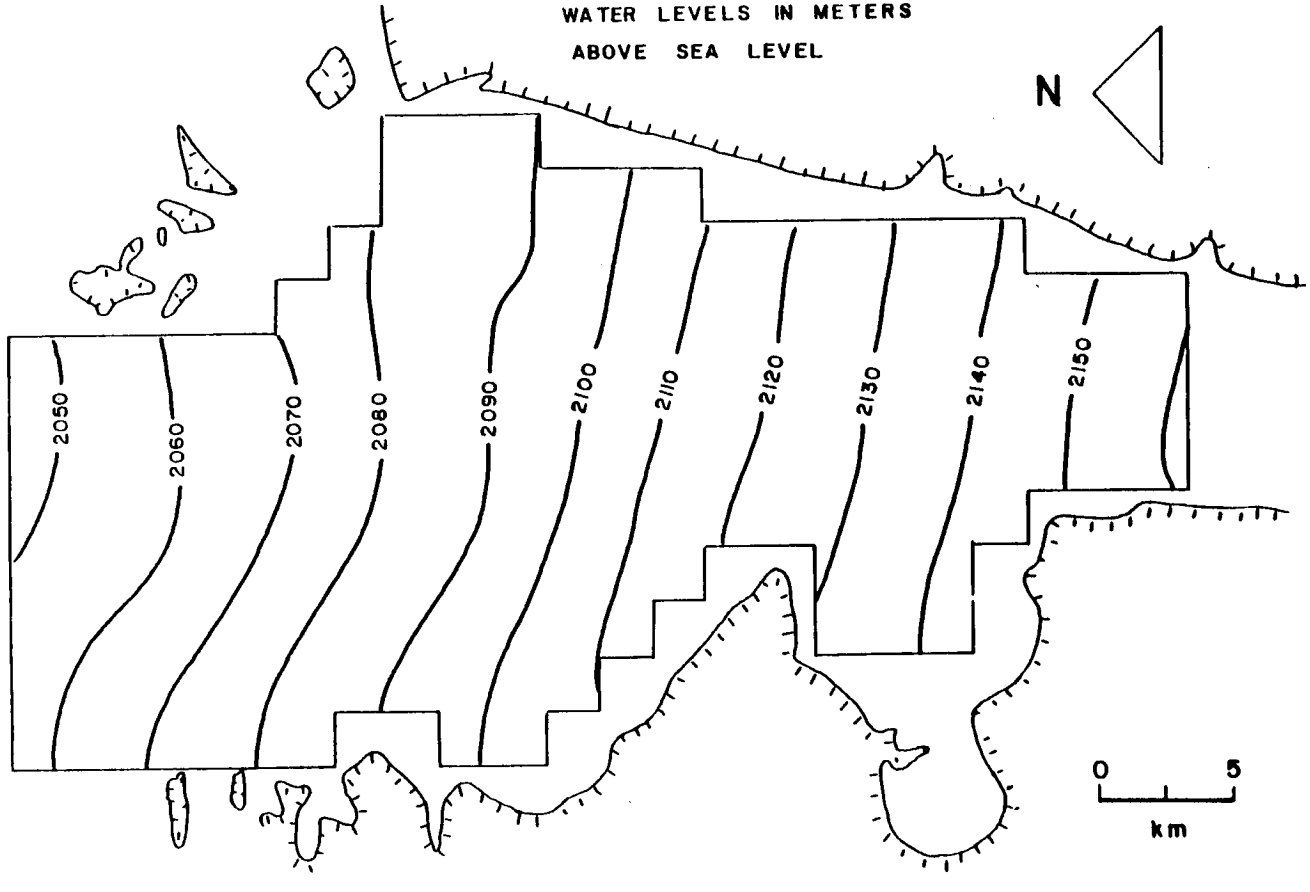

Figure 3.22 Contour map of 1956 kriged hydraulic head estimates based on results of maximum likelihood cross-validation.

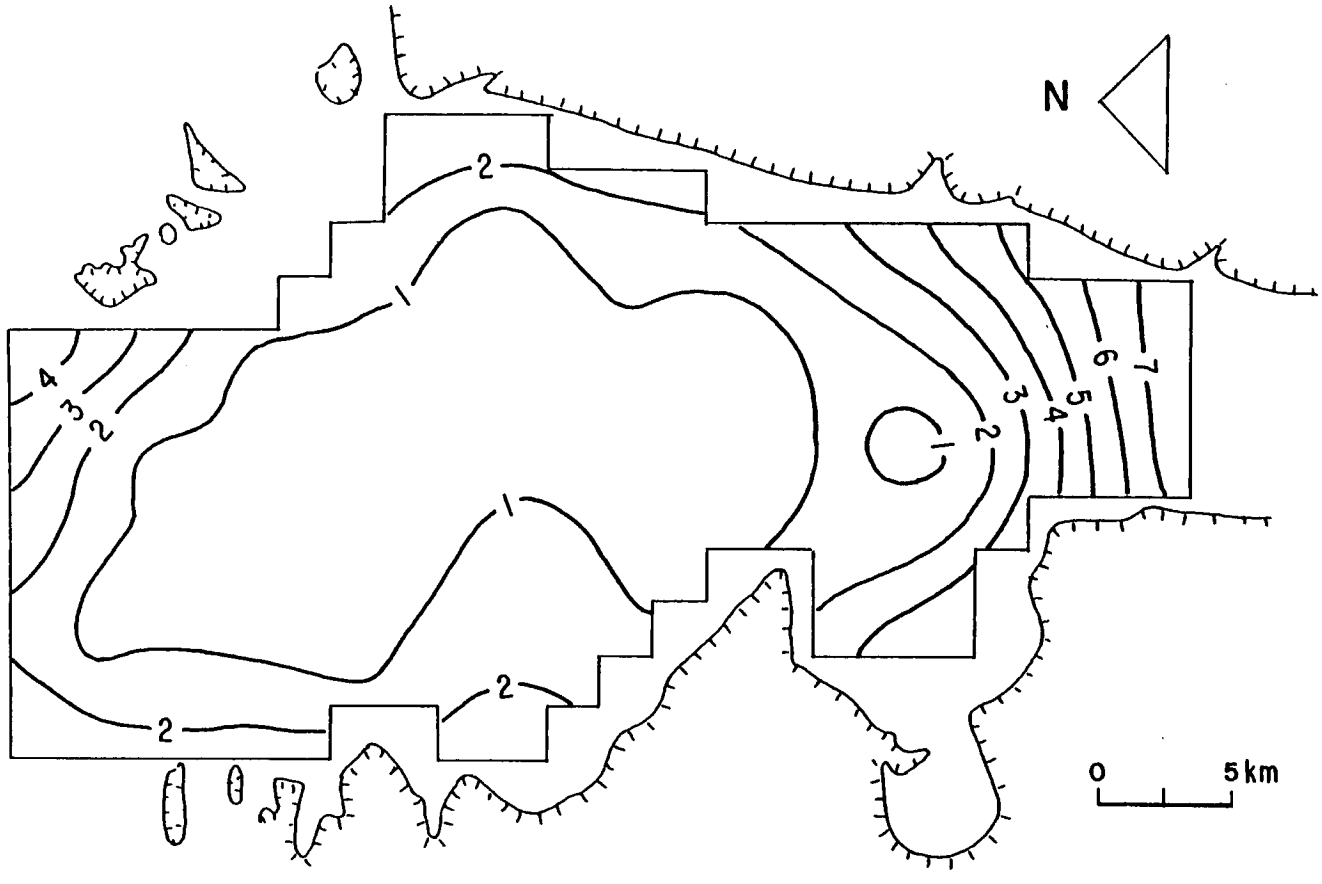

Figure 3.23 Contour map of 1956 hydraulic head kriging errors based on results of maximum likelihood cross-validation.

Table 3.5.- Hydraulic head maximum likelihood validation test (1956).

a) mean difference between measured and kriged values

$$1/N \sum_{i=1}^{N} [(Z(\underline{x}_i) - Z^*(\underline{x}_i)] = -0.014$$

b) dimensionless mean square error

$$[1/N \sum_{i=1}^{N} (e_i^2/\sigma^2_{ki})]^{1/2} = 1.000$$

c) negative log-likelihood value

$$S = 174.81$$

Water level estimates obtained with the iterative generalized least squares method are similar to those corresponding to the method that minimizes the negative loglikelihood function. The iterative generalized least squares method, however, produced higher kriging errors than those of the maximum likelihood cross-validation method, especially in the central part of the basin. In order to obtain hydraulic head estimates for 1985, the maximum likelihood cross-validation method was used again due to the fact that yielded lower residual kriging errors than the generalized least squares method in the computation of hydraulic head estimates for 1956. Figure 3.24 shows the location of water level measurements corresponding to the 1985 time period. The process of estimation was repeated as previously described in this chapter.

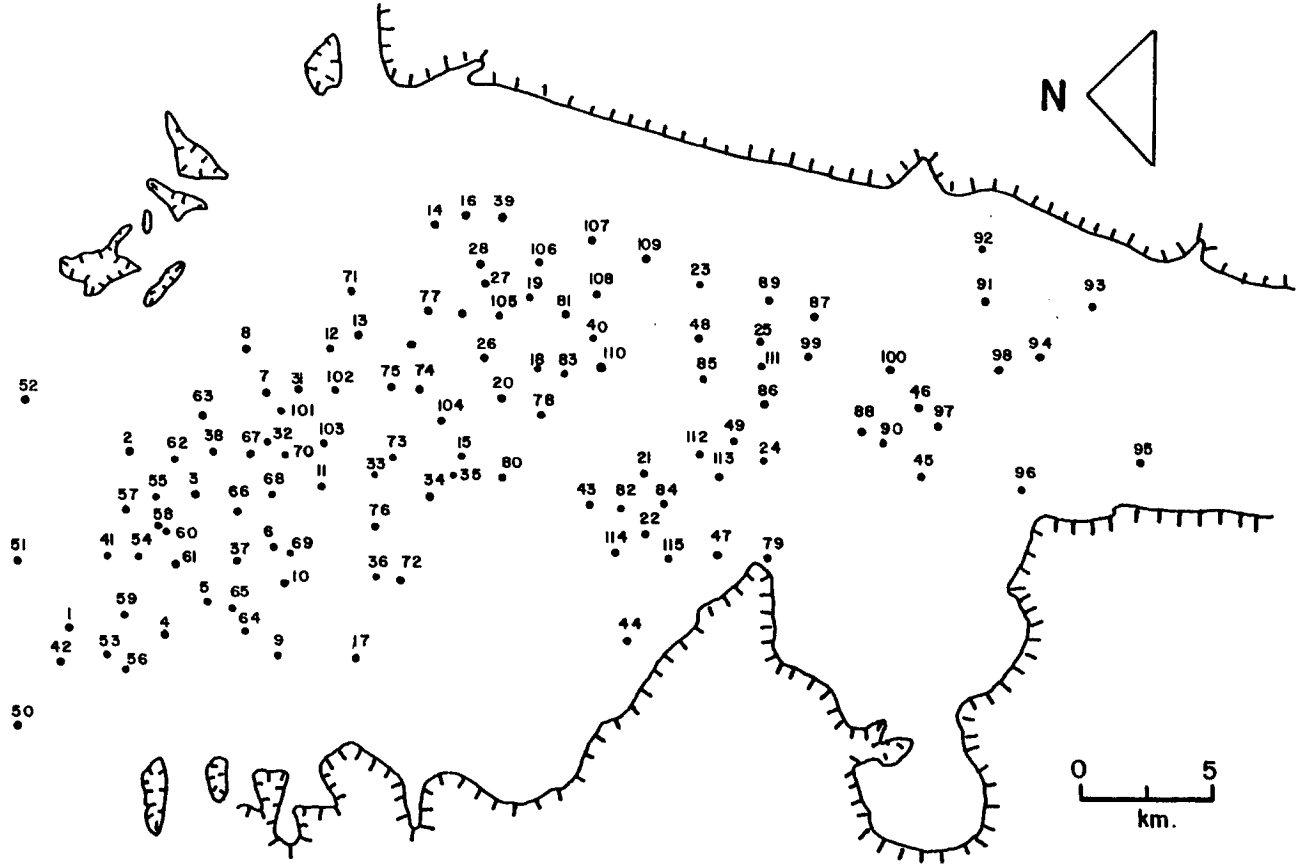

Figure 3.24 Location of 1985 water level measurement sites in Calera basin.

Clearly, the 1985 average sample semivariogram shows a rapid increase with distance indicating that a drift is present in the data (figure 3.25). Consequently, ordinary least squares was used to fit successively higher order polynomial trends to the water level data until the sample semivariogram of the residuals showed a distinct sill. A first order polynomial produced a residual semivariogram with distinct sill of the following form.

$$m(\underline{x}) = a_0 + a_1 x + a_2 y$$

This sample semivariogram was used to start the first iteration of the generalized least squares method. New residuals were calculated and a new residual semivariogram was obtained. In this case, the process required three iterations to obtain the optimum parameters. The corresponding final residual semivariogram and fitted spherical model are shown in figure 3.26. The coefficients of the polynomial representing the drift were found to be:

$$a_0 = 2028.32 \quad ; \; a_1 = 4.428 \quad ; \; a_2 = 0.392$$

The cross-validation results for the final parameters of the semivariogram of the residuals are presented in table 3.6.

Once the drift and the semivariogram of the residuals were estimated, residual kriging was used to obtain hydraulic head estimates at the center of each cell of the grid shown in figure 3.17. The kriged hydraulic head estimates and kriging estimation errors are listed in table 3.4 and contoured in figures 3.27 and 3.28, respectively. In the 1985 hydraulic head distribution a cone of depression

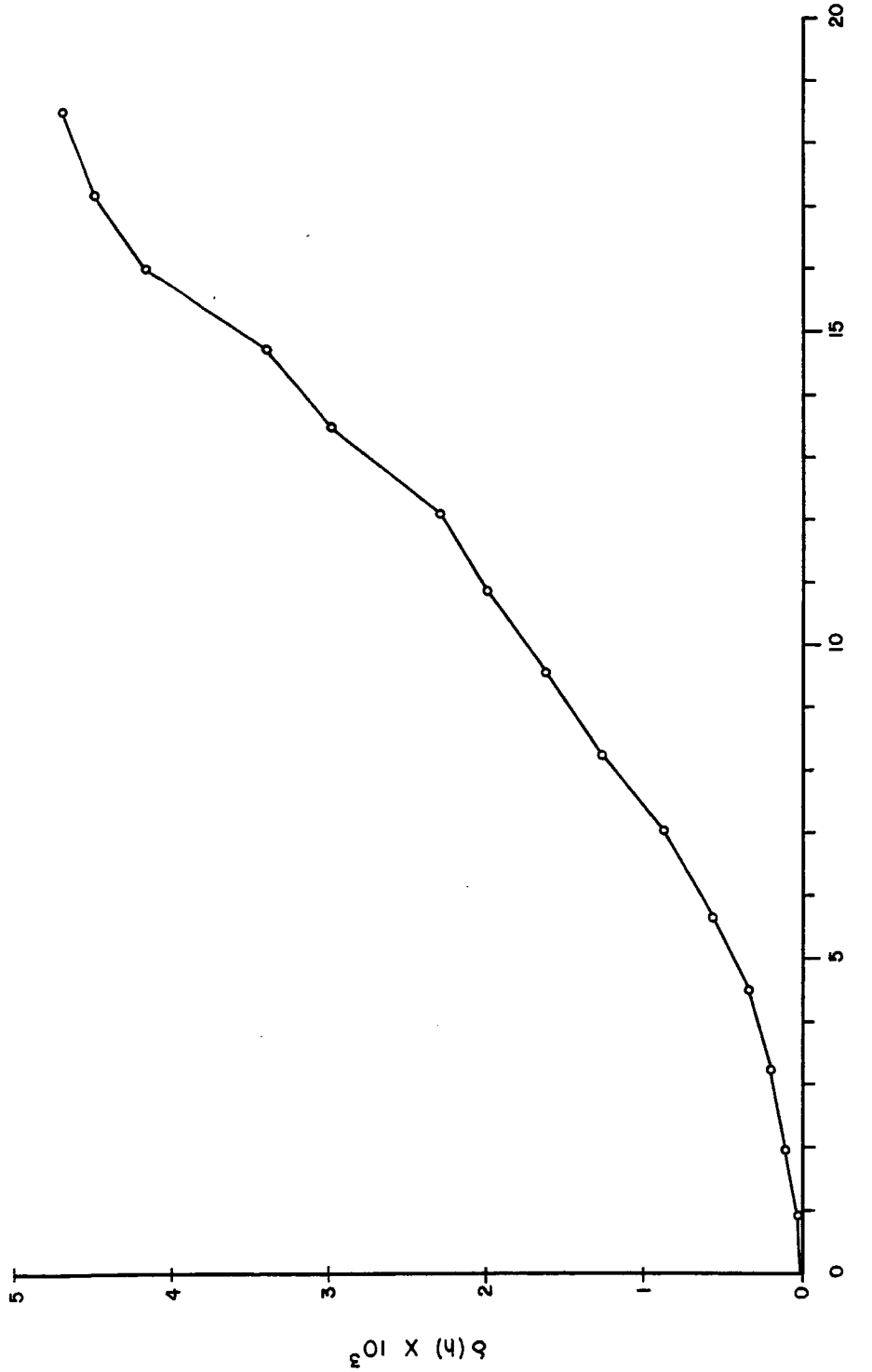

Figure 3.25 Isotropic sample semivariogram of 1985 water levels in Calera basin.

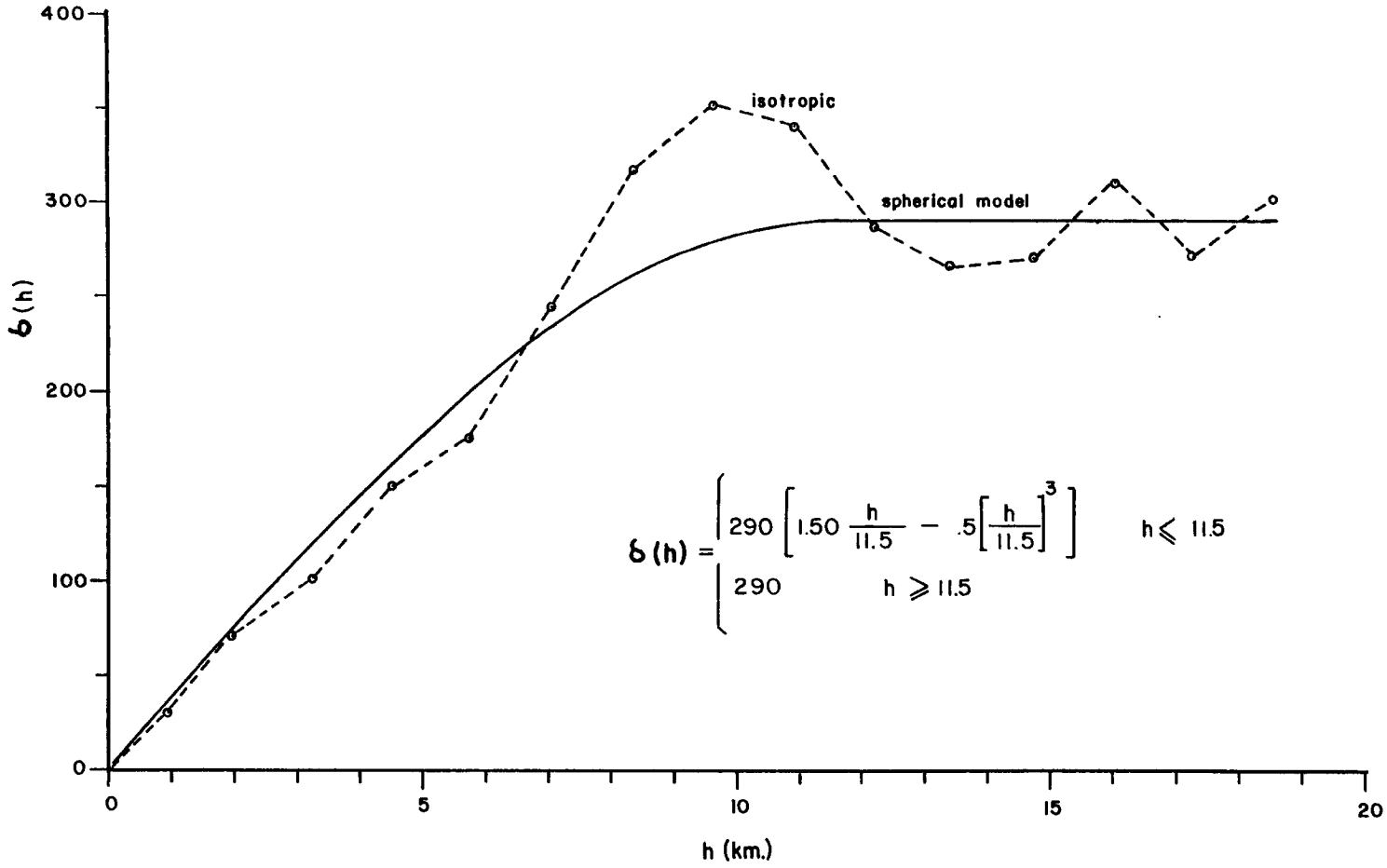

Figure 3.26 Final sample semivariogram of residual hydraulic heads based on linear drift determined by maximum likelihood cross-validation and fitted spherical model.

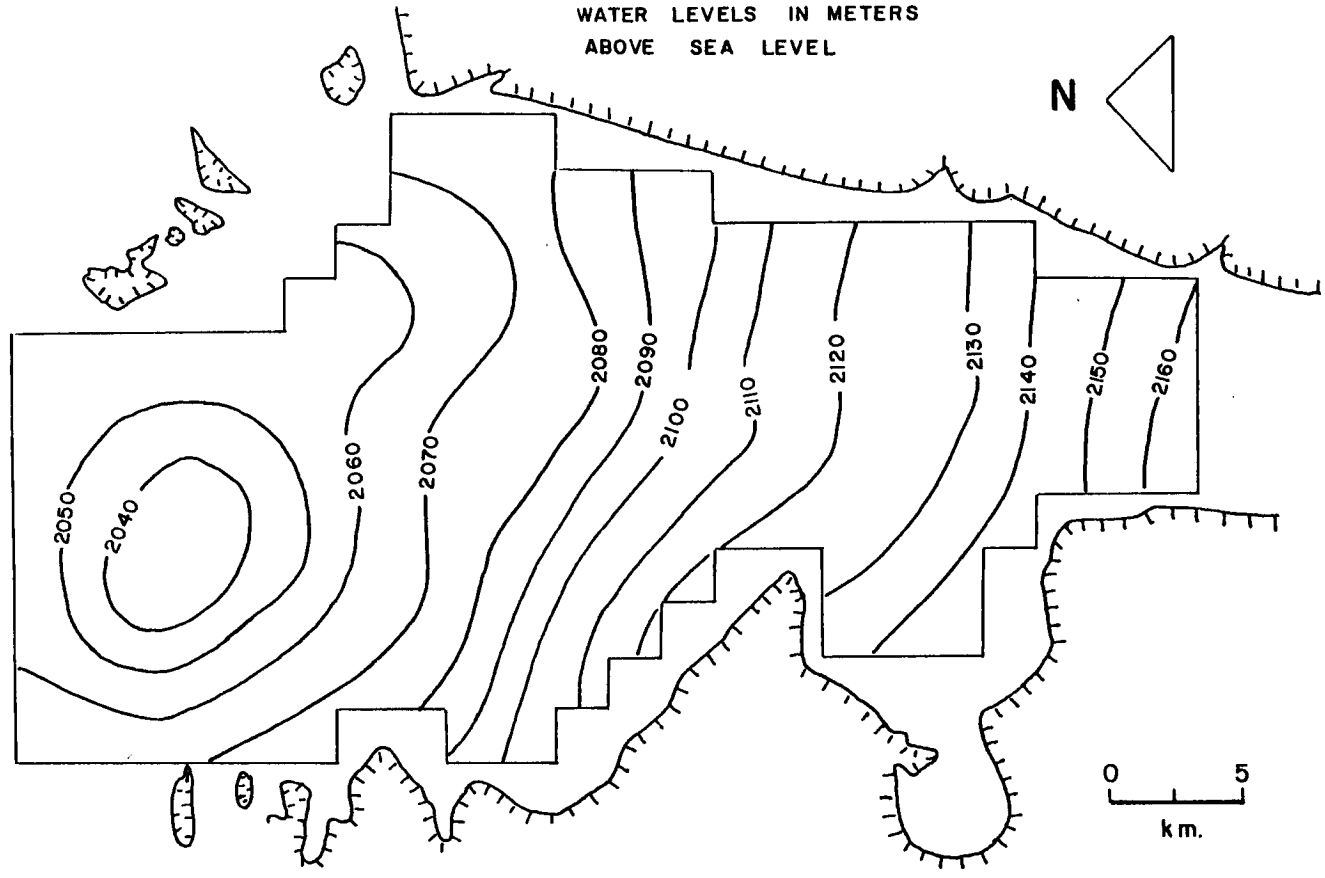

Figure 3.27 Contour map of 1985 kriged hydraulic head estimates based on results of maximum likelihood cross-validation.

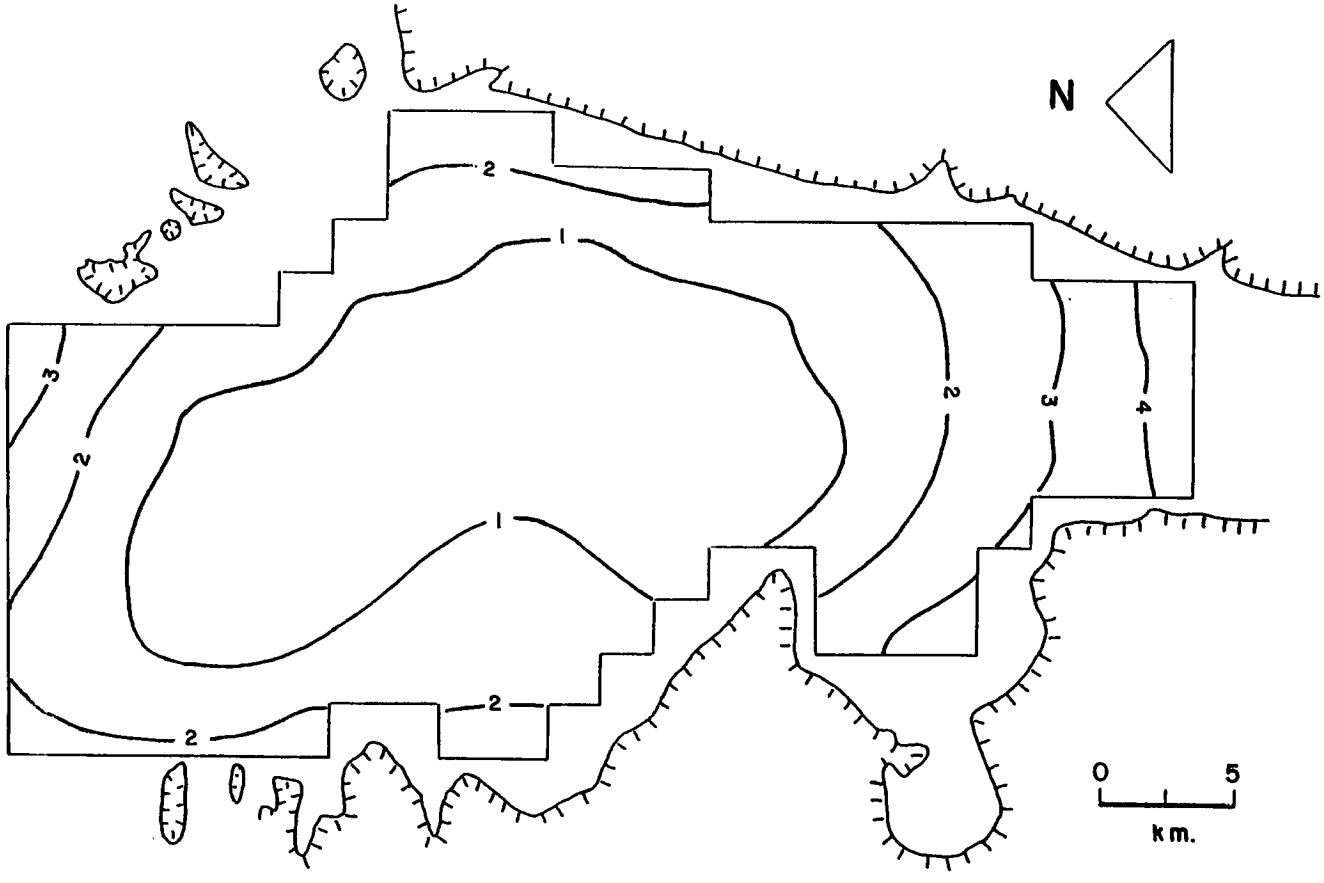

Figure 3.28 Contour map of 1985 hydarulic head kriging errors based on results of maximum likelihood cross-validation.

appeared in the northern region of the basin. Wells are narrowly-spaced in this region due to the fact that groundwater resources development began in 1956, therefore, as time evolved this region became the most heavily pumped area in the basin. Regarding the kriging estimation errors, the highest values were obtained in areas where water level measurements were scarce. Furthermore, inasmuch as more water level measurements were available along the margins of the basin in 1985, as a result, the 1985 kriging estimation errors were lower in these regions than those corresponding to the 1956 time period.

Table 3.6.- Hydraulic head maximum likelihood validation test. (1985)

a) mean difference between measured and kriged values

$$1/N \sum_{i=1}^{N} [(Z(\underline{x}_i) - Z^*(\underline{x}_i)] = -0.055$$

b) dimensionless mean square error

$$[1/N \sum_{i=1}^{N} (e_i^2/\sigma^2_{ki})]^{1/2} = 1.000$$

c) negative log-likelihood value

$$S = 320.15$$

CHAPTER 4

SIMULATION OF PRESENT BASIN CONDITIONS

Before a computer model can be used to evaluate the effects of future development on Calera basin ground water conditions, it must first be capable of simulating some known basin conditions.

According to the available data there is evidence of long-term changes in ground water levels during the period of record. Prior to the period 1956-1958 the basin was in an undeveloped steady state condition. Then, as time evolved the aquifer was subject to heavy pumpage conditions, mainly in the northern region of the basin, which caused the formation of a cone of depression. Therefore, the only means of testing the model's reliability is to test its ability to simulate the steady state condition and the prevailing transient state ground water flow regime. Inasmuch as the aquifer system responds to stress over a long period of time as a single unit, a two dimensional finite difference model was chosen to simulate the system. Hence, the Modular Three Dimensional Finite Difference Groundwater Flow Model (Michael G. Mc.Donald and Arlen W. Harbaugh, 1984) was used in developing the model. Construction of the model involves the design of the finite difference mesh, selection of initial input data, and steady state and transient state calibration. The calibration procedure consists of adjusting model parameters (transmissivity and recharge, in the case of steady state, and specific yield, in the case of transient state) by

trial and error until the computed groundwater table configuration lies within the interval H^*_i +/- σ_i. Modeling procedures and results are discussed in the remainder of this chapter.

Model Devolopment

In general, the results obtained from a computer simulation model are only as reliable as the data upon which the model is based. For this reason, the reliability of the data and assumptions must be evaluated before modeling begins.

The assessment of available hydrologic data for the present study, indicates that estimates of the quantity and distribution of recharge in the mountains areas of the basin are subject to large errors. In addition, an estimate of the specific yield for the entire aquifer was obtained from SARH. This estimate may vary in different zones, therefore, a high uncertainty is involved in the spatial distribution of the specific yield estimate. According to the writer, the order of reliability of the available data from the most to the least reliable, is as follow:

1.- Hydraulic head

2.- Transmissivity

3.- Pumpage

4.- Recharge

5.- Specific yield

In developing a model for the Calera aquifer, the area to be modeled was divided into a uniform grid with each square representing

4 Km^2 (1.55 $Miles^2$). The following factors were considered in its design: 1) spatial variations in hydraulic gradients and transmissivity 2) the quantity and quality of the input data. The data base for the present study is somewhat weak, and does not justify the use of a very refined mesh. Common practice is to describe the rectangular finite difference elements as blocks. The center of the block is the node which is the point in space for which the finite difference equation is solved. The blocks formed a grid of 25 columns and 15 rows (figure 4.1). There are currently 198 active nodes in the model. Inasmuch as the groundwater system is most highly stressed during the dry season, for this reason, drawdowns were determined during this period.

Initial Input Data

The initial values of transmissivity used in the steady state simulation of the basin are shown in figure 3.10. The transmissivity distribution was obtained by performing a geostatistical interpolation procedure called Kriging described in chapter three.

Similarly, the hydraulic head distribution was obtained by means of Kriging in chapter three. The initial values of hydraulic head used in the simulation process are shown in figure 3.22. Note, that the geostatistical interpolation procedure provided contour maps of kriging estimation errors for both transmissivity and hydraulic head estimates, these estimation errors were used in the calibration process as explain later in this chapter.

In our model, three types of boundary conditions were considered

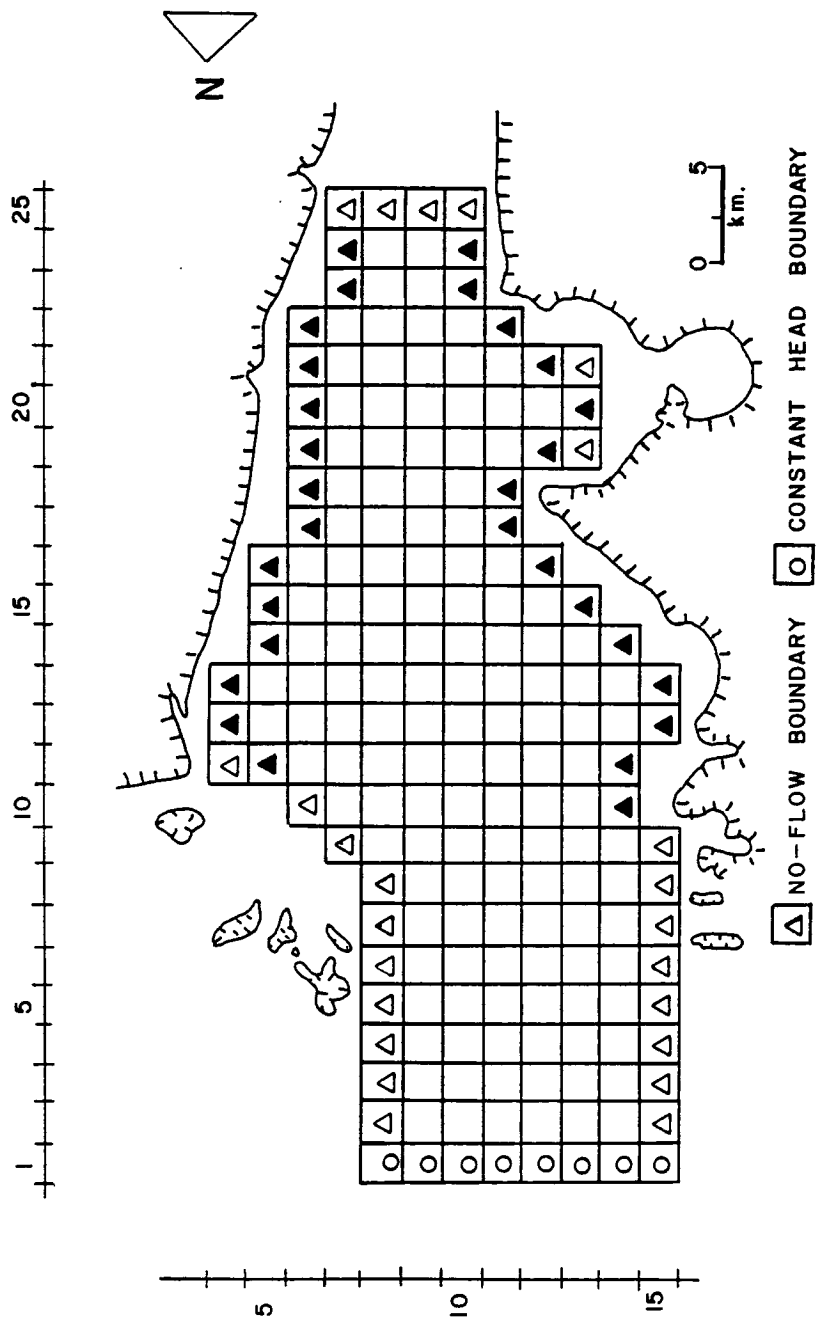

Figure 4.1 Finite difference mesh and boundary conditions.

in the Calera aquifer to simulate the natural boundaries, prescribed head, prescribed flow and no-flow boundaries. Figure 4.1 indicates the boundary conditions used in the model. The northern boundary was considered as prescribed head. For modelling purposes and prevent capture from the constant head boundary, the boundary was considered far enough from the well field located at the northern part of the study area. The southern boundary is a groundwater divide, flow to the north of the divide is independent of flow to the south. Here, the divide acts as an artificial boundary, therefore, the divide was represented by no-flow nodes. The western and eastern boundaries, The Sierra Madre Occidental and The Sierra of Zacatecas, respectively, were represented by prescribed flow boundaries to simulate the mountain front recharge.

Information about historical pumpage was provided by SARH (1985). In general, most water users do not measure pumpage directly, estimates were based on power consumption (electrical or gas) and/or records of the number of hours a pump operated. Pumpage data were separated into three use categories: agricultural, municipal and industrial. Each node has the total of these three categories as the total pumpage for that node. Most of the water pumped from the Calera aquifer is for agricultural purposes, 90 percent of the total volume. Next, municipal and industrial use take 8 and 2 percent, respectively. The historical pumpage from 1956 to 1984 is depicted in figure 4.2. In addition, a monthly pumpage pattern for the year 1984 is shown in figure 4.3. Analyzing figure 4.3 is clear that 90 percent of the total volume of water pumped ocurred during April through September.

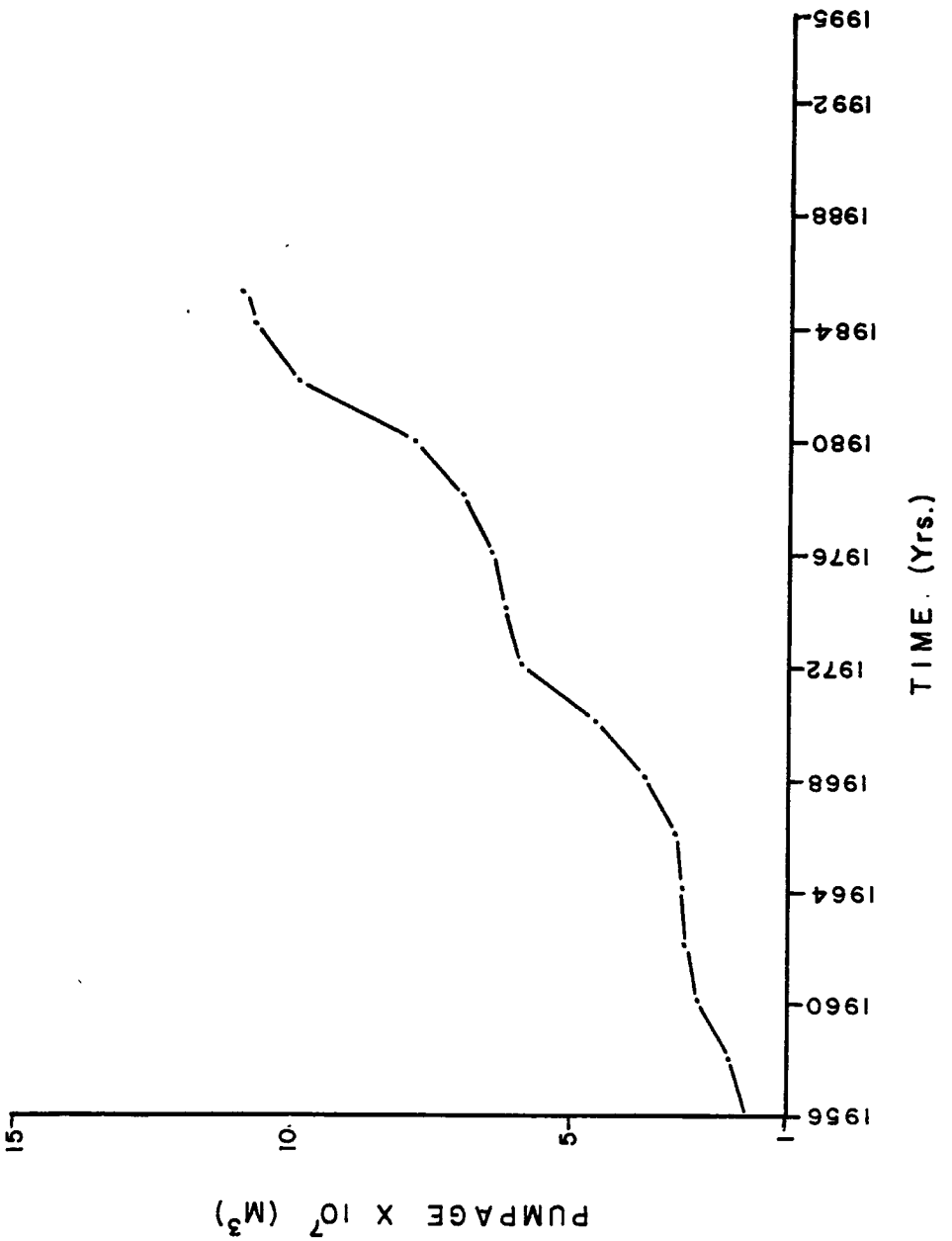

Figure 4.2 Historical pumpage for the period 1956-1984.

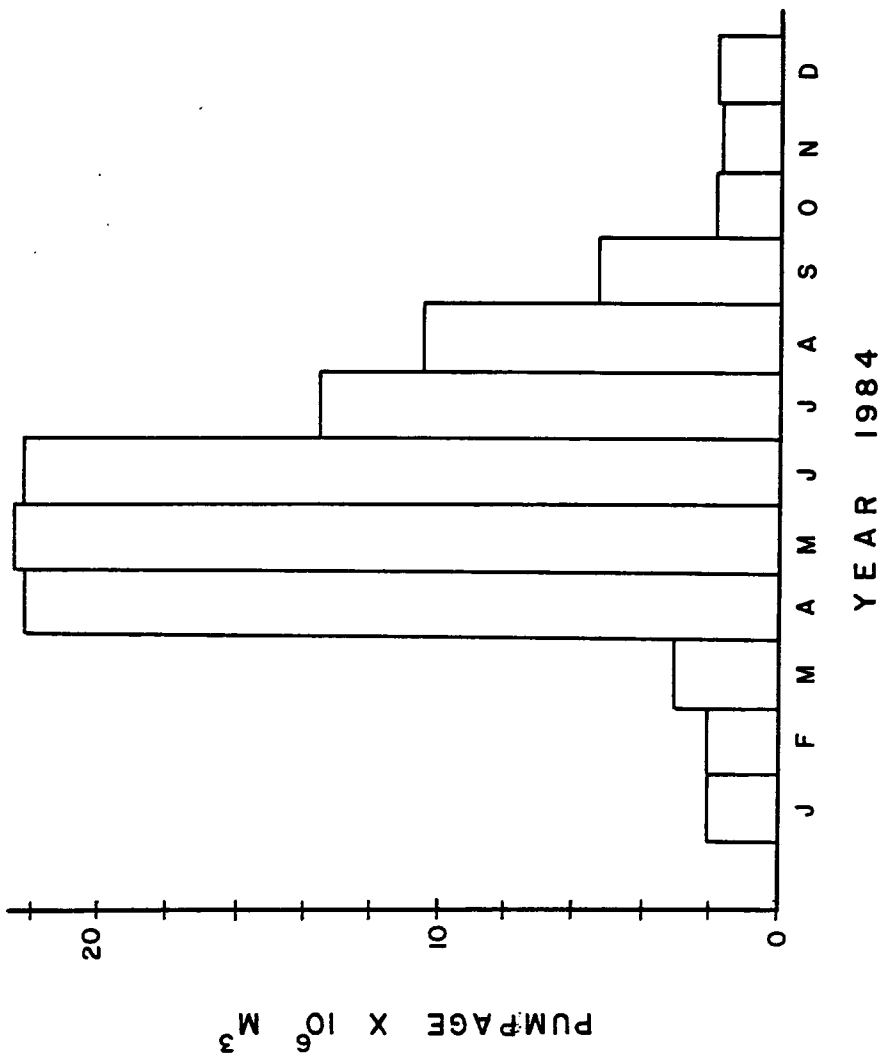

Figure 4.3 Monthly pumpage pattern for the year 1984.

This pumpage pattern has been followed by farmers for years due to land use reasons.

Recharge is an important part of the area's water budget, but unlike water levels or pumpage, it cannot be measured directly and, therefore, is difficult to quantify. Recharge varies over the modeled area depending on land use patterns, meteorological conditions, and aquifer and geologic characteristics. Potential recharge is greater in areas of high infiltration capacity, such as portions of the mountains fronts having well defined drainages and alluvial fans, and irrigated agricultural lands. An estimate of natural recharge was taken from previous work done by SARH (1980). Little is known about its spatial distribution, however, the writer assumes that recharge is taking place along the margins of the Sierra Madre Occidental and Sierra of Zacatecas based on the ground water level contours. Thus, the reported recharge estimate of 49.00E+06 M^3/Yr (39.69E+03 AF/Yr) was distributed equally among nodes which lie on the margins of the Sierra Madre Occidental and Sierra of Zacatecas. Each of these nodes was assigned as an initial value a recharge rate of 3122 M^3/day (2.53 AF/day).

Similarly, the initial value of specific yield used in the transient state simulation was obtained by performing a hydrologic budget for the Calera groundwater basin done by SARH (1980). The estimate for the entire aquifer was reported to be 0.13.

Calibration Process

Calibration of the model for steady state and transient state involved first entering the known data into the model and running the model to see if it adequately simulate the known system.

Modifications were limited to reasonable ranges for the value of each parameter. In addition to decisions on modifications of the model input data involved in the calibration, a decision had to be made as to when the model was sufficiently calibrated. The criterion to decide whether the model was sufficiently calibrated was based on the values of the hydraulic head residual kriging errors of 1985. That is, the unknown real hydraulic head values at unsample sites were assumed to lie within the interval H^*_i +/- σ_i. Where H^*_i is the kriging hydraulic head estimate and σ_i is the hydraulic head residual kriging error at each node. Clearly, analayzing the hydraulic head residual kriging errors, the allowed interval is greater in areas where data is scarce or unknown than in areas where measurements are available. Therefore, the calibration process was accepted until simulated hydraulic heads at each node lay whithin the previously mentioned interval.

Calibration Results

An initial calibration run for the steady state was made prior to adjusting the input parameters. This run was followed by a series of documented calibration runs. For each subsequent calibration run,

problem areas were isolated and attempts were made to have the calculated hydraulic heads at each node to lie within the interval H^*_i +/- σ_i. During the calibration process greatest modifications were made as expected to recharge. Next, results and contour maps under steady state and transient state.

Steady State

The calibration run using the transmissivity distribution shown in figure 3.10 and the assumed recharge distribution yielded a poor match between computed and kriged hydraulic heads. A few subsequent runs were made using modified versions of the recharge distribution with a substantial improvement in results. Once a fairly good match was obtained, a few modifications were made to the transmissivity distribution in areas where log-transmissivity kriging errors were greatest to enhance the calibration. The final steady state hydraulic head distribution is shown in figure 4.4.

With regard to the flow patterns, the conceptual model of flow can be easily tested from the contour map and the perspective plots of the piezometric surface (figure 4.5). Water table configuration resembles the topography of the basin. This implies that the lowlands are discharge zones and the interfluvial areas are recharge zones. Tables 4.1 and 4.2 present recharge rates obtained at each node which lies along the margins of the Sierra Madre Occidental and Sierra of Zacatecas, respectively. The total recharge rate obtained during the simulation process is 53.50E+06 M^3/Yr (43.33E+03 AF/Yr). Obviously,

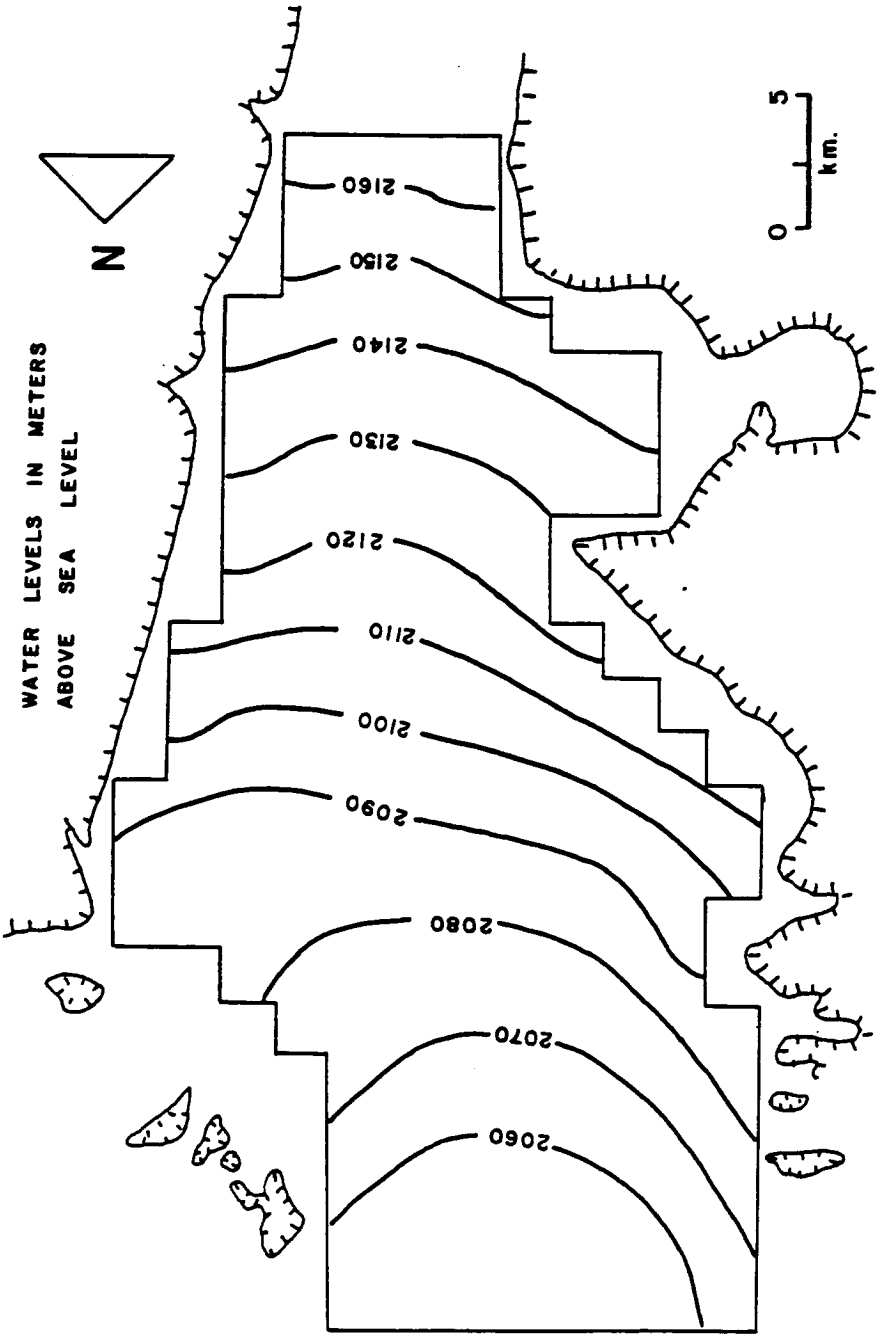

Figure 4.4 Steady state hydraulic head distribution.

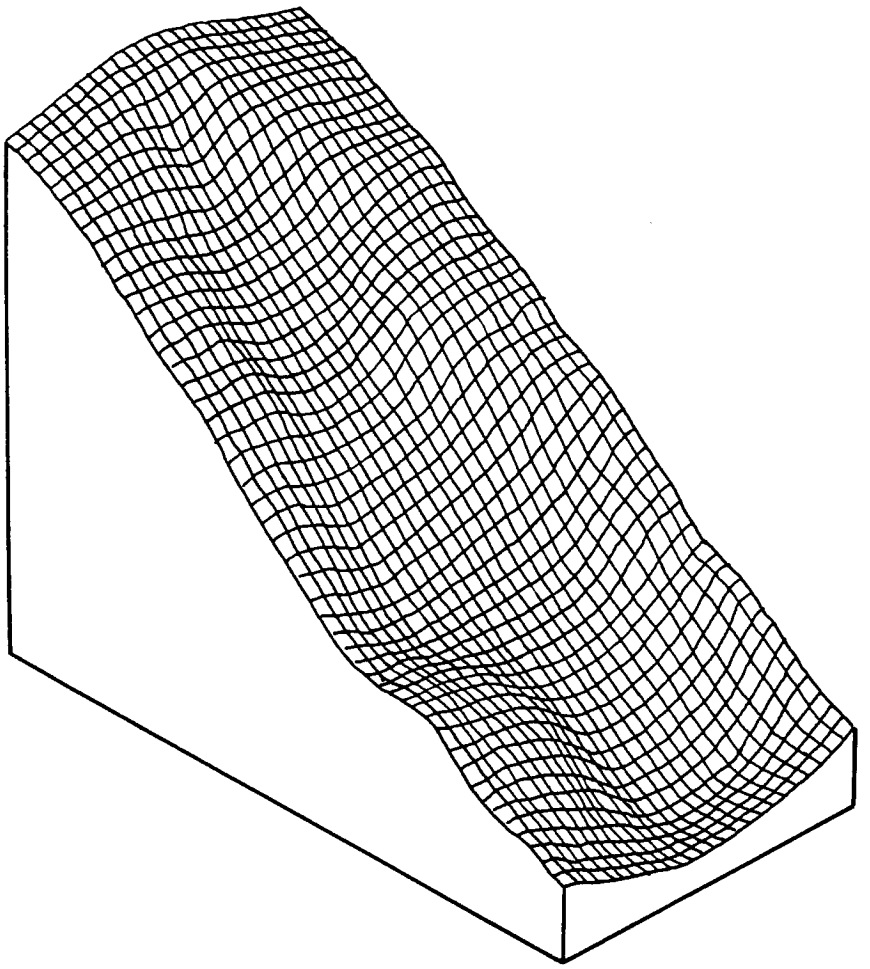

Figure 4.5 Perspective plot of 1956 piezometric surfaces.

Table 4.1

RECHARGE ESTIMATES
(Sierra Madre Occidental)

Node Row	Node Col	Recharge Computed by Model $M^3/Yr \times 10^6$	Recharge Computed by Model AF/Yr
14	10	3.8104	3086.42
14	11	1.2502	1012.66
15	12	1.2993	1052.43
15	13	1.2125	982.12
14	14	3.6213	2933.25
13	15	4.6058	3730.69
12	16	4.0583	3287.22
11	17	3.1511	2552.39
11	18	0.9275	751.27
12	19	0.7746	627.42
13	20	0.8183	662.82
12	21	2.5951	2102.03
11	22	2.7356	2215.83
10	23	3.0074	2435.99
10	24	0.8505	688.90

Total Sierra Madre Occidental Recharge = 34.7189×10^6

= 28,122.30 AF/Yr

Table 4.2

RECHARGE ESTIMATES
(Sierra of Zacatecas)

Node Row	Node Col	Recharge Computed by Model $M^3/Yr \times 10^6$	Recharge Computed by Model AF/Yr
5	11	0.7079	573.40
4	12	0.7056	571.53
4	13	0.8244	667.76
5	14	3.6882	2987.44
5	15	0.9401	761.48
5	16	0.6562	531.52
6	17	3.2592	2639.95
6	18	1.0095	817.69
6	19	0.8869	718.38
6	20	0.8343	675.78
6	21	0.7587	614.54
6	22	0.4405	356.80
7	23	3.3939	2749.05
7	24	0.6712	543.67

Total Sierra of Zacatecas Recharge = 18.7766×10^6

= 15,209.05 AF/Yr

since the aquifer is in steady state, the total balance through discharge zones is 1.465E+06 M^3/day (1.186E+03 AF/day), which is approximately equal, whithin the accuracy ranges of the calculation, to the 1.342E+06 M^3/day (1.087E+03 AF/day) assumed infiltration.

Transient State

A comparison of results between the heads obtained using the two dimensional model, and the ones obtained by kriging is presented in figure 4.6. In addition a perspective plot of the piezometric surface is presented in figure 4.7. Clearly, the maximum differences occured in areas where data were not available such as the southern and northern region of the study area. According to the hydraulic head residual kriging error map of 1985 (figure 3.28), the greatest intervals took on values of +/- 4 meters at the southern and +/- 3 meters at the northern part of the basin. Whereas the smallest interval took on the value of +/- 1 meter at the central part of the basin.

A look at the evolution of the piezometric surface after several years of pumpage confirms the conceptual model of the behavior of the Calera aquifer. Its hydrogeologic characteristic, namely fairly low transmissivity and large specific yield, suggest the simulated results. Clearly, as a result of heavy pumpage and reduction of the natural outflow a cone of depression has formed in the northern region of the aquifer. The zone of depression of the water table are very steep and restricted to a small region around the pumping area. The effects of pumping are limited to a distance of 5 Km (3.11 Miles) from

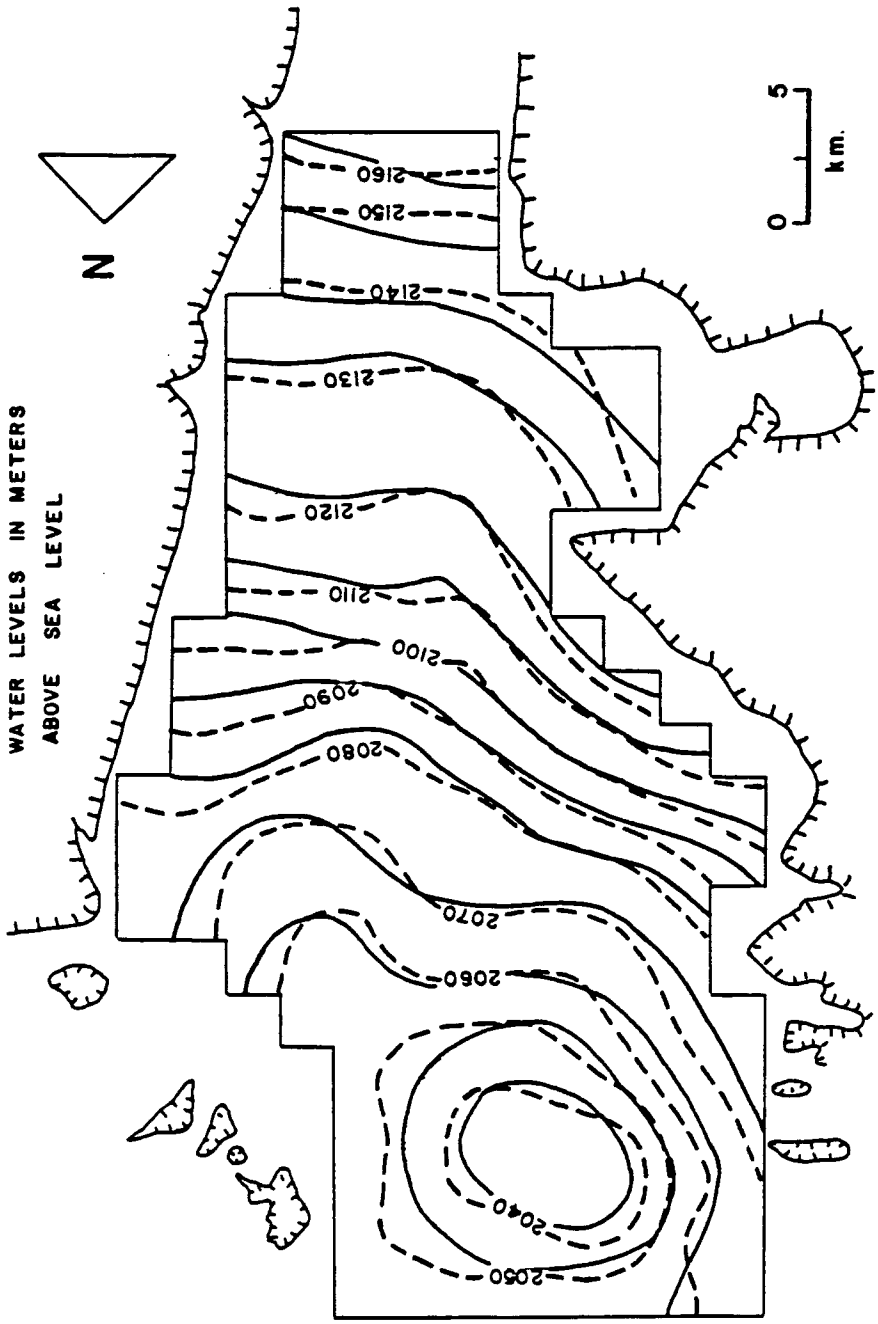

Figure 4.6 Comparison between kriged and computed hydraulic heads.

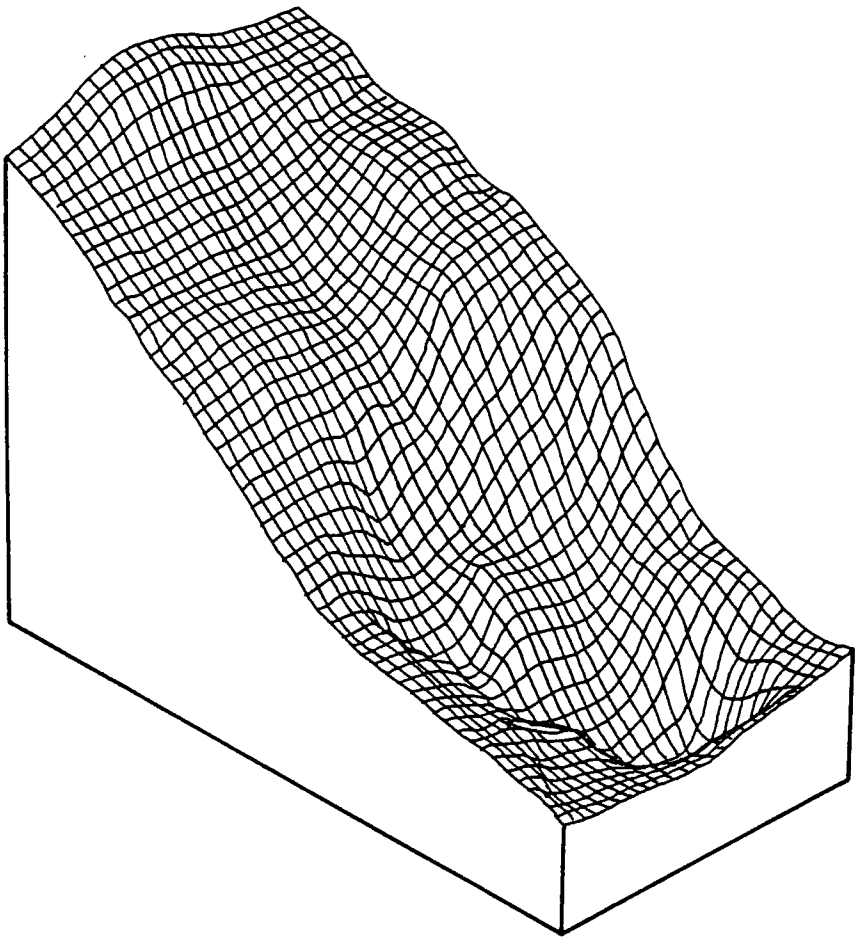

Figure 4.7 Perspective plot of 1985 piezometric surfaces.

the pumping center, after 29 years. Notice, the simulated drawdowns represent an average over the area associated with each node. Actual drawdowns in individual wells may be much larger. In terms of flow, the source of the extracted water are storage and discharge zones. Initially, most water withdrawn came from storage. As time evolves, the natural outflow was reduced and some springs became dry. This provided the additional source of water to balance the withdrawals. Therefore, the mass balance at the end of the 1956-1985 period can be summarized as follow. Inasmuch as the natural outflow became neglible, then, the total flow out of the aquifer is 293,150 M^3/day (237.45 AF/day) produced mainly by pumpage. When the infiltration is subtracted, the total balance out of the system is 146,650 M^3/day (118.79 AF/day). Obviously, this net balance out of the system is withdrawn from storage. Clearly, the total balance out of the system is almost twice the recharge rate.

Sensitivity Aanalysis

The purpose of this analysis is to determine the sensitivity of computed head values to changes in transmissivity and specific yield at different points in the model. The results of the sensitivity analysis provide insights into the reliability of calibrated transmissivities and specific yield values.

The Calera model model was analysed for sensitivity in two ways. One was to multiply specific yield and transmissivity in each node of the model by the same percentage and observe the effect of this

change on calculated water levels. The other way was to modify one parameter in a particular location, while holding the other model parameters and the review parameter in other locations the same as in the calibration run.

The effects of +/- 20% variations in transmissivity or specific yield throughout the model on calculated drawdowns for the period 1956 to 1985 along row 8 are shown in figures 4.8 and 4.9. The sensitivity of calculated water levels to +/- 20% variations in specific yield or transmissivity is generally small and dependent on location within the model. That is, +/- 20% specific yield variations have a larger effect than +/- 20% transmissivity in areas where large scale storage depletion is taking place.

Inasmuch as the specific yield parameter is the least reliable due to the fact that it was estimated for the entire aquifer from a hydrologic budget procedure, for this reason, a sensitivity analysis was performed in particular locations. The methology used for the specific yield analysis was developed by Boggs (1980). The general procedure used to measure the relative sensitivity of computed heads to changes in specific yield is outlined below.

First, twelve areas or zones of equal size and shape were selected within the basin model as shown in figure 4.10. The number and location of zones were chozen to provide a reasonably uniform distribution over the model with representation of all hydrogeologic conditions. On this basis, square zones, 4 by 4 Km (2.50 by 2.50 Miles) in area were selected. Next, the sensitivity of each zone was computed

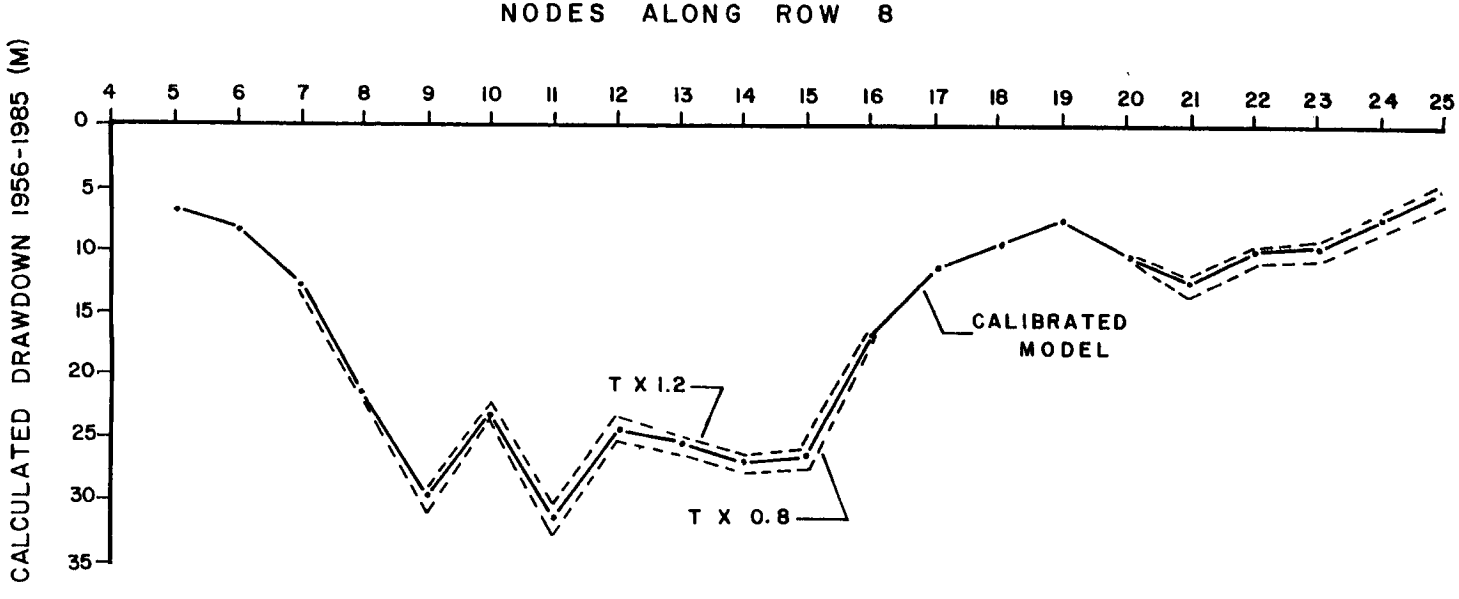

Figure 4.8 Effects of varying the aquifer transmissivity on model calculated drawdown in Calera basin.

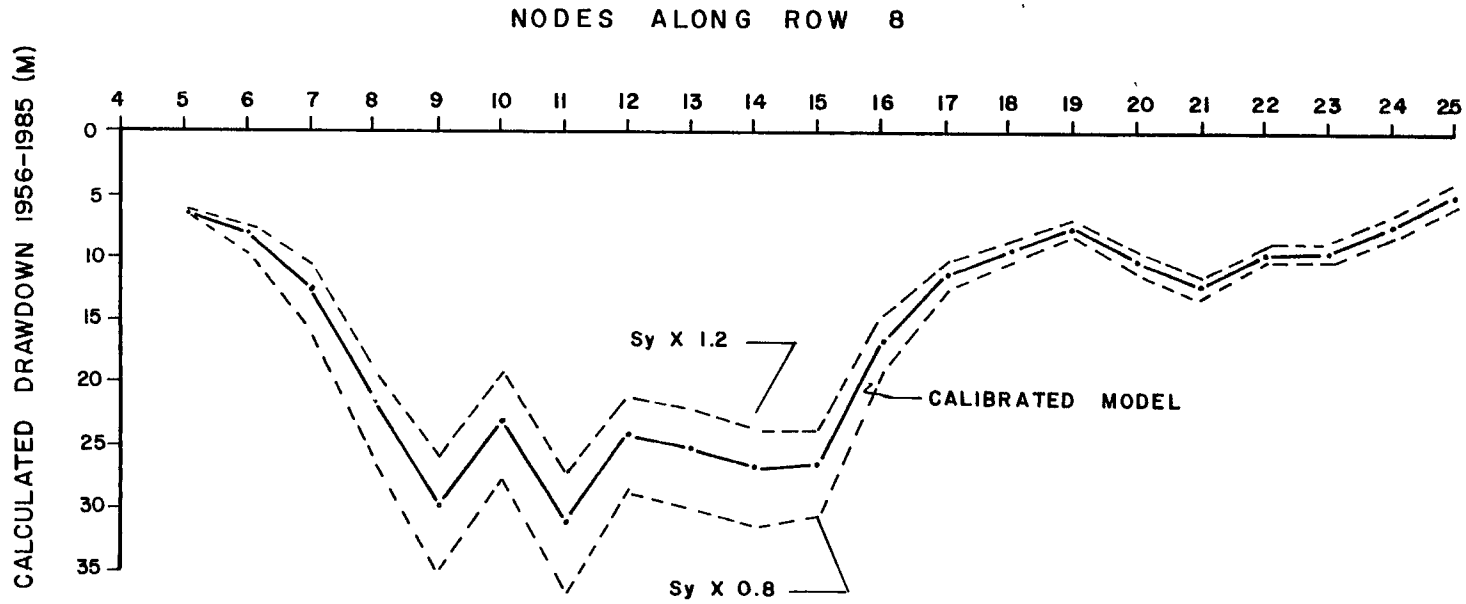

Figure 4.9 Effects of varying the aquifer specific yield on model calculated drawdown in Calera basin.

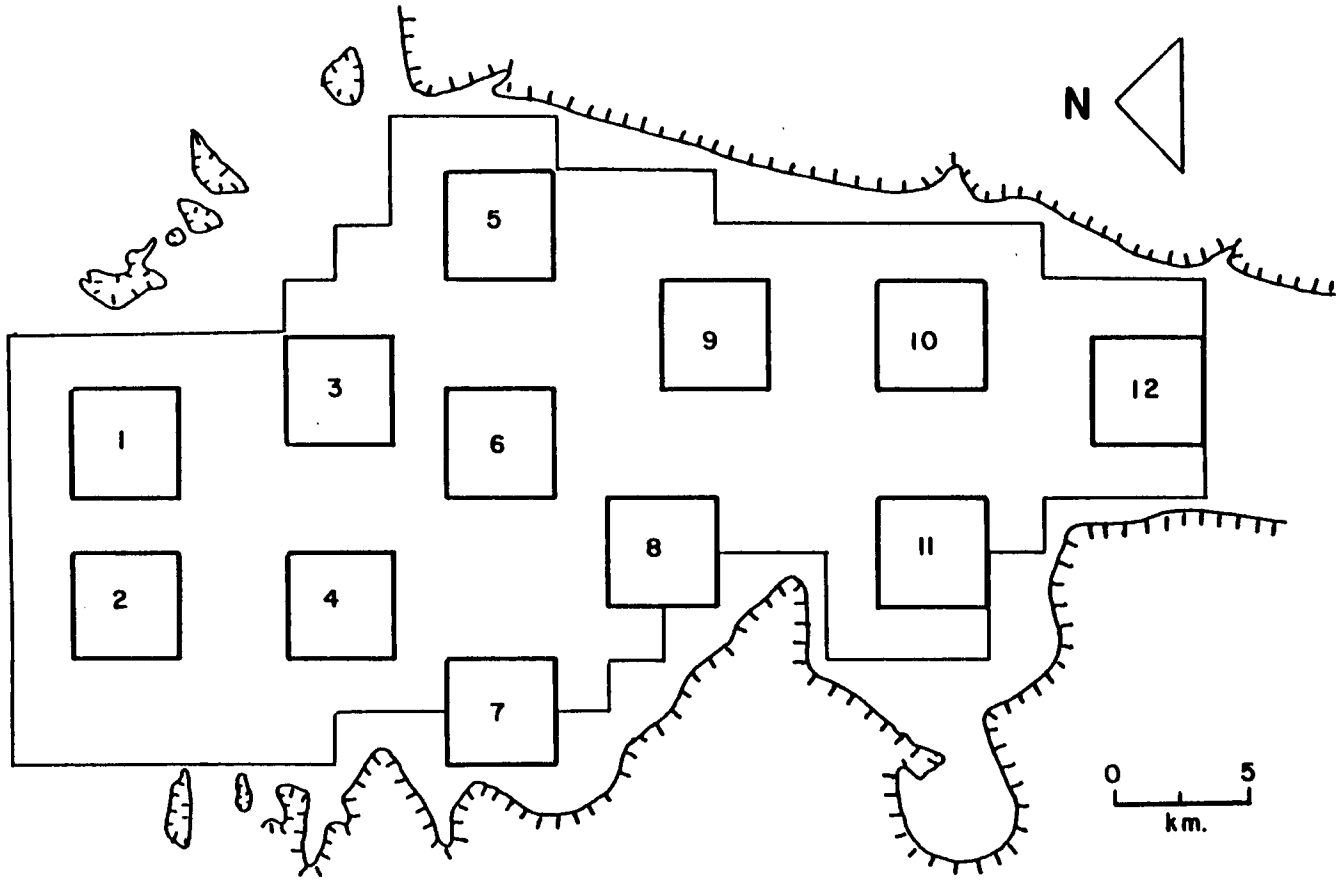

Figure 4.10 Sensitivity zones.

separately. Specific yield values within all elements of a given zone were increased by fifty percent holding the rest of the model parameters constant at their calibrated values. The model was again run with this data set for a 29 year period to calculate the new 1985 water levels. Finally, a sensitivity coefficient, Bn, was defined for each sensitivity zone. According to Boggs the sensitivity coefficient can be calculated with the following equation

$$Bm = \sum_{n=1}^{N} h_n * S_n \qquad \text{for all } h \geqslant 0.30 \text{ m and } n = 1,2,..,N$$

where h_n is the absolute value of the resulting head change at node n, S_n is the area of the subdomain associated with node n, m is the sensitivity zone number, and N is the total number of nodes in the finite difference grid. Values of normalized sensitivity coefficients, B^*, (normalized to the lowest B value, i.e $B^*_m = B_m/B_{12}$) are presented in table 4.3. A contour map of normalized sensitivity for the model is given in figure 4.11. The largest normalized sensitivity coefficients was 2.04 in zone # 3 which is an area of intensive pumping. Furthermore, the sensitivity contour map shows the zone of relatively high sensitivity extending in an arc from the northern region, through the central part of the basin, to the southern basin boundary. Within this zone, sensitivity is lowest in the Sierra Madre Occidental and Sierra of Zacatecas, becoming progressively more sensitive in the direction of the natural outflow, the northern basin boundary.

When considered in the context of hydrologic conditions, the sensitivity distribution shown in figure 4.11 suggest that sensitivity

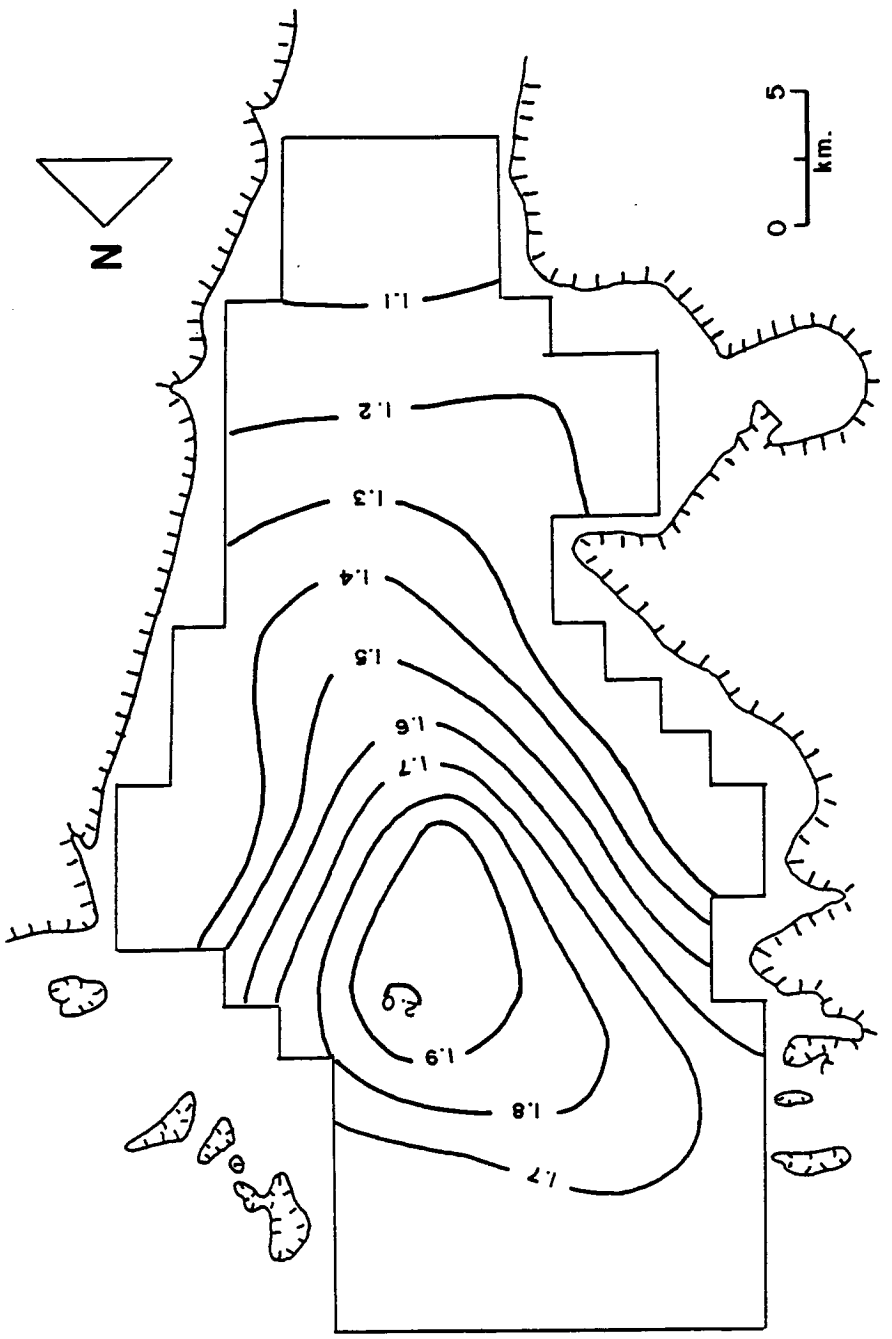

Figure 4.11 Contour map of normalized sensitivity coefficients.

is primarly a function of the dewatering process. Clearly, sensitivity is lowest in areas where little pumpage is taking place.

The results of the sensitivity analysis support earlier statements concerning the calibration of the basin model. That is, except for the northern central region, errors in specific yield in the upper land areas have little effect elsewhere. Thus, possible inaccuracies in the calibration of these areas will not affect pumping simulation results significantly. The areas of highest sensitivity occur mainly within the basin lowlands model which is believed to be accurately calibrated.

Table 4.3

SENSITIVITY ANALYSIS RESULTS

Zone	Sensitivity Coefficient, B	Normalized Sensitivity Coefficient, B*	Average Head Change
1	8.8160E+07	1.51	2.87
2	1.0712E+08	1.84	1.89
3	1.1896E+08	2.04	5.01
4	1.0408E+08	1.79	3.73
5	7.3040E+07	1.25	1.95
6	1.1600E+08	1.99	3.60
7	6.4200E+07	1.10	0.14
8	7.3120E+07	1.26	0.52
9	8.6720E+07	1.49	1.60
10	6.9120E+07	1.19	0.61
11	7.0360E+07	1.21	0.72
12	5.8200E+07	1.00	0.15

CHAPTER FIVE

GROUNDWATER HYDRAULIC MANAGEMENT MODEL

In the previous chapter, a groundwater simulation model was performed to calibrate the hydrologic parameters of the aquifer. Such a simulation model is a valuable tool to aid in the decision making process. Such decisions may include the location of production wells, pumping rates, and pumping schedules. The computer model can be used to determine the effects of the various decisions. However, because essentially an infinite number of different managements schemes can be used, it would be impossible to use the model to predict the outcome of every possible scheme. It is therefore unlikely to arrive at the optimal operating conditions. The use of systems analysis coupled with the simulation model provides the basis of a powerfull decision making tool. Two approaches to couple the groundwater simulation model with the mathematical optimization model are through the embedding technique and the response matrix technique. The coupling of these two types of models forms the management model. The output from the management model will be the optimal operating conditions. It is the response matrix technique which is applied in this study for the groundwater management. The response functions are obtained using a two dimensional iterative ADI program developed by Maddock (1974 a), and represent the relationship between pumpage at a well and the induced drawdowns in surrounding wells with time.

Objective

The growing demand for water in the Calera basin has caused substantial decline in the water table. In addition, according to the results obtained from the simulation model, the future for groundwater supplies in the Calera basin are not favorable unless the groundwater management district of the area make important decisions regarding their water supply. As a result, the major objective of this chapter is to illustrate the effects on the aquifer of an efficient groundwater development scheme which may be effective in the overall preservation of the future groundwater resources in the Calera basin. Because of the lack of data regarding the economics of water allocation, our decisions are primarily based on the groundwater hydraulics.

Response Functions

As previously mentioned, the simulation model is coupled with the linear programming algorithm by means of the response matrix technique. This technique involves determining a set of functions that relate pumping over time at wells to drawdowns to those wells (Maddock,1972). The general form of this relationship is

$$s(k,n) = \sum_{i=1}^{n} \sum_{j=1}^{N_w} Q(j,i)\, \beta(k,j,n-i+1) \text{ ---} \qquad (5.1)$$

where: $s(k,n)$, is the drawdown at the point k at the end of the period of time n; N_w, is the number of pumping wells; $Q(j,i)$, is the pumping

rate at well j during the i^{th} time period; n, is the total number of periods of time; k, is the two dimensional Cartesian space vector in the horizontal plane; ß (k,j,n-i+1), is the response coefficient. The response coefficient represents the average drawdown in the discrete cell associated with the k^{th} observation well at the end of the n^{th} pumping period due to a unit pumpage at the j^{th} well applied throughout the i^{th} pumping period. Inasmuch as the response coefficients are usually obtained from digital simulation models, equation (5.1) represents its discrete form. As the response function relates pumping to drawdown, it is a function of the type of partial differential equation being used to represent the flow regime, the spatial distribution of transmissivity, storativity, the spatial distribution of pumping, the homogeneous initial conditions and the type of boundary conditions. They are independent of pumping rate. However, equation (5.1) expresses a linear relationship between drawdown and pumping. This result is obtained only when the partial differential equation representing the flow regime is linear. In the case of an unconfined aquifer, such as in the Calera basin, the governing equation is

$$\frac{\partial}{\partial x}\left[Kh\frac{\partial h}{\partial x}\right] + \frac{\partial}{\partial Y}\left[Kh\frac{\partial h}{\partial Y}\right] = S_y\frac{\partial h}{\partial t} + \sum_{j=1}^{N_w} Q(j,t)(x-x_j) \quad \text{---} \quad (5.2)$$

However, equation (5.2) is not linear in h. A linear approximation of equation (5.2) can be produced as follow (Maddock, 1974 b)

$$\frac{\partial}{\partial x}\left[T'\frac{\partial s^*}{\partial x}\right] + \frac{\partial}{\partial Y}\left[T'\frac{\partial s^*}{\partial Y}\right] = S_y\frac{\partial s^*}{\partial t} + \sum_{j=1}^{N_w} Q(j,t)(x-x_j) \quad \text{---} \quad (5.3)$$

where:

$T' = H K$

$H = 1/A \int H_o \, dA$;A, is the areal extent of the aquifer

$s^* = 1/H \, (sH_o - 0.5 \, s^2)$

then, the initial and boundary conditions are as follow:

initial conditions.-

$$s^* = 0 \quad \text{at} \quad t = 0$$

boundary conditions.-

constant head along

$$s^* = 0 \quad \text{along} \quad \Gamma$$

unperturbed boundary condition along

$$\frac{\partial s^*}{\partial n} = 0 \quad \text{along} \quad \Gamma'$$

the error introduced by this linearization is of the order of s/H_o. Inasmuch as equation (5.3) is linear, response functions can be obtained using equation (5.1). In practice, the response functions can be obtained by subjecting a calibrated finite difference model of the flow domain to unit discharges at each pumping well utilizing known initial and boundary conditions. The procedure proposed by Maddock is as follow: a) the domain is discretizes; b) to each cell or node, values of hydraulic parameters are assigned; c) the boundary conditions are identified and quantified for input to the model; d) the location of wells are designated; e) a unit pumpage is assigned to the first well during the first time step and zero units for the rest of the time steps, the procedure is repeated for the rest of the wells; f) the drawdowns calculated at each well in this manner are the response

coefficients in equation (5.1).

Formulation of the Management Model

In this study an objective function based on the physical capability of the system is proposed. The model shows the maximum amount of water that may be pumped while mantaining the drawdowns within reasonable limits. The formulation of the model is as follow:

$$\text{Max } Q = \sum_{k=1}^{M} \sum_{n=1}^{N} q(k,n) \qquad (5.4)$$

$$q(k,n) \leqslant Q_{max}(k) \quad \text{for all k and n} \qquad (5.5)$$

$$\sum_{k=1}^{M} q(k,n) \geqslant D(n) \quad \text{for all n} \qquad (5.6)$$

$$\sum_{j=1}^{M} \sum_{i=1}^{N} q(j,i)\, \beta(k,j,n-i+1) \leqslant \rho b(k) \qquad (5.7)$$

where: Q, is the sum of pumpages of M wells for N time periods; q(k,n), is the pumpage of well k during period n; Q_{max}, is the upper limit well field capacity of well field k; D(n), is the water demand required for time period n; b(k), is the saturated thickness before pumpage started; ρ, is a value within the interval $0 < \rho > 1$; and $\rho b(k)$, is the useable saturated thickness for well k up to the end of period n.

According to this groundwater management model, the objective function, equation (5.4), tries to find the maximum quantity of pumpage from M well fields for N time periods. Constraint (5.5) states that

the quantity of water pumped from the k^{th} well field for all n may not exceed some design capacity, $Q_{max}(k,n)$. Constraint (5.6) states that the sum of pumpages from M well fields during any time period should meet the water demand during any time period, D(n). Constraint (5.7) states that the drawdown for the k^{th} well field may not exceed a limit, $\overline{b}(k)$. Clearly, constraint (5.7) considers the continuity equation that describes the flow regime through the response coefficients. The set of equations (5.4) through (5.7) form a linear programming model that can be solved by any linear programming package. For each well field and time step there are one unknown, q(k,n).

Application of the Groundwater Management Model to the Calera Basin

In order to evaluate the potential pumpage of the Calera aquifer, a number of well fields had to be designated in the area. However, a management model for the entire aquifer would have been prohibitively large. In other words, a management model for the entire aquifer involves computing response functions at each nodal point of the grid. As a result, response functions were obtained at selected nodes according to the following criterion. Inasmuch as the model was developed for a microcomputer system, the memory of the system had to be taken into account. In addition, the number of response functions were restricted by the linear programming package used to solve the set of linear equations. That is, the linear programming package used

in our model was the LP88 version 3.12 (Eastern Software Products, Inc., 1984). This linear programming package can handle efficiently as many as 255 constraints and 2255 variables and requires at least 128 K bytes of memory. Another factor that affected the number of well fields was their pumping capacity. That is, each well field represents the total pumpage from several real wells in its vecinity. Therefore, response functions were obtained at well fields which had a pumping capacity greater than 141 Lps (5 Ft^3/sec). The time horizon considered in our study consisted in two time steps, each time step consisted in five years. That is, optimal pumpage policies were obtained for the periods 1985-1990 and 1991-1995. Thus, considering these factors in mind, the total number of well fields at which response functions were computed were 63. Figure 5.1 shows the distribution of the chosen nodes. According to the number of time steps and the number of well fields; the total number of variables and constraints were 123 and 254, respectively.

Once the total number and location of well fields were defined, the response functions were obtained at each well field and for each time step by a finite difference program developed by Maddock (1974). The hydrologic parameters such as transmissivity and storativity used in the finite difference program were obtained from previous chapters. That is, transmissivity estimates were obtained from the geostatistical method called Kriging performed in chapter three; storativity estimates were obtained from the calibrated simulation model performed in chapter four. In addition, the calibrated simulation model was used to generate the steady state hydraulic heads (H_o) taking as initial

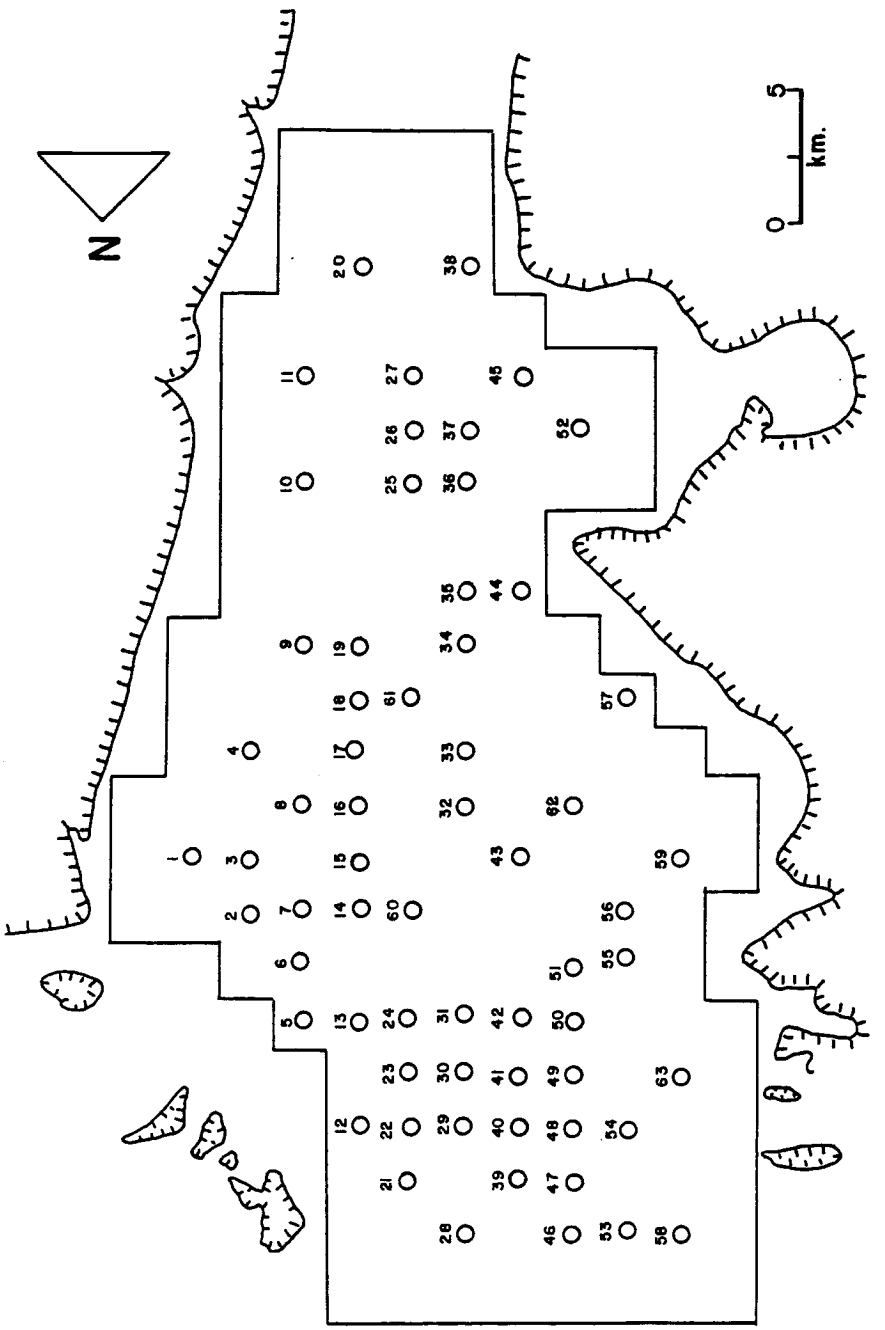

Figure 5.1 Locations at which response functions were computed.

condition the 1956 water table. In other words, according to equation (5.1), s is the drawdown at a particular time and location, therefore, to calculate the water table configuration at the end of each time step due to the optimal pumpage policy, one had to consider the drawdown produced by non-optimal pumpage during the period 1956-1985. That is, s'+s, where s' is the drawdown produced by non-optimal pumping rates. Therefore, to obtain the optimal water table at the end of each time period, one had to superimpose the total drawdown, s'+s, on the steady state water table configuration. According to the number of well fields and the number of time steps, the total number of ß's coefficients was 7938. Analyzing the response functions, their values range from 35.7 to 84 sec/M^2 (3.32 to 7.80 sec/Ft^2) and 20.6 to 76 sec/M^2 (1.91 to 7.06 sec/Ft^2) for the first and second time periods, respectively. Clearly, the highest values were obtained in well fields located near no flow boundary conditions or in areas of low transmissivity, whereas the lowest values were found in areas of high transmissivity or storativity.

Having computed the response functions at each well field and for each time period, the set of linear equations, (5.4) through (5.7), were solved to obtain the optimal pumping patterns subject to the following management schemes. Three management schemes were considered to obtain our goal. The criteria considered to come up with the three management alternatives were based on the water demands in the region, maximum well field capacity and percentage of useable saturated thickness.

First management scheme.- Two five years optimal pumpage policies will be generated for a total time of 10 years. In order to accomplish such "optimal pumpage scheme", water demand for the first five years was estimated to be 1.2E08 M^3/Yr (9.72E04 AF/Yr) and 1.5E08 M^3/Yr (1.22E05 AF/Yr) for the second five years. According to some water management from the region, the southern area of the basin has favorable conditions for agricultural purposes. Therefore, water demands were obtained based on crop consumptive use. Regarding the well field capacity, the estimate of 227 Lps (8 Ft^3/sec) was obtained taking into account the following facts. As previously mentioned, pumpage from irrigation, municipal and industrial wells which laid on the same cell were added up and assigned to a single well field or node in the grid. In the process of associating pumpage to each well field, it was found that each well field comprises in the average five or six wells. Furthermore, the actual well capacity of a production well for agricultural purpose range from 28.3 to 48 Lps (1.0 to 1.7 ft^3/sec). Thus, it was reasonable to assign a maximum well field capacity of 227 and 340 Lps (8 and 12 Ft^3/sec) for the first and second periods of time, respectively. Inasmuch as the water table has declined 30 M (80 Ft) during the period of 1956-1985 in the northern part of the aquifer, as a result, it was necessary to reduce the effects of pumping in this particular area. Therefore, a 5 percent of the 1984-1985 saturated thickness is allowed to be deplited during the first and second periods.

Second management scheme.- Another alternative to obtain the optimal pumpage policies from these 63 well fields is to consider

different values for well field capacity and allowable saturated thickness in constraints (5.5) and (5.7). That is, the well field capacity for the second period of time is reduced from 340 to 227 Lps (12 to 8 Ft^3/sec). In addition, the 5 percent useable saturated thickness is increased to 10 percent for the second time period. The reasoning to increase the useable saturated thickness in the second time period is based on the fact that, altough 340 Lps (12 Ft^3/sec) of well field capacity in the previous management scheme, the water demand could not be met by decreasing 5 percent of allowable saturated thickness. For example, the first time period might have used the total 5 percent to meet its water demand. The water demands for the two periods of time remain the same.

Third management scheme.- Similarly to the previous management schemes, the water demands for both periods of time are kept without modifications. Likewise, the 5 and 10 percent of useable saturated thickness for both period are unchanged. The only modification is the well field capacity for both periods. For instance, the well field capacity is increased from 227 to 1415 Lps (8 to 50 Ft^3/sec). According to this strategy, the well field capacity is set equal to a large enough value so that the useable saturated thickness together with continuity control the maximum allowable pumpage. Furthermore, this strategy provides a criterion to expand agricultural lands. That is, areas with low pumpage rates should not be considered for agricultural purposes, but may be considered for industrial purposes.

Evaluation of Computational Results

The purpose of this section is to assess the results obtained in each management scheme and choose the optimal pumpage policy for the Calera basin.

First management scheme.- The distributed optimal pumpage policies for the two periods are listed in tables 5.1 and 5.2 together with the allowed aquifer saturated thickness, actual saturated thickness used and well field capacity for each well field. Clearly, in this policy the water demand for the first period was met, however, the strategy failed to meet the water demand for the second period of time. That is, according to tables 5.1 and 5.2, most of the 5 percent of the useable saturated thickness was exhausted during the first period of time. As a result, pumping rates were very low during the second period, and therefore, they did not meet the required water demand. Hence, based on this fact, the first management scheme to obtain optimal pumpage policies was rejected.

Second management scheme.- Similarly, results obtained under this policy are listed in tables 5.3 and 5.4. According to the results, this strategy was capable of obtaining optimal pumpage for the two periods of time. As a result, the total amount of water that can be extracted from the 63 well fields under optimal conditions at the end of the first five years is 1.32E+08 M^3/Yr (1.07E+05 AF/Yr). The water demand for this period was 1.2E+08 M^3/Yr (9.72E+04 AF/Yr). On the other hand, some well fields used their maximum well field capacity, 227 Lps (8 Ft^3/sec), without using the full 5 percent of the

saturated thickness. Consequently, they are located in areas where groundwater hydraulic conditions are favorable to agricultural land use, for example, well fields 13, 15, and 20. For the second five years period, the total amount of water that can supply the well fields under these optimal conditions is 1.5E+08 M^3/Yr (1.2E+05 AF/Yr). Clearly, the water demand was hardly met, besides, more well fields were obtained pumping at their maximum capacity without using the 10 percent useable saturated thickness limit. As a result, the capacity of these well fields could be increased to a limit that would allow to use the full 10 percent saturated thicness bound.

Third management scheme.- In order to find out the maximum pumping rate at well fields which did not use the 5 and 10 percents of useasble saturated thickness limit, the well field capacity was increased to 1415 Lps (50 Ft^3/sec). Results for both periods are listed in tables 5.5 and 5.6. The total amount of water that can supply the 63 well fields at the end of the first five years period using 5 percent of saturated thickness is 1.47E+08 M^3/Yr (1.18E+05 AF/Yr). The water demand was exceeded by 2.68E+07 M^3/Yr (2.17E+04 AF/Yr). The pumping rates at well fields varied from 0 to 448 Lps (0 to 15.84 Ft^3/sec). The 5 percent saturated thickness ranged from 5.8 M (19 Ft), in the northwestern region, to 14.6 M (48 Ft) in the north central part of the aquifer. For the second five years period, the total amount of water that can be extracted from the system is 1.7E+08 M^3/Yr (1.38E+05 AF/Yr). The demand for this period was far exceeded by 1.99E+07 M^3/Yr (1.61E+04 AF/Yr). The maximum pumping rates fluctuated within the range of 544 and 100 Lps (19.20 and 3.53 Ft^3/sec).

Similarly, the 10 percent saturated thickness was within the interval of 30 and 8 M (97 and 39 Ft).

A general assessment of the three management schemes revealed that the first strategy failed to meet the water demand for the second period. In other words the 5 percent of useable saturated thickness was not enough to provide the water to meet the demand. Next, the second management scheme succeeded in meeting the water demands for both periods. In addition, some well fields, for example 14, 26, 39, 46, 47 and 53, can be considered inoperatives due to their low pumping rates during the first period of time. However, they should be reincorporated to the system to help meet the water demand for the second period. Clearly, the second management scheme was chosen to provide the optimal pumpage policies for the Calera aquifer. However, the third management scheme produced an optimal pumpage policy that exhausted the total useable saturated thickness. Consequently, the latter approach can be used as a criterion to increase the well field capacity at well fields operating under the second management scheme but without exhausting the useable saturated thickness.

Once the optimal pumping rates were obtained, the total drawdown at each well field was substracted from the initial water table configuration of 1956 to obtain the optimal water levels at the end of the first and second five years time piriods. That is, figures 5.2 and 5.3 show the final water level configuration at the end of 1990 and 1995, respectively. In an attempt to show the effects on the aquifer of non-optimal pumping rates, the simulation model was run to obtain non-optimal water levels at the end of 1990 and 1995. For this purpose,

the 1985 water demand remained constant for both periods. According to this criterion, drawdowns may be underestimated at the end of each time period due to the fact that the amount of water required in 1985 is less than the water demands considered during the management model. Figures 5.4 and 5.5 show the non-optimal hydraulic head distribution at the end of 1990 and 1995, respectively. According to the optimal hydraulic head distribution at the end of 1990, the cone of depression in the northern area of the basin increased. In addition, a small cone appeared in the south central part of the basin. However, the non-optimal head distribution shows steeper hydraulic gradients and the cone of depression with much larger radius. According to the hydraulic head distribution at the end of 1995, as expected, the radius of the cones of depression and the hydraulic gradient increased. For example, heads declined 10 M (32.8 Ft) in the northern area and the cone of depression increased approximately five times in the south central area after an increased of pumpage to meet the water demand for this period. However, by pumping at the non-optimal rates, the results were not satisfactory, that is, the radius of the cones of depression were larger than those produced under optimal conditions and the hydraulic gradient was steeper in heavily pumped areas. In addition, the non-optimal heads were obtained as a result of affecting the aquifer with pumping rates that only met the 1985 water demand. Clearly, the results showed that the water demand can be met under optimal pumping rates for the two time periods. However, 5 and 10 percent of the 1985 saturated thickness should be used up. Furthermore, the effects on the aquifer under optimal stresses help to keep the hydraulic heads at a

desirable level while meeting the water demands. On the other hand, non-optimal pumping rates produced drawdowns that were even greater than the 5 and 10 percent allowable saturated thickness while just meeting the 1985 water demand. As a result, groundwater decision makers will have to consider this fact in mind for future agricultural, municipal or industrial water allocations.

Table 5.1

OPTIMAL PUMPING RATES ACCORDING TO THE FIRST MANAGEMENT SCHEME FOR THE FIRST PERIOD. WELL FIELD CAPACITY 227 LPS (8 FT^3/SEC).

WELL FIELD	OPTIMAL PUMPING RATES		5% SAT. THICKNESS		OPTIMAL DRAWDOWN	
	LPS	FT^3/SEC	M	FT	M	FT
1	201.5	7.12	9.4	31	9.4	31.0
2	226.2	7.99	8.8	29	8.8	29.0
3	226.5	8.00	8.8	29	8.8	29.0
4	226.5	8.00	11.5	38	9.5	31.2
5	0.0	0.00	8.8	29	0.0	0.0
6	226.5	8.00	8.5	28	8.5	28.0
7	0.0	0.00	8.5	28	0.0	0.0
8	226.5	8.00	11.2	37	10.6	34.9
9	226.5	8.00	10.3	34	10.3	34.0
10	226.5	8.00	11.5	38	9.5	31.3
11	226.5	8.00	13.7	45	8.3	27.5
12	191.7	6.77	9.4	31	8.8	28.9
13	226.5	8.00	10.6	35	9.0	29.5
14	161.4	5.70	8.5	28	8.5	28.0
15	226.5	8.00	10.9	36	10.9	36.0
16	216.9	7.66	10.9	36	10.9	36.0
17	180.1	6.36	8.8	29	8.8	29.0

Table 5.1--Continued

WELL FIELD	OPTIMAL PUMPING RATES LPS	OPTIMAL PUMPING RATES FT^3/SEC	5% SAT. THICKNESS M	5% SAT. THICKNESS FT	OPTIMAL DRAWDOWN M	OPTIMAL DRAWDOWN FT
18	0.0	0.00	8.8	29	0.0	0.0
19	184.9	6.53	9.1	30	9.1	30.0
20	226.5	8.00	11.5	38	8.7	28.6
21	194.2	6.86	9.1	30	9.1	30.0
22	0.0	0.00	11.5	38	0.0	0.0
23	226.5	8.00	14.6	48	8.6	28.2
24	226.5	8.00	14.6	48	9.0	29.6
25	186.0	6.57	9.4	31	9.4	31.0
26	161.7	5.71	8.8	29	8.8	29.0
27	206.4	7.29	9.1	30	9.1	30.0
28	136.1	4.81	6.7	22	6.7	22.0
29	0.0	0.00	10.9	36	0.0	0.0
30	0.0	0.00	13.7	45	0.0	0.0
31	226.5	8.00	13.7	45	8.1	26.7
32	188.8	6.67	8.8	29	8.8	29.0
33	180.3	6.37	9.1	30	9.1	30.0
34	226.5	8.00	9.1	30	9.1	30.0
35	186.3	6.58	9.4	31	9.4	31.0
36	180.6	6.38	9.4	31	9.4	31.0
37	183.2	6.47	9.4	31	9.4	31.0

Table 5.1--Continued

WELL FIELD	OPTIMAL PUMPING RATES LPS	OPTIMAL PUMPING RATES FT^3/SEC	5% SAT. THICKNESS M	5% SAT. THICKNESS FT	OPTIMAL DRAWDOWN M	OPTIMAL DRAWDOWN FT
38	226.5	8.00	10.3	34	10.3	34.0
39	135.1	4.77	6.4	21	6.4	21.0
40	0.0	0.00	10.3	34	0.0	0.0
41	0.0	0.00	13.7	45	0.0	0.0
42	226.5	8.00	13.7	45	8.1	26.8
43	210.6	7.44	9.1	30	9.1	30.0
44	174.1	6.15	9.1	30	9.1	30.0
45	217.4	7.68	9.7	32	9.7	32.0
46	96.0	3.39	6.4	21	5.5	16.8
47	0.0	0.00	5.7	19	0.0	0.0
48	0.0	0.00	8.5	28	0.0	0.0
49	226.5	8.00	10.6	35	8.0	26.4
50	226.5	8.00	10.9	36	9.0	29.7
51	226.5	8.00	10.9	36	8.9	29.3
52	218.6	7.72	9.7	32	9.7	32.0
53	0.0	0.00	6.4	21	0.0	0.0
54	169.9	6.00	8.2	27	8.2	27.0
55	171.8	6.07	7.9	26	7.9	26.0
56	178.9	6.32	8.2	27	8.2	27.0
57	178.6	6.31	9.4	31	9.4	31.0

Table 5.1--Continued

WELL FIELD	OPTIMAL PUMPING RATES LPS	OPTIMAL PUMPING RATES FT^3/SEC	5% SAT. THICKNESS M	5% SAT. THICKNESS FT	OPTIMAL DRAWDOWN M	OPTIMAL DRAWDOWN FT
58	174.6	6.17	8.8	29	8.8	29.0
59	196.7	6.95	8.5	28	8.5	28.0
60	205.0	7.24	9.1	30	9.1	30.0
61	191.7	6.77	9.1	30	9.1	30.0
62	189.4	6.69	9.1	30	9.1	30.0
63	226.5	8.00	9.4	31	9.4	31.0

Table 5.2

OPTIMAL PUMPING RATES ACCORDING TO THE FIRST MANAGEMENT SCHEME FOR THE SECOND PERIOD. WELL FIELD CAPACITY 340 LPS (12 FT^3/SEC).

WELL FIELD	OPTIMAL PUMPING RATES LPS	FT^3/SEC	5% SAT. THICKNESS M	FT	OPTIMAL DRAWDOWN M	FT
1	33.4	1.18	9.4	31	9.4	31.0
2	16.1	0.57	8.8	29	8.8	29.0
3	15.3	0.54	8.8	29	8.8	29.0
4	116.4	4.11	11.5	38	11.5	38.0
5	170.2	6.01	8.8	29	8.8	29.0
6	14.4	0.51	8.5	28	8.5	28.0
7	162.2	5.73	8.5	28	8.5	28.0
8	63.7	2.25	11.2	37	11.2	37.0
9	49.3	1.74	10.3	34	10.3	34.0
10	116.4	4.11	11.5	38	11.5	38.0
11	229.3	8.10	13.7	45	13.7	45.0
12	21.8	0.77	9.4	31	9.4	31.0
13	52.1	1.84	10.6	35	10.6	35.0
14	5.7	0.20	8.5	28	8.5	28.0
15	38.5	1.36	10.9	36	10.9	36.0
16	25.2	0.89	10.9	36	10.9	36.0
17	10.8	0.38	8.8	29	8.8	29.0

Table 5.2--Continued

WELL FIELD	OPTIMAL PUMPING RATES LPS	OPTIMAL PUMPING RATES FT^3/SEC	5% SAT. THICKNESS M	5% SAT. THICKNESS FT	OPTIMAL DRAWDOWN M	OPTIMAL DRAWDOWN FT
18	125.4	4.43	8.8	29	8.8	29.0
19	16.7	0.59	9.1	30	9.1	30.0
20	154.9	5.47	11.5	38	11.5	38.0
21	17.6	0.62	9.1	30	9.1	30.0
22	138.4	4.89	11.5	38	0.0	0.00
23	161.9	5.72	14.6	48	14.6	48.0
24	184.6	6.52	14.6	48	14.6	48.0
25	17.8	0.63	9.4	31	9.4	31.0
26	9.9	0.35	8.8	29	8.8	29.0
27	36.0	1.27	9.1	30	9.1	30.0
28	15.6	0.55	6.7	22	6.7	22.0
29	168.5	5.95	10.9	36	10.9	36.0
30	229.6	8.11	13.7	45	0.0	0.0
31	157.4	5.56	13.7	45	13.7	45.0
32	26.6	0.94	8.8	29	8.8	29.0
33	20.1	0.71	9.1	30	9.1	30.0
34	20.7	0.73	9.1	30	9.1	30.0
35	20.1	0.71	9.4	31	9.4	31.0
36	16.1	0.57	9.4	31	9.4	31.0
37	15.3	0.54	9.4	31	9.4	31.0

Table 5.2--Continued

WELL FIELD	OPTIMAL PUMPING RATES LPS	OPTIMAL PUMPING RATES FT^3/SEC	5% SAT. THICKNESS M	5% SAT. THICKNESS FT	OPTIMAL DRAWDOWN M	OPTIMAL DRAWDOWN FT
38	46.1	1.63	10.3	34	10.3	34.0
39	7.1	0.25	6.4	21	6.4	21.0
40	153.2	5.41	10.3	34	0.0	0.0
41	265.0	9.36	13.7	45	0.0	0.0
42	173.8	6.14	13.7	45	13.7	45.0
43	46.4	1.64	9.1	30	9.1	30.0
44	13.3	0.47	9.1	30	9.1	30.0
45	40.8	1.44	9.7	32	9.7	32.0
46	25.8	0.91	6.4	21	6.4	21.0
47	88.3	3.12	5.7	19	5.7	19.0
48	115.2	4.07	8.5	28	8.5	28.0
49	66.8	2.36	10.6	35	10.6	35.0
50	59.5	2.10	10.9	36	10.9	36.0
51	95.1	3.36	10.9	36	10.9	36.0
52	46.7	1.65	9.7	32	9.7	32.0
53	100.8	3.56	6.4	21	6.4	21.0
54	17.3	0.61	8.2	27	8.2	27.0
55	16.4	0.58	7.9	26	7.9	26.0
56	32.8	1.16	8.2	27	8.2	27.0
57	17.0	0.60	9.4	31	9.4	31.0

Table 5.2--Continued

WELL FIELD	OPTIMAL PUMPING RATES LPS	OPTIMAL PUMPING RATES FT^3/SEC	5% SAT. THICKNESS M	5% SAT. THICKNESS FT	OPTIMAL DRAWDOWN M	OPTIMAL DRAWDOWN FT
58	17.6	0.62	8.8	29	8.8	29.0
59	44.5	1.57	8.5	28	8.5	28.0
60	39.1	1.38	9.1	30	9.1	30.0
61	17.6	0.62	9.1	30	9.1	30.0
62	34.8	1.23	9.1	30	9.1	30.0
63	57.2	2.02	9.4	31	9.4	31.0

Table 5.3

OPTIMAL PUMPING RATES ACCORDING TO THE SECOND MANAGEMENT SCHEME FOR THE FIRST PERIOD. WELL FIELD CAPACITY 227 LPS (8 FT^3/SEC).

WELL FIELD	OPTIMAL PUMPING RATES		5% SAT. THICKNESS		OPTIMAL DRAWDOWN	
	LPS	FT^3/SEC	M	FT	M	FT
1	201.5	7.12	9.4	31	9.4	31.0
2	205.5	7.26	8.8	29	8.2	27.4
3	226.5	8.00	8.8	29	8.8	29.0
4	226.5	8.00	11.5	38	9.5	31.2
5	161.9	5.72	8.8	29	7.1	23.4
6	201.3	7.11	8.5	28	7.9	26.0
7	185.7	6.56	8.5	28	7.3	24.0
8	226.5	8.00	11.2	37	10.6	34.9
9	226.5	8.00	10.3	34	10.3	34.0
10	226.5	8.00	11.5	38	9.5	31.3
11	226.5	8.00	13.7	45	8.3	27.5
12	167.6	5.92	9.4	31	8.8	28.9
13	226.5	8.00	10.6	35	9.2	30.5
14	36.2	1.28	8.5	28	3.4	11.4
15	226.5	8.00	10.9	36	10.9	36.0
16	217.7	7.69	10.9	36	10.9	36.0
17	176.6	6.24	8.8	29	8.8	29.0

Table 5.3-- Continued

WELL FIELD	OPTIMAL PUMPING RATES LPS	OPTIMAL PUMPING RATES FT^3/SEC	5% SAT. THICKNESS M	5% SAT. THICKNESS FT	OPTIMAL DRAWDOWN M	OPTIMAL DRAWDOWN FT
18	56.6	2.00	8.8	29	3.9	12.9
19	182.3	6.44	9.1	30	9.1	30.0
20	226.5	8.00	11.5	38	8.7	28.6
21	176.9	6.25	9.1	30	9.1	30.0
22	216.5	7.65	11.5	38	11.5	38.0
23	226.5	8.00	14.6	48	11.1	36.6
24	226.5	8.00	14.6	48	9.5	31.2
25	195.0	6.89	9.4	31	9.4	31.0
26	64.2	2.27	8.8	29	4.5	14.9
27	213.4	7.54	9.1	30	9.1	30.0
28	136.1	4.81	6.7	22	6.7	22.0
29	215.7	7.62	10.9	36	10.9	36.0
30	226.5	8.00	13.7	45	10.6	34.9
31	226.5	8.00	13.7	45	9.4	31.1
32	188.8	6.67	8.8	29	8.8	29.0
33	180.3	6.37	9.1	30	9.1	30.0
34	226.5	8.00	9.1	30	9.1	30.0
35	186.8	6.60	9.4	31	9.4	31.0
36	121.4	4.29	9.4	31	6.7	22.0
37	192.5	6.80	9.4	31	9.4	31.0

Table 5.3-- Continued

WELL FIELD	OPTIMAL PUMPING RATES LPS	OPTIMAL PUMPING RATES FT^3/SEC	5% SAT. THICKNESS M	5% SAT. THICKNESS FT	OPTIMAL DRAWDOWN M	OPTIMAL DRAWDOWN FT
38	226.5	8.00	10.3	34	10.3	34.0
39	0.0	0.00	6.4	21	0.0	0.0
40	199.6	7.05	10.3	34	10.3	34.0
41	226.5	8.00	13.7	45	10.3	34.1
42	226.5	8.00	13.7	45	9.5	31.2
43	210.6	7.44	9.1	30	9.1	30.0
44	160.8	5.68	9.1	30	8.4	27.8
45	217.1	7.67	9.7	32	9.7	32.0
46	0.0	0.00	6.4	21	0.0	0.0
47	0.0	0.00	5.7	19	0.0	0.0
48	150.3	5.31	8.5	28	8.5	28.0
49	226.5	8.00	10.6	35	9.6	31.5
50	226.5	8.00	10.9	36	9.3	30.8
51	226.5	8.00	10.9	36	8.9	29.3
52	225.3	7.96	9.7	32	9.7	32.0
53	0.0	0.00	6.4	21	0.0	0.0
54	162.2	5.73	8.2	27	8.2	27.0
55	171.8	6.07	7.9	26	7.9	26.0
56	178.9	6.32	8.2	27	8.2	27.0
57	178.6	6.31	9.4	31	9.4	31.0

Table 5.3-- Continued

WELL	OPTIMAL PUMPING RATES		5% SAT. THICKNESS		OPTIMAL DRAWDOWN	
FIELD	LPS	FT^3/SEC	M	FT	M	FT
58	174.6	6.17	8.8	29	8.8	29.0
59	196.7	6.95	8.5	28	8.5	28.0
60	213.4	7.54	9.1	30	9.1	30.0
61	189.1	6.68	9.1	30	9.1	30.0
62	189.4	6.69	9.1	30	9.1	30.0
63	226.5	8.00	9.4	31	9.4	31.0

Table 5.4

OPTIMAL PUMPING RATES ACCORDING TO THE SECOND MANAGEMENT SCHEME FOR THE SECOND PERIOD. WELL FIELD CAPACITY 227 LPS (8 FT^3/SEC).

WELL FIELD	OPTIMAL PUMPING RATES		10% SAT. THICKNESS		OPTIMAL DRAWDOWN	
	LPS	FT^3/SEC	M	FT	M	FT
1	224.0	7.91	18.9	62	18.9	62.0
2	226.5	8.00	17.7	58	17.7	58.0
3	226.5	8.00	17.7	58	17.7	58.0
4	226.5	8.00	23.2	76	16.0	52.6
5	226.5	8.00	17.7	58	17.7	58.0
6	226.5	8.00	17.1	56	17.1	56.0
7	226.5	8.00	17.1	56	17.1	56.0
8	226.5	8.00	22.6	74	19.3	63.4
9	226.5	8.00	20.7	68	19.1	62.8
10	226.5	8.00	23.2	76	16.2	53.3
11	226.5	8.00	27.4	90	13.9	45.5
12	197.1	6.96	18.9	62	18.9	62.0
13	226.5	8.00	21.3	70	17.7	58.1
14	226.5	8.00	17.1	56	17.1	56.0
15	226.5	8.00	21.9	72	20.5	67.1
16	226.5	8.00	21.9	72	21.5	70.5
17	173.6	6.14	17.7	58	17.7	58.0

Table 5.4--Continued

WELL FIELD	OPTIMAL PUMPING RATES LPS	OPTIMAL PUMPING RATES FT^3/SEC	10% SAT. THICKNESS M	10% SAT. THICKNESS FT	OPTIMAL DRAWDOWN M	OPTIMAL DRAWDOWN FT
18	226.5	8.00	17.7	58	17.7	58.0
19	186.6	6.59	18.3	60	18.3	60.0
20	226.5	8.00	23.2	76	14.2	46.6
21	187.4	6.62	18.3	60	18.3	60.0
22	221.1	7.81	23.2	76	23.2	76.0
23	226.5	8.00	29.3	96	21.1	69.1
24	226.5	8.00	29.3	96	18.3	59.9
25	194.2	6.86	18.9	62	18.9	62.0
26	226.5	8.00	17.7	58	17.7	58.0
27	226.5	8.00	18.3	60	18.3	60.0
28	151.2	5.34	13.4	44	13.4	44.0
29	224.8	7.94	21.9	72	21.9	72.0
30	226.5	8.00	27.4	90	20.9	68.6
31	226.5	8.00	27.4	90	18.3	60.2
32	211.5	7.47	17.7	58	17.7	58.0
33	193.7	6.84	18.3	60	18.3	60.0
34	226.5	8.00	18.3	60	17.9	58.7
35	196.8	6.95	18.9	62	18.9	62.0
36	226.5	8.00	18.9	62	18.9	62.0
37	191.1	6.75	18.9	62	18.9	62.0

Table 5.4--Continued

WELL FIELD	OPTIMAL PUMPING RATES LPS	OPTIMAL PUMPING RATES FT^3/SEC	10% SAT. THICKNESS M	10% SAT. THICKNESS FT	OPTIMAL DRAWDOWN M	OPTIMAL DRAWDOWN FT
38	226.5	8.00	20.7	68	19.1	62.8
39	205.3	7.25	12.8	42	12.8	42.0
40	193.4	6.83	20.7	68	20.7	68.0
41	226.5	8.00	27.4	90	20.3	66.5
42	226.5	8.00	27.4	90	18.1	59.4
43	226.5	8.00	18.3	60	17.3	56.8
44	194.5	6.87	18.3	60	18.3	60.0
45	226.5	8.00	19.2	63	18.8	61.6
46	220.8	7.80	12.8	42	12.8	42.0
47	191.7	6.77	11.6	38	11.6	38.0
48	142.1	5.02	17.1	56	17.1	56.0
49	226.5	8.00	21.3	70	18.6	60.9
50	226.5	8.00	21.9	72	17.7	58.1
51	226.5	8.00	21.9	72	16.5	54.2
52	225.3	8.00	19.5	64	18.3	60.2
53	217.4	7.68	12.8	42	12.8	42.0
54	174.1	6.15	16.5	54	16.5	54.0
55	195.9	6.92	15.8	52	15.8	52.0
56	205.3	7.25	16.5	54	16.5	54.0
57	186.0	6.57	18.9	62	18.9	62.0

Table 5.4--Continued

WELL FIELD	OPTIMAL PUMPING RATES LPS	OPTIMAL PUMPING RATES FT^3/SEC	10% SAT. THICKNESS M	10% SAT. THICKNESS FT	OPTIMAL DRAWDOWN M	OPTIMAL DRAWDOWN FT
58	186.0	6.57	17.7	58	17.7	58.0
59	226.5	8.00	17.1	56	17.1	56.0
60	226.5	8.00	18.3	60	18.2	59.7
61	195.1	6.89	18.3	60	18.3	60.0
62	217.2	7.67	18.3	60	18.3	60.0
63	226.5	8.00	18.9	62	17.1	56.1

Table 5.5

OPTIMAL PUMPING RATES ACCORDING TO THE THIRD MANAGEMENT SCHEME FOR THE FIRST PERIOD. WELL FIELD CAPACITY 1415 LPS (50 FT^3/SEC).

WELL FIELD	OPTIMAL PUMPING RATES		5% SAT. THICKNESS		OPTIMAL DRAWDOWN	
	LPS	FT^3/SEC	M	FT	M	FT
1	201.5	7.12	9.4	31	9.4	31.0
2	217.2	7.67	8.8	29	8.8	29.0
3	231.3	8.17	8.8	29	8.8	29.0
4	303.2	10.71	11.5	38	11.5	38.0
5	203.3	7.18	8.8	29	8.8	29.0
6	214.6	7.58	8.5	28	8.5	28.0
7	211.8	7.48	8.5	28	8.5	28.0
8	265.0	9.36	11.2	37	11.2	37.0
9	234.1	8.27	10.3	34	10.3	34.0
10	300.7	10.62	11.5	38	11.5	38.0
11	408.8	14.44	13.7	45	13.7	45.0
12	197.3	6.97	9.4	31	9.4	31.0
13	266.1	9.40	10.6	35	10.6	35.0
14	150.6	5.32	8.5	28	8.5	28.0
15	238.7	8.43	10.9	36	10.9	36.0
16	216.3	7.64	10.9	36	10.9	36.0
17	176.6	6.24	8.8	29	8.8	29.0

Table 5.5--Continued

WELL FIELD	OPTIMAL PUMPING RATES LPS	OPTIMAL PUMPING RATES FT^3/SEC	5% SAT. THICKNESS M	5% SAT. THICKNESS FT	OPTIMAL DRAWDOWN M	OPTIMAL DRAWDOWN FT
18	159.7	5.64	8.8	29	8.8	29.0
19	182.3	6.44	9.1	30	9.1	30.0
20	330.1	11.66	11.5	38	11.5	38.0
21	176.9	6.25	9.1	30	9.1	30.0
22	0.0	0.00	11.5	38	0.0	0.00
23	425.3	15.02	14.6	48	14.6	48.0
24	410.8	14.51	14.6	48	14.6	48.0
25	195.0	6.89	9.4	31	9.4	31.0
26	161.7	5.71	8.8	29	8.8	29.0
27	213.4	7.54	9.1	30	9.1	30.0
28	136.2	4.81	6.7	22	6.7	22.0
29	289.1	10.21	10.9	36	10.9	36.0
30	0.0	0.00	13.7	45	0.0	0.0
31	412.8	14.58	13.7	45	13.7	45.0
32	188.8	6.67	8.8	29	8.8	29.0
33	180.3	6.37	9.1	30	9.1	30.0
34	237.0	8.37	9.1	30	9.1	30.0
35	186.8	6.60	9.4	31	9.4	31.0
36	180.6	6.38	9.4	31	9.4	31.0
37	192.5	6.80	9.4	31	9.4	31.0

Table 5.5--Continued

WELL FIELD	OPTIMAL PUMPING RATES LPS	OPTIMAL PUMPING RATES FT^3/SEC	5% SAT. THICKNESS M	5% SAT. THICKNESS FT	OPTIMAL DRAWDOWN M	OPTIMAL DRAWDOWN FT
38	226.5	8.00	10.3	34	10.3	34.0
39	128.0	4.52	6.4	21	6.4	21.0
40	0.0	0.00	10.3	34	0.0	0.0
41	0.0	0.00	13.7	45	0.0	0.0
42	448.5	15.84	13.7	45	13.7	45.0
43	210.6	7.44	9.1	30	9.1	30.0
44	174.1	6.15	9.1	30	9.1	30.0
45	217.1	7.67	9.7	32	9.7	32.0
46	113.8	4.02	6.4	21	6.4	21.0
47	100.8	3.56	5.7	19	5.7	19.0
48	150.3	5.31	8.5	28	8.5	28.0
49	317.7	11.22	10.6	35	10.6	35.0
50	270.4	9.55	10.9	36	10.9	36.0
51	310.9	10.98	10.9	36	10.9	36.0
52	225.3	7.96	9.7	32	9.7	32.0
53	114.4	4.04	6.4	21	6.4	21.0
54	162.2	5.73	8.2	27	8.2	27.0
55	171.8	6.07	7.9	26	7.9	26.0
56	178.9	6.32	8.2	27	8.2	27.0
57	178.9	6.31	9.4	31	9.4	31.0

Table 5.5--Continued

WELL FIELD	OPTIMAL PUMPING RATES LPS	OPTIMAL PUMPING RATES FT^3/SEC	5% SAT. THICKNESS M	5% SAT. THICKNESS FT	OPTIMAL DRAWDOWN M	OPTIMAL DRAWDOWN FT
58	174.6	6.17	8.8	29	8.8	29.0
59	196.7	6.95	8.5	28	8.5	28.0
60	213.4	7.54	9.1	30	9.1	30.0
61	189.1	6.68	9.1	30	9.1	30.0
62	189.4	6.69	9.1	30	9.1	30.0
63	234.7	8.29	9.4	31	9.4	31.0

Table 5.6

OPTIMAL PUMPING RATES ACCORDING TO THE THIRD MANAGEMENT SCHEME FOR THE SECOND PERIOD. WELL FIELD CAPACITY 1415 LPS (50 FT^3/SEC).

WELL	OPTIMAL PUMPING RATES		10% SAT. THICKNESS		OPTIMAL DRAWDOWN	
FIELD	LPS	FT^3/SEC	M	FT	M	FT
1	224.0	7.91	18.9	62	18.9	62.0
2	222.3	7.85	17.7	58	17.7	58.0
3	226.5	8.00	17.7	58	17.7	58.0
4	368.3	13.01	23.2	76	23.2	76.0
5	192.0	6.78	17.7	58	17.7	58.0
6	217.7	7.69	17.1	56	17.1	56.0
7	205.8	7.27	17.1	56	17.1	56.0
8	301.0	10.63	22.6	74	22.6	74.0
9	265.6	9.38	20.7	68	20.7	68.0
10	361.3	12.76	23.2	76	23.2	76.0
11	513.3	18.13	27.4	90	27.4	90.0
12	180.4	6.37	18.9	62	18.9	62.0
13	265.9	9.39	21.3	70	21.3	70.0
14	149.2	5.27	17.1	56	17.1	56.0
15	260.2	9.19	21.9	72	21.9	72.0
16	222.3	7.85	21.9	72	21.9	72.0
17	169.6	5.99	17.7	58	17.7	58.0

Table 5.6--Continued

WELL FIELD	OPTIMAL PUMPING RATES LPS	OPTIMAL PUMPING RATES FT^3/SEC	10% SAT. THICKNESS M	10% SAT. THICKNESS FT	OPTIMAL DRAWDOWN M	OPTIMAL DRAWDOWN FT
18	154.6	5.46	17.7	58	17.7	58.0
19	182.1	6.43	18.3	60	18.3	60.0
20	416.8	14.72	23.2	76	23.2	76.0
21	182.1	6.43	18.3	60	18.3	60.0
22	291.1	10.28	23.2	76	23.2	76.0
23	375.4	13.26	29.3	96	29.3	96.0
24	447.3	15.80	29.3	96	29.3	96.0
25	193.7	6.84	18.9	62	18.9	62.0
26	163.9	5.79	17.7	58	17.7	58.0
27	225.7	7.97	18.3	60	18.3	60.0
28	143.3	5.06	13.4	44	13.4	44.0
29	188.6	6.66	21.9	72	21.9	72.0
30	455.6	16.09	27.4	90	27.4	90.0
31	374.3	13.22	27.4	90	27.4	90.0
32	205.8	7.27	17.7	58	17.7	58.0
33	188.0	6.64	18.3	60	18.3	60.0
34	241.5	8.53	18.3	60	18.3	60.0
35	190.3	6.72	18.9	62	18.9	62.0
36	187.7	6.63	18.9	62	18.9	62.0
37	185.7	6.56	18.9	62	18.9	62.0

Table 5.6--Continued

WELL FIELD	OPTIMAL PUMPING RATES LPS	OPTIMAL PUMPING RATES FT^3/SEC	10% SAT. THICKNESS M	10% SAT. THICKNESS FT	OPTIMAL DRAWDOWN M	OPTIMAL DRAWDOWN FT
38	262.7	9.28	20.7	68	20.7	68.0
39	112.1	3.96	12.8	42	12.8	42.0
40	289.9	10.24	20.7	68	20.7	68.0
41	543.6	19.20	27.4	90	27.4	90.0
42	404.6	14.29	27.4	90	27.4	90.0
43	246.0	8.69	18.3	60	18.3	60.0
44	178.4	6.30	18.3	60	18.3	60.0
45	240.1	8.48	19.2	63	19.2	63.0
46	115.2	4.07	12.8	42	12.8	42.0
47	100.0	3.53	11.6	38	11.6	38.0
48	131.1	4.63	17.1	56	17.1	56.0
49	256.5	9.06	21.3	70	21.3	70.0
50	271.0	9.57	21.9	72	21.9	72.0
51	341.5	12.06	21.9	72	21.9	72.0
52	256.8	9.07	19.5	64	19.5	64.0
53	113.3	4.00	12.8	42	12.8	42.0
54	168.2	5.94	16.5	54	16.5	54.0
55	172.4	6.09	15.8	52	15.8	52.0
56	199.0	7.03	16.5	54	16.5	54.0
57	180.9	6.39	18.9	62	18.9	62.0

Table 5.6--Continued

WELL FIELD	OPTIMAL PUMPING RATES LPS	OPTIMAL PUMPING RATES FT^3/SEC	10% SAT. THICKNESS M	10% SAT. THICKNESS FT	OPTIMAL DRAWDOWN M	OPTIMAL DRAWDOWN FT
58	180.4	6.37	17.7	58	17.7	58.0
59	231.3	8.17	17.1	56	17.1	56.0
60	231.0	8.16	18.3	60	18.3	60.0
61	189.7	6.70	18.3	60	18.3	60.0
62	211.2	7.46	18.3	60	18.3	60.0
63	272.4	9.62	18.9	62	18.9	62.0

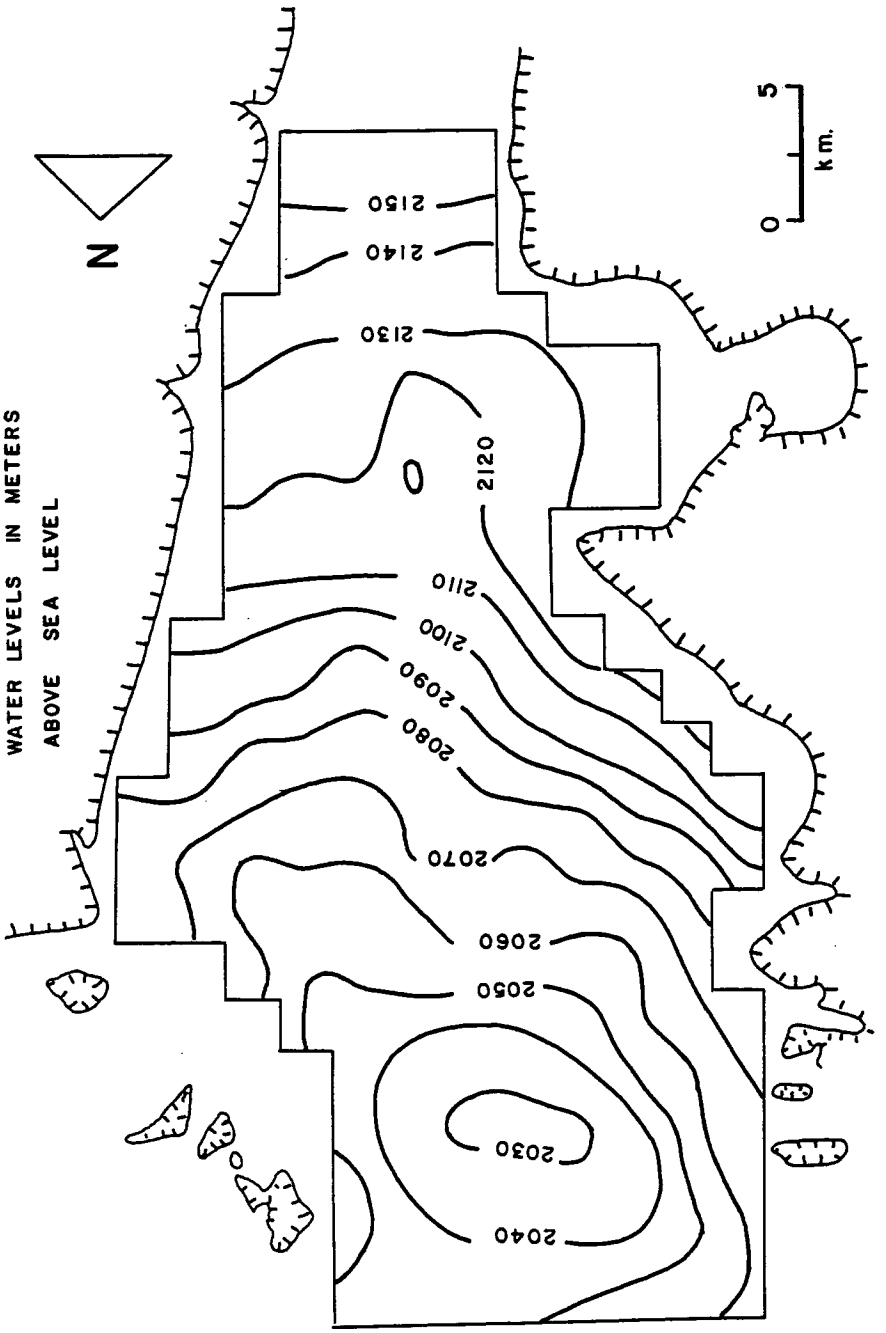

Figure 5.2 Optimal hydraulic heads at the end of 1990.

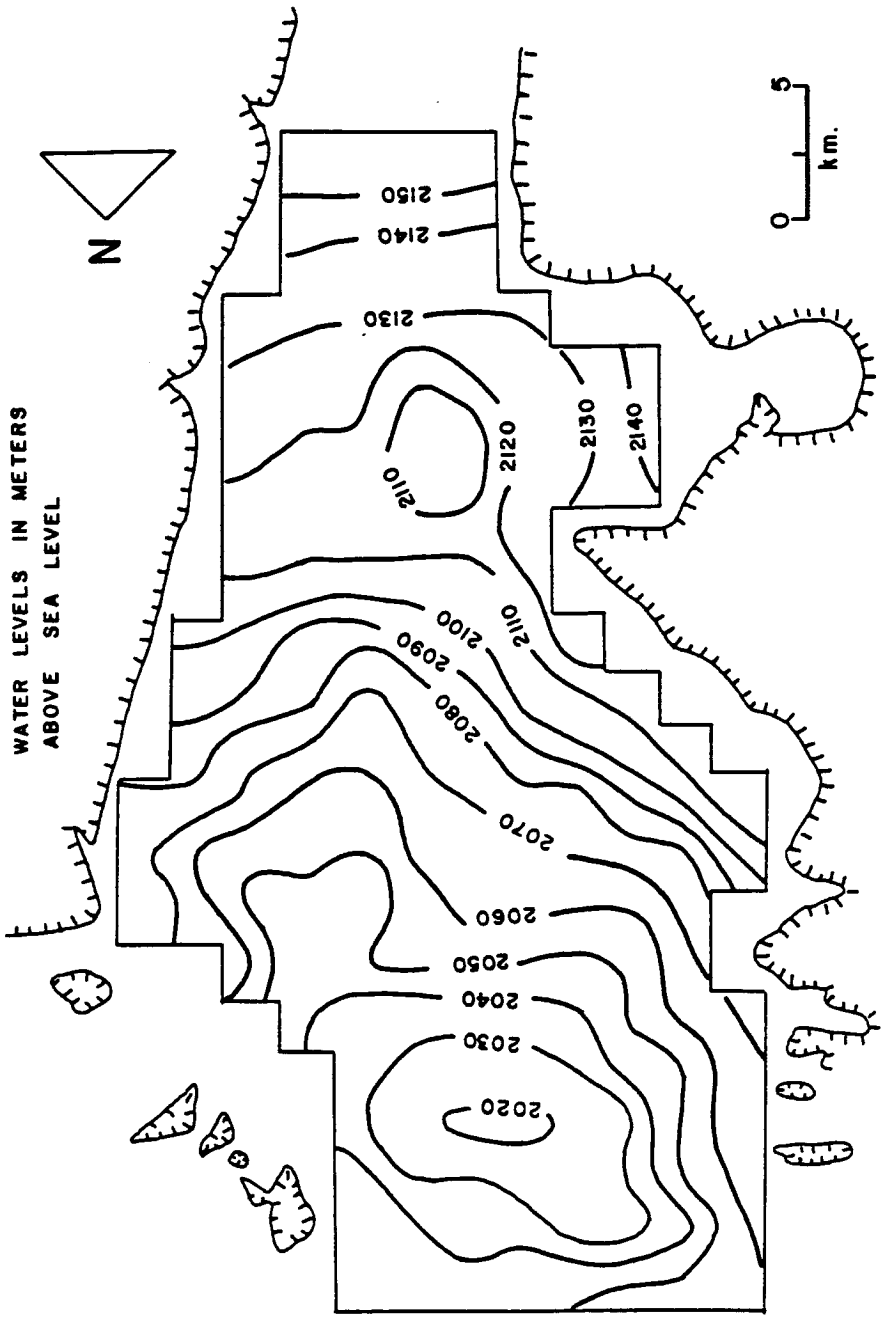

Figure 5.3 Optimal hydraulic heads at the end of 1995.

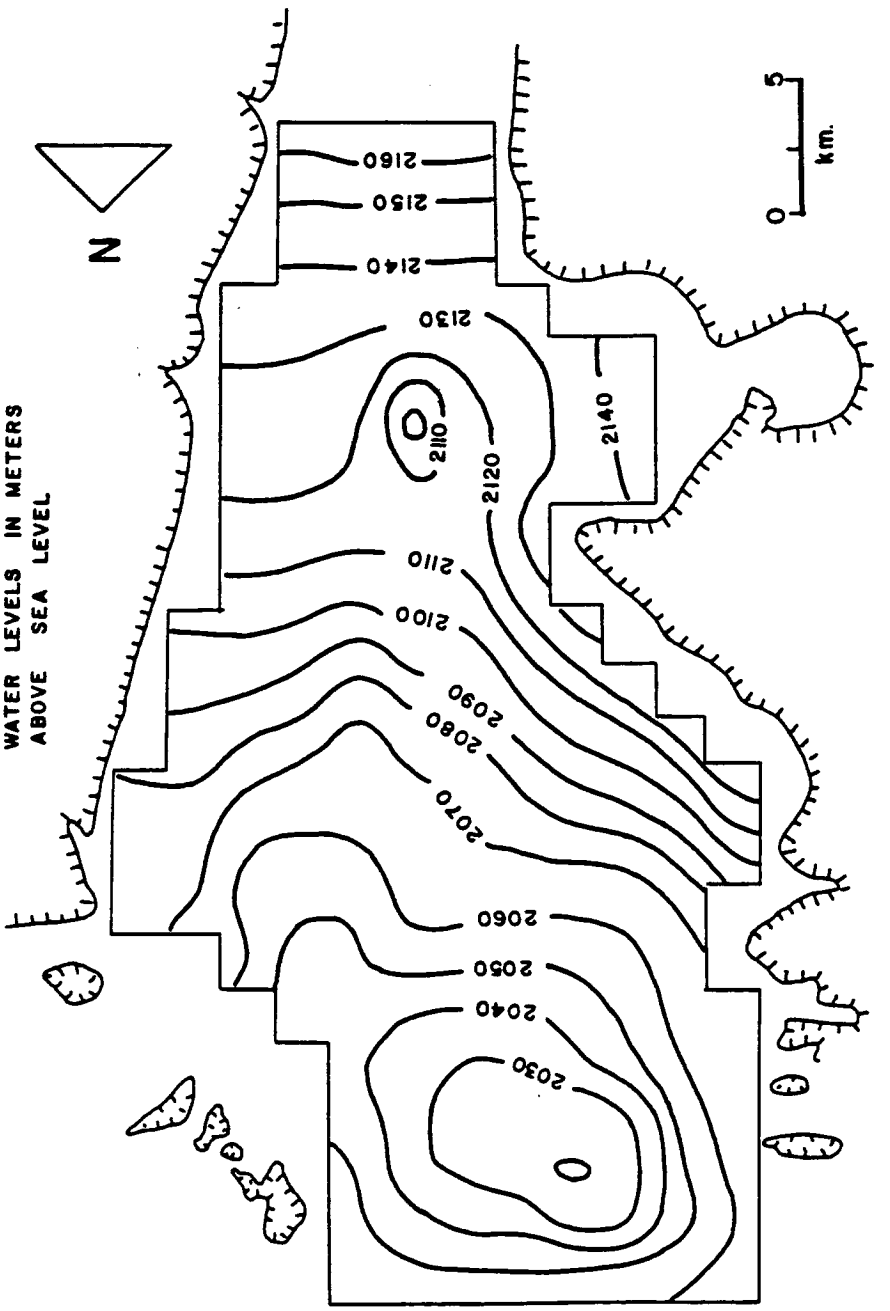

Figure 5.4 Non-optimal hydraulic heads at the end of 1990.

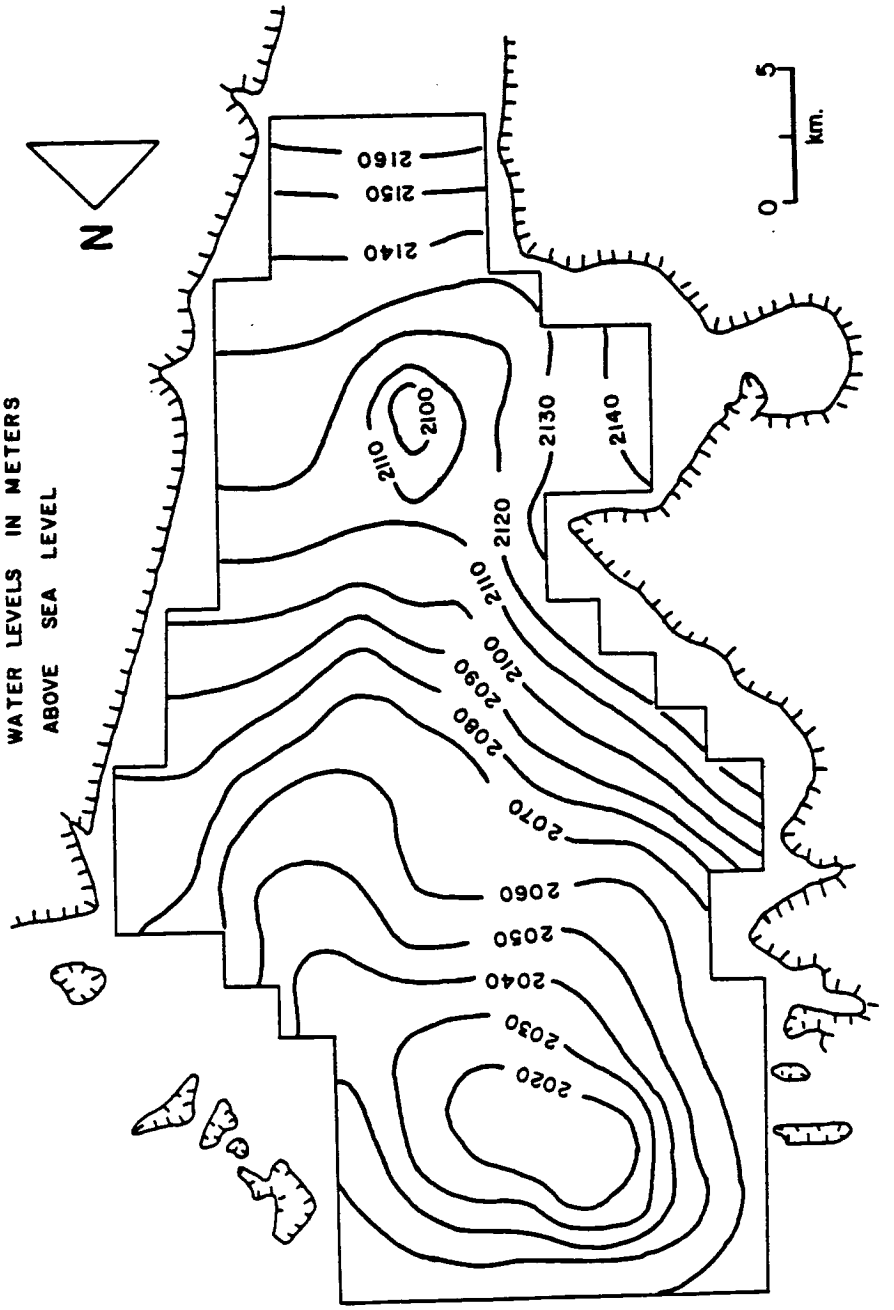

Figure 5.5 Non-optimal hydraulic heads at the end of 1995.

CHAPTER 6

SUMMARY AND CONCLUSIONS

The primary objectives of this study were to: 1) Estimate log-transmissivities and hydraulic heads given measured spatial data from the Calera basin, 2) Quantify the uncertainty in estimation, 3) Develop a groundwater management model which is capable of calculating the best pumpage policies "optimal" subject to physical constraints.

The first two objectives were accomplished by performing a geostatistical estimation technique called Kriging, which was used to estimate log-transmissivities, hydraulic heads and their associated estimation error. Regarding log-transmissivity, a spherical model was fitted to the isotropic semivariogram. Although the range is small, there is a relatively high correlation between transmissivity values at two close locations. According to the log-transmissivity estimation kriging errors, the least reliable areas were along the boundaries and southern region of the basin.

Initial and transient state hydraulic heads were represented by water levels measured in 1956 and 1985, respectively. Because hydraulic head is a non-intrinsic phenomenon, the drift or trend function had to be determined from the data before kriging could be applied. A first order polynomial was fitted to the initial and transient state water level data by using an iterative generalized least squares procedure. This method allowed for simultaneous determination of the

trend surface and residual semivariogram. The method required two steps: 1) ordinary least squares was used to select the order of the polynomial used to fit the trend and 2) iterative generalized least squares was used to calculate the trend and the semivariogram of the residuals. The second step was repeated until successive semivariograms were coincident. Kriging was used to estimate hydraulic head residuals at grid points over the aquifer. The drift was added to the kriged residuals to provide total head estimates. Hydraulic head residual kriging errors were also calculated. Clearly, the highest errors occured in areas where water level measurements were not available or scarce. In addition, a cross-validation method using the maximum likelihood approach developed by Samper was performed to the available water level data. Hydraulic head residual kriging errors obtained by the latter method were lower than those by the generalized least squares method in the central region of the basin.

Before the groundwater management model was developed, it was necessary to simulate some known basin conditions. Consequently, a two dimensional finite difference model was used to simulate actual conditions on the Calera Basin. The process of simulation was carried out in two steps. The first step consisted of obtaining the steady state hydraulic head configuration. The second step involved matching the computed transient hydraulic heads with the 1985 kriging hydraulic head estimates. In obtaining the steady state hydraulic head configuration, the transmissivity distribution from the Kriging interpolation technique remained unchanged, while minor adjustments in recharge were made along the boundaries of the basin. Total recharge was computed

using the model to be approximately 53.50E+06 M^3/Yr (43.37E+03 AF/Yr). Approximately 65 percent of the total recharge occurs in the Sierra Madre Occidental and 35 percent in the Sierra of Zacatecas. In the second step, an average storativity value of 0.13 was used for the first run. Further modifications were made to the storativity value in areas where the match between computed hydraulic heads and kriging hydraulic head estimates was poor. The final values of storativity were within the interval of 0.1 and 0.2. The hydraulic head residual kriging errors were used as a criterion to stop the calibration process. That is, the calibration process was considered to be satisfactory when the computed hydraulic heads lay within the interval H^*_i +/- σ_i. Consequentely, the larger discrepancies between computed and kriged hydraulic heads were permitted in areas where water level measurements were not available or scarce. A sensitivity analysis performed on the calibrated model suggests that groundwater levels are most sensitive to changes in storativity than in transmissivity. The greatest water level changes occured in heavily pumped areas. Consequently, sensitivity is primarly a function of the dewatering process.

The third objective of this study was to develop a groundwater management model based on the use of linear programming and the response function technique. The model is capable of calculating the optimal pumpage policy subject to physical constraints of the system. The application of the management model to the Calera basin was done for 63 well fields for two time periods, five years each. For the two time periods, three optimal pumpage policies were generated allowing

five and ten percent of the 1985 saturated thickness at each well field to be used up while meeting the water demand during each time period. The water demand for the first and second time periods were set equal to 1.20E+08 M^3/Yr (9.72E+04 AF/Yr) and 1.50E+08 M^3/Yr (1.22E+05 AF/Yr), respectively. The first optimal pumpage policy was generated allowing five percent to be used up for the two time periods, and a maximum well field capacity of 227 lps (8 ft^3/sec) for the first period and 340 lps (12 ft^3/sec) for the second time period. This management scheme failed to meet the water demand for the second time period. That is, most of the five percent of the saturated thickness at each well field was used up during the first period. As a result, the pumping rates during the second time period were very low. Consequently, in order to meet the water demand during the second time period, no less than the five percent of the 1985 saturated thickness has to be used up. Hence, the second management scheme generated an optimal pumpage policy that used up five and ten percent of the 1985 saturated thickness during the first and second time period, respectively. In addition, the maximum well field capacity was set equal to 227 lps (8 ft^3/sec) for the two time periods. According to this optimal pumpage policy the water demands were met during the two time periods. In addition, 29 well fields did not use up the full five percent of the saturated thickness during the first time period. The location of these well fields are primarly in the north central, eastern and southeastern regions of the basin which have fairly high transmissivity values. However, 9 of the 29 well fields are in the area where greatest drawdowns have occured. Therefore, it is desirable not to use up the full five percent of the

saturated thickness to prevent further declining of water levels in this area. Similarly, in the second time period 25 well fields did not use up the full ten percent of the saturated thickness. The location of these well fields were the same as those previously mentioned in the first time period, except, the well field # 52 that was located in the northwestern region of the basin. Clearly, based on these results, the system is capable of supplying more water if the five and ten percent of the 1985 saturated thickness is fully used up in some regions. Therefore, the purpose of the third management scheme was to find out the maximum amount of water that the 63 well fields could pump from the system exhausting the five and ten percent of the 1985 saturated thickness. The results showed that the water demand was far exceeded in both time periods.

In order to obtain the effects on the aquifer produced by non-optimal pumping rates, the simulation model was run using the 1985 pumpage scheme, which would able to provide 89 and 71 of the water demand at the end of 1990 and 1995, respectively. The results showed that indeed, the optimal pumpage policy reduced the drawdowns in all over the aquifer. That is, the drawdown at the end of 1990 in the north central region of the basin produced by optimal pumping rates was 10 m (32 ft) less than the one produced by non-optimal pumping rates. Similarly, at the end of 1995, the drawdown in the north and south central regions of the basin was 10 m (32 ft) less than the one produced by nonoptimal pumping rates. Therefore, the groundwater management model proved to obtain an optimal pumping distribution which may be effective in the overall preservation of the groundwater

resources in the Calera Basin.

The following conclusions can be made from this study:

1.- Kriging is an effective method of estimating spatially values of transmissivity and hydraulic head. Kriging has the advantage over other estimation techniques of providing unbiased linear estimates with minimum estimation error variance.

2.- The quality of the estimate can be judged by the magnitude of its kriging estimation error. In other words, kriging errors are largest in areas where data are scarce.

3.- The maximum likelihood cross-validation method produced lower kriging estimation errors than the conventional "jacknife" cross-validation method.

4.- Kriging estimation errors proved to be a useful criterion to stop the calibration process. That is, the calibration process was continued until computed hydraulic heads were within the interval H^*_i +/- σ_i.

5.- Groundwater resources in the Calera Basin are highly over appropiated. However, water demands at the end of 1990 and 1995 can be met if five and ten percent of the 1985 saturated thickness is allowed to be used up.

6.- In addition, if groundwater resources in the Calera basin are developed according to the actual non-optimal pumping rates to meet future water demands, drawdowns will be much greater than the ten percent allowable saturated thickness limit at the end of 1995.

7.- Areas which may be recomended for further development are in the eastern and south central regions of the basin. Well fields in

these areas pump at their maximum capacity without exhausting the five or ten percent of the allowable saturated thickness.

An option to prolong the life of the groundwater resources in the Calera Basin is to stop further development in the north central region of the aquifer. In addition, according to the optimal pumpage policy, well fields such as # 39, 46, 47 and 53 located in this region can be shut down over the next five years.

It should be kept in mind that water is not plentiful in the area and that the actual appropriation is twice the estimated natural recharge. However, following the proposed optimal pumpage scheme may help to enhance future development of groundwater resources in the Calera Basin.

APPENDIX A

CALERA BASIN DATA

TABLE A-1

Transmissivity Data. Reported by Secretaria de Agricultura y Recursos Hidraulicos (1980).

Well No	X (km)	Y (km)	Transmissivity (m^2/day)
1	3.95	13.15	22.98
2	4.60	12.00	35.40
3	5.00	13.40	20.74
4	5.90	12.90	37.80
5	7.00	17.35	417.00
6	7.10	17.55	432.24
7	7.40	11.25	177.12
8	7.45	13.85	374.11
9	7.35	14.85	501.12
10	8.05	10.55	210.38
11	8.15	15.40	346.40
12	8.05	16.85	380.18
13	8.00	18.35	75.34
14	8.80	15.85	148.61
15	8.45	18.20	103.68
16	8.55	19.00	54.43
17	9.30	19.70	38.62
18	9.40	18.00	70.55
19	9.45	18.20	31.10
20	9.75	16.30	114.91
21	9.65	18.25	59.96
22	9.95	18.20	59.27
23	10.65	12.00	90.72
24	10.80	17.70	101.20
25	10.90	18.75	329.18
26	11.00	18.50	280.28
27	11.15	19.55	112.32
28	11.45	10.65	53.22
29	11.55	19.55	120.10
30	12.00	20.50	99.36
31	12.12	11.60	135.65
32	11.70	18.05	230.62
33	13.45	20.50	252.29
34	13.75	19.10	88.99
35	13.97	17.20	66.53

Table A-1--Continued

Well No	X (km)	Y (km)	Transmissivity (m^2/day)
36	13.95	16.60	39.57
37	13.95	14.72	22.29
38	14.10	17.50	32.83
39	14.50	19.45	114.05
40	15.30	14.37	56.16
41	15.40	16.00	86.40
42	15.55	14.60	36.30
43	18.27	16.85	61.34
44	18.65	16.17	69.98
45	22.50	16.00	114.91
46	24.00	16.37	93.31
47	25.35	15.72	190.08
48	27.65	13.92	183.17
49	28.75	16.05	189.22

TABLE A-2

Water level data measured in 1956. Reported by Secretaria de Agricultura y Recursos Hidraulicos (1980).

Well No	X (km)	Y (km)	Water Level (m)
1	4.00	12.90	2059.5
2	5.08	16.08	2059.1
3	6.43	15.45	2066.7
4	5.90	12.90	2070.5
5	6.55	13.30	2071.2
6	7.95	14.40	2076.4
7	7.70	17.25	2068.3
8	7.25	18.00	2069.0
9	7.95	12.30	2084.5
10	8.00	13.58	2080.3
11	8.60	15.50	2077.1
12	8.92	18.00	2076.5
13	9.45	18.20	2081.4
14	10.83	20.40	2086.7
15	11.35	16.03	2089.7
16	11.42	20.50	2087.2
17	9.40	12.34	2091.5
18	12.60	17.75	2097.2
19	12.50	19.00	2095.1
20	12.00	17.10	2093.2
21	14.65	15.73	2111.6
22	14.87	14.58	2114.2
23	15.55	19.35	2110.1
24	16.95	16.02	2123.7
25	16.95	18.27	2120.0
26	11.75	17.95	2092.6
27	11.80	19.25	2091.5
28	11.55	19.55	2090.8
29	11.25	18.85	2089.2
30	10.45	18.13	2085.9

Table A-2--continued

Well No	X (km)	Y (km)	Water Level (m)
31	8.11	17.30	2070.1
32	7.70	16.43	2069.6
33	9.65	15.60	2082.4
34	10.75	15.40	2087.3
35	11.15	15.90	2089.4
36	9.85	13.75	2087.0
37	7.10	14.00	2072.3
38	6.60	16.14	2066.0
39	12.00	20.50	2090.1
40	13.80	18.17	2102.6
41	4.85	14.35	2059.9
42	3.90	12.20	2060.0
43	13.83	15.22	2108.6
44	14.35	12.60	2116.8
45	19.62	15.60	2138.8
46	19.65	17.00	2136.6
47	16.00	14.35	2121.6
48	15.55	18.35	2113.6
49	16.40	16.25	2120.0
50	3.00	11.00	2058.6

TABLE A-3

Water level data measured in 1985. Reported by Secretaria de Agricultura y Recursos Hidraulicos, (1985, personal communication).

Well No	X (km)	Y (km)	Water Level (m)
1	4.00	12.90	2050.5
2	5.08	16.08	2054.8
3	6.43	15.45	2056.7
4	5.90	12.90	2054.5
5	6.55	13.30	2054.2
6	7.95	14.40	2058.4
7	7.70	17.25	2060.3
8	7.25	18.00	2060.0
9	7.95	12.30	2067.5
10	8.00	13.58	2060.3
11	8.60	15.50	2061.0
12	8.92	18.00	2065.5
13	9.45	18.20	2065.4
14	10.83	20.40	2070.7
15	11.35	16.03	2076.5
16	11.42	20.50	2069.2
17	9.40	12.34	2075.5
18	12.60	17.75	2070.2
19	12.50	19.00	2070.1
20	12.00	17.10	2076.8
21	14.65	15.73	2108.6
22	14.87	14.58	2125.2
23	15.55	19.35	2109.8
24	16.95	16.02	2120.5
25	16.95	18.27	2120.6
26	11.75	17.95	2070.6
27	11.80	19.25	2069.5
28	11.55	19.55	2065.8
29	11.25	18.85	2062.2
30	10.45	18.13	2059.9

Table A-3--Continued

Well No	X (km)	Y (km)	Water Level (m)
31	8.11	17.30	2058.9
32	7.70	16.43	2055.5
33	9.65	15.60	2067.4
34	10.75	15.40	2076.6
35	11.15	15.90	2077.3
36	9.85	13.75	2069.0
37	7.10	14.00	2050.2
38	6.60	16.14	2049.0
39	12.00	20.50	2070.9
40	13.80	18.17	2085.5
41	4.85	14.35	2030.9
42	3.90	12.20	2060.0
43	13.83	15.22	2110.0
44	14.35	12.60	2126.8
45	19.62	15.60	2133.8
46	19.65	17.00	2127.0
47	16.00	14.35	2127.2
48	15.55	18.35	2113.7
49	16.40	16.25	2115.5
50	3.00	11.00	2070.0
51	3.05	14.00	2060.4
52	3.10	17.05	2054.7
53	4.60	12.40	2062.2
54	5.25	14.15	2030.9
55	5.60	15.20	2033.6
56	5.10	12.04	2057.0
57	5.03	15.00	2036.3
58	5.75	14.80	2032.5
59	5.08	13.01	2045.1
60	5.80	14.85	2031.7
61	6.07	14.10	2036.4
62	6.10	16.08	2037.0
63	6.50	16.70	2039.1
64	7.30	12.90	2062.9
65	7.05	13.10	2060.2

Table A-3--Continued

Well No	X (km)	Y (km)	Water Level (m)
66	7.08	15.01	2040.3
67	7.30	16.10	2040.7
68	7.80	15.40	2048.5
69	8.02	14.20	2055.4
70	8.04	16.04	2050.8
71	9.20	19.10	2058.2
72	10.18	13.70	2070.1
73	10.05	16.06	2070.0
74	10.50	19.20	2060.7
75	10.00	17.25	2070.9
76	9.80	14.90	2067.0
77	10.90	18.85	2060.4
78	12.70	16.95	2079.6
79	17.00	14.00	2129.8
80	12.00	15.70	2080.1
81	13.23	18.67	2080.2
82	14.35	15.08	2105.3
83	13.30	17.65	2082.5
84	15.06	15.03	2115.6
85	15.65	17.50	2105.0
86	16.95	17.00	2113.1
87	17.85	18.67	2119.3
88	18.70	16.50	2121.5
89	17.00	19.00	2113.7
90	19.10	16.40	2125.9
91	21.00	19.00	2134.0
92	21.00	20.00	2133.7
93	23.00	19.00	2146.4
94	22.00	18.00	2145.1
95	23.90	16.00	2160.2
96	21.60	15.50	2147.5
97	20.20	16.60	2134.6
98	21.25	17.75	2142.3
99	17.65	18.05	2120.7
100	19.30	17.80	2122.5

Table A-3--Continued

Well No	X (km)	Y (km)	Water Level (m)
101	8.00	17.00	2059.1
102	8.95	17.45	2064.8
103	8.75	16.30	2053.0
104	10.90	16.80	2075.1
105	12.00	18.70	2069.4
106	12.70	7.65	2070.6
107	13.65	20.10	2088.3
108	13.80	19.05	2085.9
109	14.60	19.80	2095.7
110	13.95	17.55	2087.5
111	16.80	17.90	2119.6
112	15.60	16.10	2107.0
113	16.00	15.80	2112.8
114	14.10	14.40	2110.2
115	15.00	14.20	2121.4

LIST OF REFERENCES

Beck, J. V., and K. J. Arnold, 1977, Parameter Estimation in Engineering and Science, John Wiley and Sons, Inc., New York, N. Y., 501 p.

Boggs, M. J., 1980, Impact of Future Ground-Water Development in Cienega Creek Area, Pima, Santa Cruz and Cochise Counties, Arizona. M.S. Thesis, Dept. of Hydrology and Water Resour., University of Arizona, Tucson, 131 p.

Clifton, P. M., and S. P. Neuman, 1982, Effect of Kriging and Inverse Modeling on Conditional Simulation of the Avra Valley aquifer in Southern Arizona, Water Resour. Res., 18 (4) 1215-1234.

Delhomme, J. P., 1978, Kriging in the Hydrosciencies, Advances in Water Resources, 1 (5), 251-266.

Delhomme, J. P., 1979 a, Spatial Variability and Uncertainty in Groundwater Flow Parameters, Water Resour. Res., 15 (2), 269-280.

Delhomme, J. P., 1979 b, Kriging Under Boundary Conditions, Abstr. in Transactions, Am. Geophys. Union, 60 (46), 820.

Eastern Software Products, Inc., 1983, Linear Programming for IBM Personal Computer, Version 3.12.

Fennessy, P. J., 1982, Geostatistical Analysis and Stochastic Modeling of the Tajo Basin Aquifer, Spain. M.S. Thesis, Dept. of Hydrology and Water Resour., University of Arizona, Tucson, 124 p.

Hines, W. W., and D. C. Montgomery, 1980, Probability and Statistics in Engineering and Management Science, John Wiley and Sons, Inc., New York, N. Y., 634 p.

Journel, A. G., and Ch. J. Huijbregts, 1978, Mining Geostatistics, Academic Press, New York, N. Y., 600 p.

Maddock, T. III, 1972, Algebraic Technological Function From a Simulation Model, Water Resour. Res., 8 (1), 129-134.

Maddock, T. III, 1974 a, A Program to Compute Aquifer Response Coefficients. U.S. Geological Survey Open File Report, 75-612.

Maddock, T. III, 1974 b, Nonlinear Technological Functions For Aquifers Whose Transmissivity Vary With Drawdown. Water Resour. Res., 10 (4), 877-881.

Maddock, T. III, 1984, Ground-Water Management Modelling, Brief Lecture Notes, Dept. of Hydrology and Water Resour., University of Arizona, Tucson, 58 p.

Matheron, G., 1963, Principles of Geostatistics, Econ. Geol., 58, 1246-1266.

Matheron, G., 1971, The Theory of Regionalized Variables and Its Applications, Ecole des Mines, Fontainebleau, France.

Mc.Donald G. M., and Harbaugh W. A., 1984, A Modular Three Dimensional Finite-Difference Ground-Water Flow Model., U.S. Geological Survey, Reston Virginia, 528 p.

Neuman, S. P., 1984, Role of Geostatistics in Subsurface Hydrology, Geostatistics For Natural Resour. Characterization, G. Verly et al. (eds.), Part 2, 787- 816.

Neuman, S. P., E. A. Jacobson and P. J. Fennessy, 1983, Analysis of NonIntrinsic Spatial Variability by Residual Kriging with Application to Regional Groundwater Levels, Math. Geol., 16 (5), 499-521.

Samper, J., 1986, Statistical Methods of Analyzing Hydro Chemical, Isotropic and Hydrological Data from Regional Aquifers. Ph.D. Dissertation, Dept. of Hydrology and Water Resour., University of Arizona, Tucson, 520 p.

Secretaria de Agricultura y Recursos Hidraulicos, 1980. Estudio Geohidrologico de la Zona de Calera, Zacatecas, Mexico.